INVESTIGATIONS ON METAMATERIAL AND FRACTAL BASED MICROSTRIP FILTERS

Submitted in partial fulfilment of the requirements for the award of the degree of

DOCTOR OF PHILOSOPHY

by

AMPAVATHINA SOWJANYA

(Roll No. 717131)

Under the guidance of

Prof. D. VAKULA

DEPARTMENT OF ELECTRONICS AND COMMUNICATION ENGINEERING

NATIONAL INSTITUTE OF TECHNOLOGY WARANGAL

TELANGANA STATE-506004, INDIA

2023

Dedicated to

My Family, Teachers and Friends

APPROVAL SHEET

This Dissertation work entitled **"Investigations on Metamaterial and Fractal based Microstrip Filters"** by **Ampavathina Sowjanya, Roll No. 717131** is approved for the degree of Doctor of Philosophy.

Examiners

_____

_____

_____

Supervisor

_____

Chairman

_____

Date: Place:

DECLARATION

This is to certify that the work presented in the thesis entitled "**Investigations on metamaterial and fractal based microstrip filters**" is a bonafide work done by me under the supervision of **Prof. D. Vakula,** Department of Electronics and Communication Engineering, National Institute of Technology Warangal was not submitted elsewhere for the award of any degree.

I declare that this written submission represents my ideas in my own words and where others' ideas or words have been included. I have adequately cited and referenced the original sources. I also declare that I have adhered to all principles of academic honesty and integrity and have not misrepresented or fabricated or falsified any idea/ data/ fact/ source in my submission. I understand that any violation of the above will be a cause for disciplinary action by the institute and can also evoke penal action from the sources which have thus not been properly cited or from whom proper permission has not been taken when needed.

A. Sowjanya
(Roll No: 717131)
Date:……

DEPARTMENT OF ELECTRONICS AND COMMUNICATION ENGINEERING
NATIONAL INSTITUTE OF TECHNOLOGY WARANGAL
TELANGANA STATE-506004, INDIA

CERTIFICATE

This is to certify that the thesis entitled "**Investigations on Metamaterial and Fractal based Microstrip Filters**", which is being submitted by **Mrs. A. Sowjanya (Roll No: 717131),** in partial fulfilment for the award of the degree of Doctor of Philosophy to the Department of Electronics and Communication Engineering of National Institute of Technology Warangal, is a record of bonafide research work carried out by her under our supervision and guidance and has not been submitted elsewhere for any degree.

Signature of Supervisor

Prof. D. Vakula
(Supervisor)
Department of ECE
NIT Warangal
Warangal-506004,
Telangana, India.

ACKNOWLEDGEMENTS

I am indebted to my parents who have given me all that I have today and educating me with values and virtues and making my life fruitful.

I owe my deepest gratitude to my research supervisor, Prof. D. Vakula, Professor, Department of Electronics and Communication Engineering, National Institute of Technology Warangal who has been my mentor not only in research, but for many other things in life for help, kindness, patience, unwavering support and constant encouragement more than I could ever ask for throughout my years as a graduate student. She has been instrumental in often returning me to the correct point of view at various points during my research. Her advice and guidance on matters both academic and non-academic have proved invaluable time. I feel very thankful not only for the research guidance but also for the humanity shown on me.

I express my sincere thanks to Prof. P. Srihari Rao, HOD, ECE Department for his invaluable assistance and suggestions that he shared during my research tenure.

I take the privilege to thank all my DSC members Prof. D. M. Vinod Kumar, EEE Department, Prof. N.V.S.N. Sarma, Prof. L. Anjaneyulu and Dr. G. Arun Kumar of ECE Department for their detailed review, apt guidance, constructive suggestions and encouragement throughout the progress of my research work.

I am thankful to Prof. L. Anjaneyulu former HOD, ECE Department, Prof. N Bheema Rao, former HOD, ECE Department for their encouragement and suggestions. I would also like to thank all the faculty members, research scholars and friends for their continuous support and encouragement.

I thank the Government of India and MHRD for providing financial support.

I express thanks to the team of Microwave wing headed by Mr. Rakesh Singh (scientist RCI), for their support in carrying out research with the inhouse facilities available in RCI and M/s Cosmic Enterprises, Hyderabad for providing measurement and fabrication facility.

I would like to acknowledge my biggest debt to my sons Abhi ram, Akshay Krishna, family members for their cooperation, encouragement, and cheerful support.

Ampavathina Sowjanya

ABSTRACT

In modern communication systems, several applications are evolving with different frequency ranges. Each application must be selected without getting interfered with other systems. Bandpass filter is a device that can be used for selection of frequency range of a particular application in communication system. Bandstop filter is used to avoid interference and to suppress the unintended signal in the system. Now a days, devices used for communication systems are portable. To obtain portability, there is a need to design compact systems. For a system to be compact, the devices used in communication systems should be small in size. There is a requirement to select frequencies for multiple applications using a single device. The works proposed in this thesis is focused to design compact single band and multiband bandpass filters and a bandstop filter.

The development of microwave and millimeter wave communication systems, demands the low insertion loss in passband and high attenuation in stop band. Microstrip single and multiple bandpass filters are designed using metamaterials and slotted stubs. Symmetrical ring resonators, Moore fractal symmetrical ring resonators, EI shaped resonators are some of resonators which can be loaded on either side of the transmission line. Vias are also used in combination with metamaterial resonators along the transmission line to design compact single wide band bandpass filters for C band, X band and higher 5G communication applications. A triple bandpass filter is designed using EIE shaped resonators and slotted stubs for satellite communication applications.

Compact wide bandpass filter, bandstop filter are designed using complementary metamaterials. To design a compact wide bandpass filter triple concentric complementary split ring resonators are used in the ground plane below the gaps along the microstrip line for S band applications. Compact wide bandstop filter with high stop band attenuation is realised with complementary symmetrical ring resonators for Ku band applications.

Multi-band bandpass filters are designed using combination of metamaterials and complementary metamaterials. EI shaped resonators and complementary split ring resonators are used to design quint bandpass filter for higher 5G applications. Spiral resonators and complementary triple concentric split ring resonators are used to design dual bandpass filter for GPS and WLAN applications. Spiral resonators, stepped impedance resonators, stubs and complementary triple concentric split ring resonators are used to design triple bandpass filter for GPS, WLAN and Wimax applications.

Microstrip coupled resonators are used to design compact bandpass filters. A compact dual bandpass filter using dual split rings resonators coupled to the microstrip line is designed for

Upper Microwave Flexible Use Services. A compact single bandpass filter is designed using EC shaped resonators coupled to the microstrip line for 37 GHz band 5G applications.

High frequency structure simulator is used to simulate the designed filters. The filter designs are fabricated, evaluated, and measured results are validated with simulation results.

The outcome of the research work led to the development of compact wide bandpass, bandstop and multiband filters. Metamaterials, coupled resonators are used for compactness. Fractals are used for bandwidth enhancement. Slotted stubs are used to improve return loss and insertion loss.

The designed filters are useful for GPS, WLAN, Wi-Max, radar, fixed/mobile satellite communications and upper microwave flexible use services applications.

CONTENTS

LIST OF FIGURES

LIST OF TABLES

LIST OF ABBREVIATIONS

GPS	Global Positioning System
Wi-Fi	Wireless Fidelity
Wi-Max	Worldwide Interoperability for Microwave Access
WLAN	Wireless Local Area Network
UMFUS	Upper Microwave Flexible Use Services
LPF	Lowpass Filter
HPF	Highpass Filter
BPF	Bandpass Filter
BSF	Bandstop Filter
IEEE	Institute of Electrical and Electronics Engineering
FCC	Federal Communications Commission
PCB	Printed Circuit Board
HFSS	High Frequency Structural Simulator
AWR	Applied Wave Research
VNA	Vector Network Analyser
SRR	Split Ring Resonator
CSRR	Complementary Split Ring Resonator
UHF	Ultra High Frequency
5G	Fifth Generation
EM	Electromagnetic
MHz	Mega Hertz
GHz	Giga Hertz
mm	millimeter
ns	nanoseconds
FBW	Fractional Bandwidth
IL	Insertion Loss
L	Inductance
C	Capacitance
dB	Decibel

LIST OF SYMBOLS

f	Frequency
ε	Permittivity
ε_0	Free space dielectric constant
ε_r	Relative dielectric constant
μ	Permeability
μ_0	Free space permeability
μ_r	Relative permeability
λ_0	Free space wavelength
λ_g	Guided wavelength

Chapter 1

Introduction

1.1 Overview

Most of today's UHF, microwave and millimeter wave applications operate in the frequency range of 0.4 GHz to 300 GHz [1]. In modern communication systems, numerous applications are existing in microwave and millimeter wave regions. Satellite communications, radar, electronic warfare, metrology, remote sensing systems, etc., are different applications in the above-mentioned frequency range. Mobile communication which is operated in the UHF band currently is also shifting to microwave range in 5G technology.

Filters, diplexers & multiplexers are essential components of communication systems with different applications. Diplexers and multiplexers are essentially two and multiple filters that are combined through a beamforming network at the common port. In communications applications, filters are used to either select a frequency of interest or reject a particular band of frequencies. The four basic types of filters are Lowpass filter (LPF), Highpass filter (HPF), Bandpass filter (BPF) and Bandstop filter (BSF). Out of all the filters, bandpass filters are most essential for communication applications.

The parameters, which are detailed below, represent how well the filter performs. The response of the practical filter is illustrated in Fig 1.1.

Insertion loss: The power loss when transmitting or receiving frequencies in the pass band is usually represented as insertion loss (IL) given in the following expression, where S_{21} is the transmission coefficient.

$$IL = 10\log\left|\frac{P_i}{P_t}\right| \ dB \qquad (1.1)$$

where P_i is incident power, P_t is transmitted power

$$IL = -20\log\left|S_{21}\right| \ dB \qquad (1.2)$$

Return loss: Return loss (RL) is the loss of power due to impedance mismatch along the transmission line as given below, where S_{11} is the reflection coefficient.

$$RL = 10\log\left|\frac{P_i}{P_r}\right| dB \qquad (1.3)$$

where P_r is reflected power

$$RL = -20\log\left|S_{11}\right| dB \qquad (1.4)$$

Bandwidth: The bandwidth of the bandpass filter is defined as the difference between the lower and upper cut-off frequencies where the return loss is 10 dB or any desired value in the passband.

$$BW = f_H - f_L \qquad (1.5)$$

Center frequency: The center frequency of either passband or stopband is defined as geometric mean of the lower cut-off frequency and upper cut-off frequency. If the ratio of upper cut off frequency to lower cut off frequency is less than 1.1, then center frequency is considered as arithmetic mean of lower and upper cut off frequencies.

$$f_c = \frac{f_H + f_L}{2} \qquad (1.6)$$

Fractional bandwidth is defined as the ratio of the bandwidth to the center frequency.

$$\%\ FBW = \frac{f_2 - f_1}{f_c} \times 100 \qquad (1.7)$$

Isolation: Isolation refers to the ability of the filter to prevent or attenuate signals from one frequency band from affecting or leaking in to another frequency band.

Stop band: The frequency range in a microwave filter where the transmission of signals is significantly attenuated or blocked.

For ideal response in the passband region, the insertion loss is to be 0 dB. The variation of amplitude in the passband is termed as ripple. The insertion loss changes from 0 dB in the passband to a large value in stopband. The sharpness of variation with respect to frequency is represented by roll off. In the filter, the number of elements indicate the order of the filter.

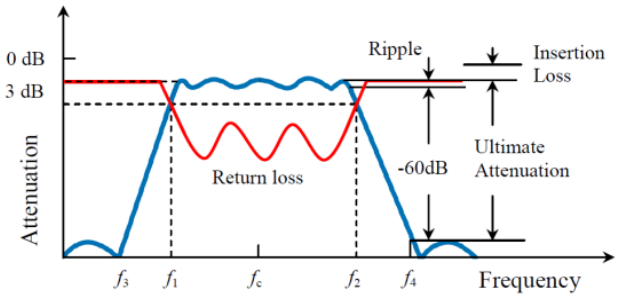

Fig 1.1 Typical bandpass filter response

Microwave and millimeter wave filters may be built from transmission lines like coaxial lines, waveguides and microstrip lines as distributed networks. The coaxial line has a very high bandwidth but is difficult to design for microwave components. Waveguide has the advantages of high power-handling capability and low loss but is bulky. Microstrip line is the planar transmission line technology suited for realizing elements with low characteristic impedance.

Microstrip filter design is based on a printed circuit board (PCB) and can be easily fabricated. Microstrip filter is the best choice as it is appropriate for monolithic and hybrid integrated circuit fabrication.

Filters can be designed using image impedance matching. The transition from passband to stopband is gradual which can be considered as one of the limitations in filter design. Filters can also be designed based on power insertion loss. The network parameters are designed based on the considered frequency response. The popular design methods are maximally flat response, Chebyshev response, elliptical response and Taylor's approximation response. Initially, LPF prototype is designed then scaled to the appropriate impedance level and cut off frequency to design any filter in insertion loss method. From the above methods, the elements of the network are obtained as lumped element values which are to be realised using transmission lines as distributed parameters at microwave and millimeter wave frequencies. Microwave elements are realised by distributed elements such as transmission lines which is done using transformations, such as Richard's transformation and the Kuroda identities. Microstrip filters can also be designed using parallel coupled lines, open loop resonators, coupled structures.

Microwave and millimeter wave frequency spectrum is divided in to different bands with specific range of frequencies. Microwave frequency bands and its applications are listed in Table 1.1. Many applications are also emerging using 5G technology. 5G communication frequency spectrum is classified in to two regions FR1 and FR2 as in Table1.2. Upper Microwave Flexible Use Service (UMFUS) applications are also emerging for mobile communications which are listed in Table 1.3.

Table 1.1 Microwave frequency bands and applications

Name	**Frequency range**	**Common applications**
UHF band	300 MHz – 3 GHz	Military applications, satellite television
L Band	1 to 2 GHz	Military telemetry, GPS, Air traffic control, Radar
S Band	2 to 4 GHz	Weather radar, Surface ship radar, WLAN, Wimax
C Band	4 to 8 GHz	WLAN, Wimax, Long distance radio telecommunications
X Band	8 to 12 GHz	Radar, Terrestrial broadband, Space Communications
Ku Band	12 to 18 GHz	Cable TV, Satellite Communications
K Band	18 to 26.5 GHz	Radar, Satellite Communications, Automotive Radar, Upper Microwave Flexible Use Services
Ka band (Millimeter wave)	26.5 to 40 GHz	Satellite Communications, Upper Microwave Flexible Use Services

Table 1.2 5G communication frequency spectrum

Name	Frequency range
Low band FR1 region	450 MHz – 1 GHz
Mid band FR1 region	1 GHz – 7 GHz
High band/ millimeter wave FR2 region	24 GHz – 52 GHz

Table 1.3 Frequency bands of Upper microwave flexible use services

Name	Frequency range (GHz)
24 GHz band	24.25 – 24.5, 24.75 – 25.25
28 GHz band	27.5 – 28.35
Lower 37 GHz band	37 - 37.6
Upper 37 GHz band	37.6 – 38.6
39 GHz band	38.6 – 40
47 GHz band	47.2 – 48.2

Bandpass filters are used in both transmitter and receiver modules of communication system at different stages. Filters are used to reduce harmonics generated in the amplifiers at the transmitter. At receivers, filters are used in optimizing signal-to-noise ratio and to improve the frequency selectivity. Filters realised with microstrip technology for different applications are discussed below. The receiver filter in mobile phone is shown in Fig 1.2.

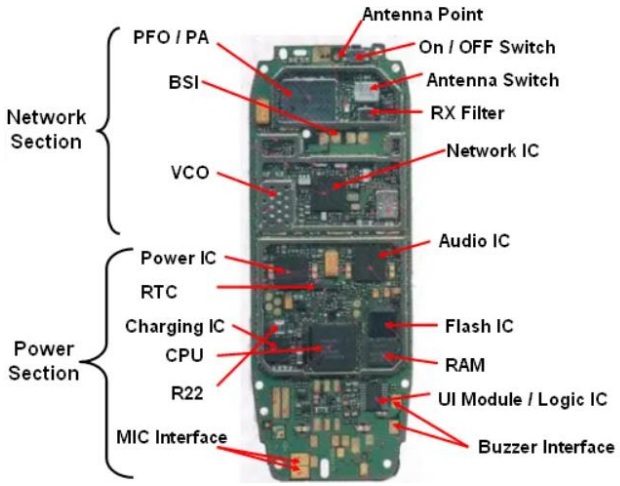

Fig 1.2 Receiver filter in mobile phone

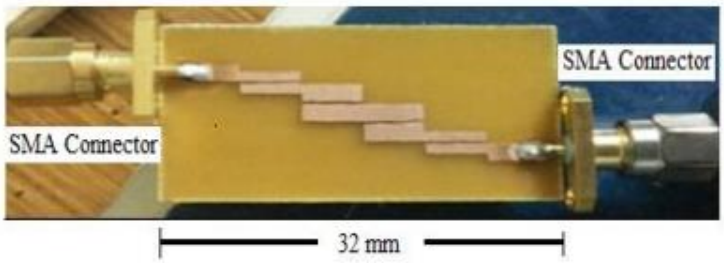

Fig 1.3 Microstrip parallel coupled bandpass filter for C band applications [2]

The microstrip parallel coupled filter shown in Fig 1.3 operating at 6 GHz with an insertion loss of 7 dB used for C band applications.

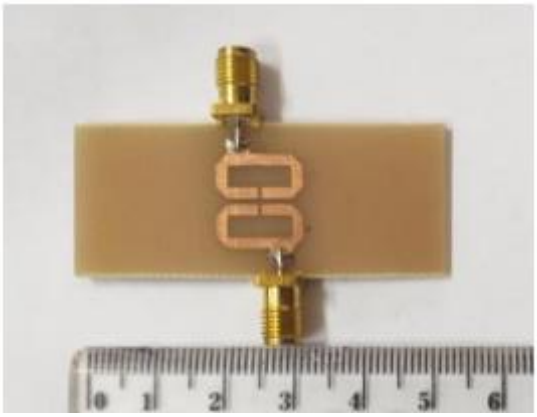

Fig 1.4 Microstrip bandpass filter using square open loop resonator [3]

Square open loop resonator bandpass filter shown in Fig 1.4 has center frequency at 3 GHz. The filter has insertion loss of 3.56 dB for S-band radar applications.

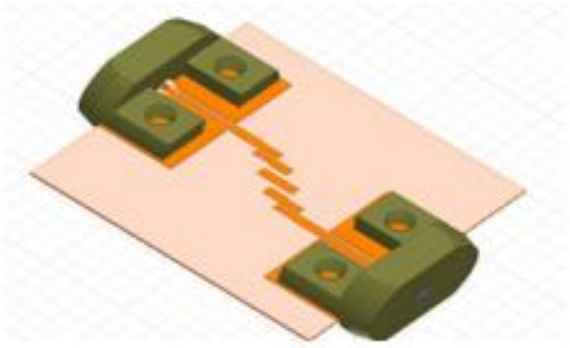

Fig 1.5 Microstrip parallel coupled bandpass filter for 5G applications [4]

The bandpass filter shown in Fig 1.5 has fractional bandwidth of 9.1 % at center frequency 36.51 GHz. The insertion loss of the filter is 3.37 dB used for 5G applications.

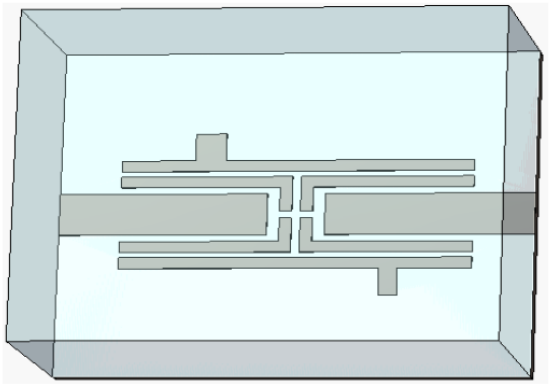

Fig 1.6 A dual bandpass filter using parallel coupled structure [5]

The dual bandpass filter using parallel coupled structure shown in Fig 1.6 resonates at 17 GHz and 35 GHz. The proposed filter has high insertion loss of 3 dB and 4 dB respectively for both bands for 5G applications.

Fig 1.7 Coaxial bandpass filter

The coaxial bandpass filter shown in Fig 1.7 has frequency range from 2.4 GHz – 2.5 GHz frequency with an insertion loss of 1.3 dB at 2.4 GHz.

Fig 1.8 Five resonator waveguide bandpass filter

The five-resonator waveguide bandpass filter shown in Fig 1.8 operates at 7.2 GHz frequency is useful for WLAN applications.

Fig 1.9 Communication between devices

Electronic gadgets like smart watch, mobile, laptop are portable devices. Portable devices should be compact. There is a need of designing compact components like filters, switches, amplifiers etc., for any electronic device to be compact.

1.2 Motivation

Microwave and millimeter wave bands are used for many applications which include GPS, WLAN, Wimax, radar, satellite communications and Upper microwave flexible-use services. Each application has its specific range of frequencies for communication. Filters are required at various stages in these applications and also microwave and millimeter wave communication systems, demands the need for filters with reduced dimensions and wide bandwidth. To have compact filters, filters can also be realised using resonators. There are many types of resonators such as cavity resonators, dielectric resonators, quartz crystal resonators, transmission line resonators and coupled resonators.

Compact filters can be realised using metamaterial resonators. Metamaterials of sub-wavelength dimensions such as split ring resonator (SRR) or complementary split ring resonator (CSRR) are also used for filter design. Size reduction is one of the main advantages of such resonators since the dimension of these resonators are much smaller than signal wavelength at resonance. Microstrip bandpass filter with metamaterial resonator is shown in Fig 1.10. Achieving wideband, compactness with low insertion loss within a single filter becomes challenging. Bandwidth enhancement can be obtained using fractals and complementary metamaterial resonators. Filters must have low insertion loss in passband and high attenuation in stopband.

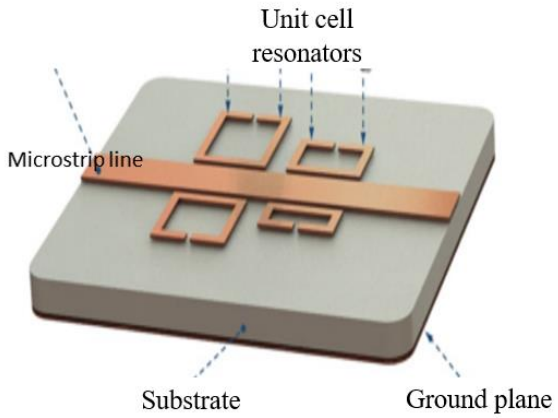

Fig 1.10 Microstrip bandpass filter using metamaterials

Microwave filters can be designed using coupled resonators. Power transferred along the transmission line is achieved by placing the resonators close to each other. In many applications, multiband filters are in great demand due to their advantages which are to be explored at microwave and millimeter wave frequencies. Multiple frequencies can be allowed or rejected using multiband filters. These filters can optimize space, improve system design and performance. The design of such filters with optimal characteristics is difficult to obtain. Hence a combination of different techniques must be applied for the realization of compact multi-band filters. Metamaterial microstrip planar technology enhance the functionality of the miniature filter which is helpful for a variety of applications.

1.3 Methodology

In the present thesis work, an attempt is made to design compact filters with microstrip technology for bandpass and bandstop responses. Broadly, microstrip filters are realised by using metamaterial unit cells or complementary metamaterial unit cells. Further, compact wide band bandpass filter is realised by employing fractals on the metamaterials. Compactness and multibands can be obtained by introducing stubs to the microstrip line in addition to metamaterials. Bandstop filters are designed with complementary split ring resonators in the ground plane to produce stop bands. Complementary split ring resonators are also used for coupling across the gaps along the microstrip line to realise a bandpass filter. Multi band BPFs are obtained combing the metamaterials and complementary metamaterials. Microstrip coupled resonators are also used for design of single and multiband BPF.

The methodology followed for the design of filters is illustrated below:

Initially, the frequency of operation for the filter is identified. Microstrip line is designed based on the permittivity of the substrate material to match with 50Ω impedance feed line. The length and width of the microstrip line are calculated based on the design expressions.

Resonators are chosen with dimensions related to the operating frequencies. Vias, gaps and stubs with optimum dimensions are used to improve the performance of the filter. Filters are designed using Ansys HFSS software. Equivalent circuits are drawn based on the HFSS frequency response of filter and the response of the circuit is simulated using an AWR software. The designed filters are fabricated and scattering parameters are measured using a vector network analyser. The S-parameters (S_{11}, S_{21}) from simulation and measurements are plotted. The passband bandwidth is determined when S_{11} is less than -10 dB and stopband bandwidth is determined when S_{21} is less than -10 dB.

1.4 Research Objective

- To design, simulate and fabricate compact, wide bandpass filters, bandstop filters and multi-bandpass filters for microwave and millimeter wave applications.
- To improve the bandwidth of the filter by applying fractals on the metamaterial resonators.
- To reduce the size of the filter using complementary metamaterial resonators, microstrip coupled resonators.
- To design compact multi-bandpass filters using a combination of metamaterial resonators and complementary metamaterial resonators.
- To enhance the performance of the filter like return loss, insertion loss and stopband attenuation.
- To design compact wide bandpass filters/bandstop filters and multiband pass filters while getting above performance characteristics.
- To validate the above filter designs experimentally and compare them with simulation results.

1.5 Contributions of research work

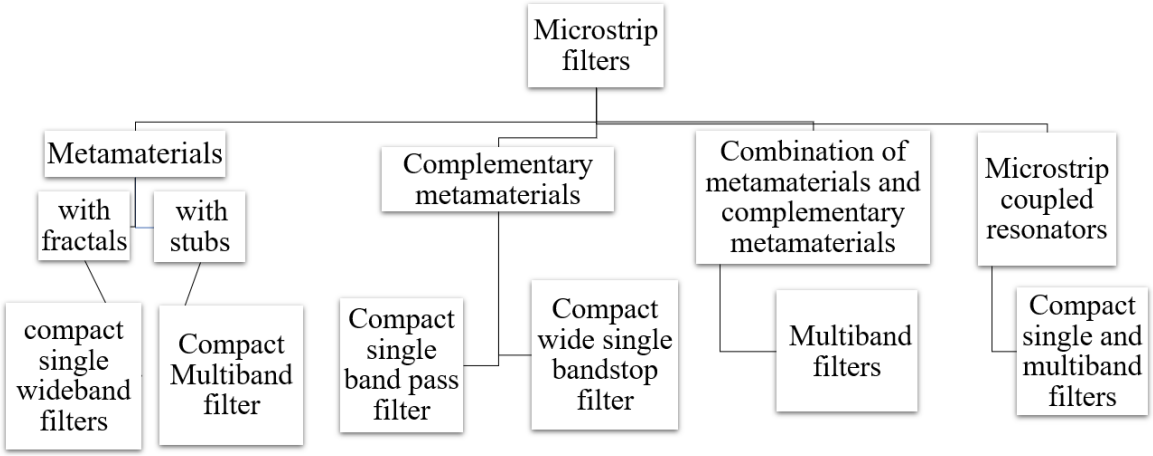

Fig 1.11 Contributions of research work

The key contributions are as shown in Fig 1.11 and summarized as follows:

(1) A bandpass filter designed on RT Duroid 3010 substrate material with 0.13mm thickness using symmetrical ring resonators and vias has frequency range from 5.47 GHz - 6 GHz with an insertion loss of 1.2 dB. The fractional bandwidth is 9.8%. The size of the filter is 0.64 λ_g^2 and is useful for C band applications.

(2) A bandpass filter is designed by applying moore fractal on the boundary of symmetrical ring resonators. The pass band frequency range varies from 6.95 GHz - 7.8 GHz with fractional bandwidth of 11.5%. The realized insertion loss is 0.4 dB. The proposed filter is realized for C band applications has size of 0.75 λ_g^2.

(3) A bandpass filter designed by loading symmetrical ring resonators on either side of the transmission line and vias are placed along the transmission line on RT Duroid 3010 substrate material with 1.28mm thickness operates in the X-band between 10 GHz - 11.8 GHz. The fractional bandwidth of the filter is 19.3%. The insertion loss and return loss obtained are less than 0.6 dB and 13 dB respectively. The area occupied by the filter is 2.8 λ_g^2.

(4) EI shaped unit cell based bandpass filter is designed for higher 5G communications. The passband frequency range is from 39.7 GHz to 40.7 GHz with fractional bandwidth of 2%. The realized insertion loss is 2.5 dB with filter area of 7 λ_g^2.

(5) EIE shaped metamaterial resonators and slotted stubs are used to design a triple bandpass filter used for fixed/mobile satellite communications has central frequencies at 7.29 GHz, 10.67 GHz and 13 GHz with fractional bandwidth of 5.4%, 2.5% and 4.58% respectively. The obtained insertion loss is 1.2 dB, 1 dB and 1.4 dB. The area of the filter is 0.32 λ_g^2.

(6) A bandpass filter is designed using complementary triple concentric split ring resonators. The frequency range of the filter is 2.85 GHz-3.15 GHz with an insertion loss of 1.5 dB. The fractional bandwidth of the filter is 3%. The filter size is 0.13 λ_g^2 useful for S band applications.

(7) A Ku band bandstop filter is designed using complementary symmetrical ring resonators has stopband frequency range from 12.1 GHz – 13.7 GHz with fractional bandwidth of 11.9 %. The obtained maximum stop band attenuation of 31 dB. The occupied area of the filter is 0.55 λ_g^2.

(8) A quintband bandpass filter is designed for higher 5G communications using EI shaped unit cell, complementary symmetrical ring resonators has passband frequency ranges from 38.65-38.85 GHz, 39.06-39.1 GHz, 39.9-40.28 GHz,41.96-42.06 GHz and 42.87-42.97 GHz. The insertion loss obtained is 1.67 dB, 2 dB, 1.54 dB, 2.45 dB and 2 dB with fractional bandwidth of 0.5%, 0.1%, 0.94%, 0.23%, 0.23% respectively. The size of the filter is 7 λ_g^2.

(9) A dual bandpass filter is designed using complementary triple concentric split ring resonators, spiral resonators have fractional bandwidth of 7.5% and 4.85 % at center frequencies 1.32 GHz and 2.47 GHz with an insertion loss of 1.3 dB and 1.8 dB respectively. The filter size is 0.039 λ_g^2. The dual band filter is useful for GPS, WLAN applications.

(10) A triple band bandpass filter is designed using complementary triple concentric split ring resonators, spiral resonators, stepped impedance resonators, stubs have fractional bandwidth of 1.16%, 11.4% and 1.86% at center frequencies 1.29 GHz, 2.27 GHz and 3.21 GHz respectively. The attained insertion loss is 1.6 dB, 1.3 dB and 1.8 dB. The area of the filter is 0.06 λ_g^2. This triband filter is useful for GPS, WLAN and Wimax applications.

(11) A dual bandpass filter is designed by coupling the dual split rings resonators directly to the microstrip line has center frequencies at 24.79 GHz and 28.37 GHz with an insertion loss of less than 4.2 dB and less than 4.2 dB. The fractional bandwidth obtained is 8.8% and 2.2% for both bands respectively. The size of the dual bandpass filter useful for upper microwave flexible use services is 0.1 λ_g^2.

(12) A bandpass filter is designed using EC shaped coupled lines coupled to the microstrip transmission line has pass band frequency range from 37 GHz - 39 GHz with fractional bandwidth of 5.26%. The realized insertion loss is 0.4 dB. The filter size is 0.96 λ_g^2. The proposed filter is useful for 37 GHz band 5G communications.

1.6 Chapter Organization

Chapter1 Introduction

This chapter gives a brief idea on the significance of the filters. The performance parameters and applications are explained. Different design methodologies to design filters are discussed. The motivation and methodology to design the filter is explained. Research objectives and contributions of work are discussed. The thesis organization is elaborated.

Chapter 2 Review of Literature

In this chapter, the concepts of microstrip lines, metamaterials, split ring resonators, thin wires are explained. Literature on different methods of designing microstrip filters are reported.

Chapter 3 Bandpass filters with single and multiple passbands using metamaterials

This chapter explains the design of a metamaterial based bandpass filter. The performance of the filter can be enhanced by using fractal structures and slotted stubs. The bandwidth of the filter is improved by applying the moore fractal on the boundary of the metamaterial structure. The return loss and stopband attenuation are improved by using slotted stubs. An equivalent circuit for a symmetrical ring resonator bandpass filter is discussed.

Chapter 4 Bandpass and Bandstop filter using complementary metamaterials

This chapter discusses the design of a compact bandpass filter using a complementary triple split ring resonator structure, gaps are introduced on the microstrip line and vias are placed to connect the patch and ground structure to improve the performance of the filter. A Compact and wideband bandstop filter design is explained using a complementary symmetrical ring resonator and its equivalent circuit is explained.

Chapter 5 Multi-bandpass filters using a combination of metamaterials and complementary metamaterials

This chapter explains the design of multi-bandpass filters. Initially, the quint bandpass filter using EI-shaped metamaterial resonators and complementary split ring resonators is discussed. A dual bandpass filter design using spiral resonators and complementary triple concentric split ring resonators are elaborated. A triple bandpass filter design using stepped impedance resonators, spiral resonators and complementary triple concentric split ring resonators is presented.

Chapter 6 Bandpass filters using Microstrip coupled resonators

This chapter discusses the design of a compact dual bandpass filter using dual split ring resonators directly coupled to the microstrip line. An equivalent circuit is proposed for the dual bandpass filter. A single bandpass filter using EC-shaped coupled lines with proximity coupling is explained.

Chapter 7 Conclusion and Future scope

The outcomes of the proposed filter in the thesis work are compared with appropriate conclusions and future scope is discussed.

1.7 Conclusion

Filters play a major role in any communication system. The performance parameters and methods to design filters are reported. The motivation to design metamaterial microstrip filters is elaborated. Methodology used to design microstrip filters is explained. Research objectives to design compact, wide band microstrip filters are framed. The contributions of research work are discussed. Chapters are organized for the achievement of the research objectives.

Chapter 2

Review of Literature

2.1 Introduction

Filters with microstrip technology have become popular due to low profile, compact structure and easy integration with other circuits. Microwave and millimeter wave filters can be designed using the microstrip technology due to its advantages. The geometry and design expressions for microstrip line are explained. The significance of metamaterials, split ring resonators and thin wires in filter design are elaborated. The literature published on microstrip filters are discussed.

2.2 Microstrip line

Microstrip line consists of a ground plane and conducting strip of width 'W' separated by a dielectric substrate of dielectric constant 'ε_r' and thickness 'h'. Usually, the thickness is considered very much less than operating wavelength ($h<<\lambda$). The structure of the microstrip line is depicted in Figure 2.1. The distribution of electric and magnetic field lines is shown in Figure 2.2.

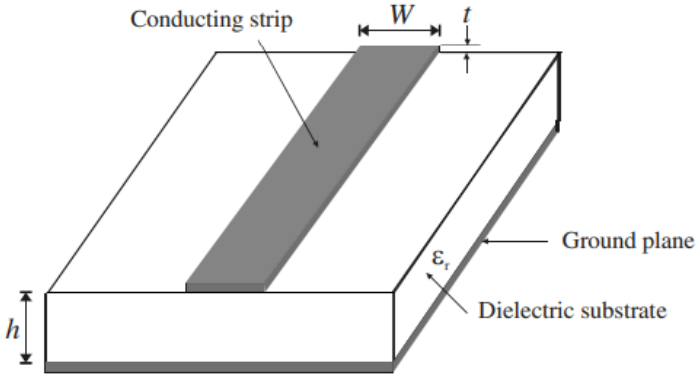

Fig 2.1 Geometry of microstrip line

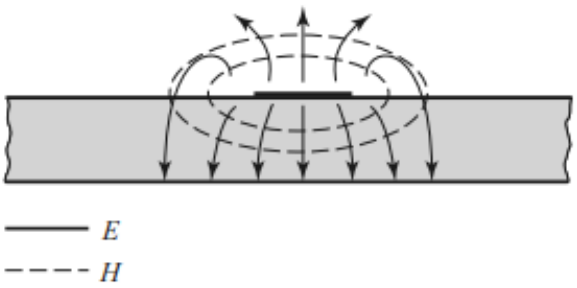

Fig 2.2 Electric and magnetic fields of a microstrip line

While the transmission of the signal takes place along the microstrip line, the fields due to current travel through the dielectric and also free space. So, the wave propagation is quasi-TEM mode instead of TEM mode. When the longitudinal components are much smaller than the transverse components, a quasi-TEM mode is applicable to facilitate the design. The phase velocity, propagation constant and characteristic impedance approximations can be obtained from static, or quasi-static solutions. The phase velocity and propagation constant can be expressed as

$$v_p = \frac{c}{\sqrt{\varepsilon_e}} \qquad (2.1)$$

$$\beta = k_0\sqrt{\varepsilon_e} \qquad (2.2)$$

where ε_e is the effective dielectric constant of the microstrip line. Because some of the field lines are in the dielectric region and some are in the air, the effective dielectric constant satisfies the relation and depends on dielectric constant and thickness of the substrate and width of microstrip line.

$$1 < \varepsilon_e < \varepsilon_r \qquad (2.3)$$

The effective dielectric constant of a microstrip line is given approximately by

$$\varepsilon_e = \frac{\varepsilon_r + 1}{2} + \frac{\varepsilon_r - 1}{2\sqrt{1 + 12h/W}} \qquad (2.4)$$

The characteristic impedance of the line depends on the width of the top conductor, effective dielectric constant and height of the substrate. The characteristic impedance of microstrip line are given below.

$$Z_0 = \frac{60}{\sqrt{\varepsilon_e}} \ln\left(\frac{8h}{W} + \frac{W}{4h}\right) \quad \text{for } \frac{W}{h} \leq 1 \tag{2.5}$$

$$Z_0 = \frac{120\pi}{\sqrt{\varepsilon_e}\left(\frac{W}{h} + 1.393 + 0.667\ln\left(\frac{W}{h} + 1.444\right)\right)} \quad \text{for} \frac{W}{h} \geq 1 \tag{2.6}$$

2.3 Metamaterials

Metamaterials are described as engineered periodic materials for altering electromagnetic properties to obtain responses that are not observed naturally. The word metamaterial is a combination of "meta" and "material". Meta is a greek word that means something beyond, altered, changed. Metamaterial can be engineered by changing its dimensions rather than the material with which it is composed of. Metamaterials control the electromagnetic properties of microwave devices such as filters, antennas, couplers, power dividers, etc., to design compact devices with better performance characteristics.

The metamaterial structures can be designed to have either negative permittivity using metallic thin wires or negative permeability using metallic ring resonators. A single metamaterial resonator is called as unit cell. The dimensions of the unit cell should be much smaller than the guided wavelength dimensions. For effective homogeneity, structural average cell size P is much smaller than the guided wavelength λ_g [6].

$$P \leq \frac{\lambda_g}{4} \tag{2.7}$$

These unit cells are the building blocks for creating metamaterial periodic surface to enhance performance parameters of the device.

2.3.1 Thin wires

To introduce negative permittivity in a medium, thin wires are introduced in a dielectric medium as shown in Fig 2.3. A lattice of conducting wires with small radii ‘r’ compared to the lattice periods ‘a’ and guided wavelength λ_g can exhibit negative permittivity. By adjusting the spacing and size of the elements in metallic thin wire arrays, a material’s electric permittivity can be varied.

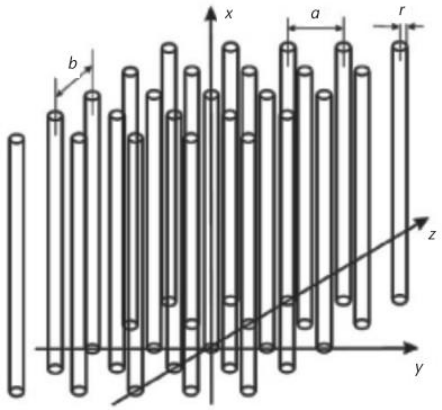

Fig 2.3 Lattice of parallel conducting thin wires [7]

In the proposed work, the thin metallic wires are placed by creating metallic vias from patch to ground along the microstrip line.

2.3.2 Split ring resonator (SRR)

Split ring resonator consists of a closed conducting loops with gaps in between which are called as splits. There can be one or more concentric loops called as rings. When magnetic field incidents on the rings, current is induced in the rings and an electric field developed across the gaps. The spacing between the gaps with induced opposite charges give the effect of capacitance. The dimensions of the gaps decide the capacitance which in turn controls the resonant frequency. The length in the conducting path or loop determines the inductance which in turn effects the resonant frequency. To use the resonators at microwave frequencies, the dimensions of the resonator must be very much less than wavelength as a result the resonators are called as sub wavelength resonators.

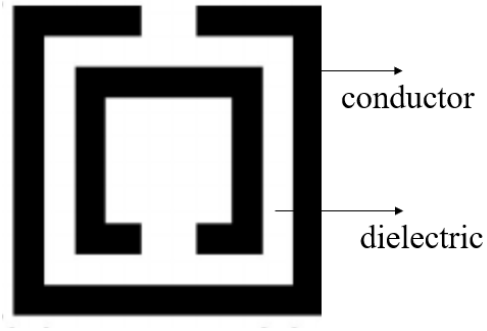

Fig 2.4 Split ring resonator

By combination of thin wires and SRRs both permittivity and permeability can be made negative at same frequency to get double negative properties.

2.4 Literature review

Microstrip filter design with small size, wide bandwidth and low insertion loss is an interesting and challenging research area because insertion loss of the filter is inversely related to bandwidth, directly related to the size of the filter. Different techniques are used in various literature to design filters with small sizes but with narrow bands and high insertion loss, wide bandwidth with low insertion loss and wide bandwidth with large sizes.

Numerous papers are published to reduce the size of the microstrip filters at microwave and millimeter wave frequencies. One such technique is using metamaterials. Metamaterial structures loaded on either side of the planar transmission line is one approach to designing bandpass filters. M. Gil (2008) et al. presented a review of the compact metamaterial filter design approach [8]. R. Bojanic (2014) et al. studied the orientation of metamaterials placed near the microstrip lines and their performance and explained their equivalent circuits [9]. Mohammad Syahral (2016) et al. investigated the effect of several SRR elements on its BPF characteristics resulting in sharp selectivity with an increase in the number of resonators at the cost of high insertion loss [10]. J. Bonache (2005) et al. proposed a left-handed microstrip line with periodic loaded SRRs and metallic vias. The proposed bandpass filter resulted in a frequency range from 2.99 GHz - 3.11 GHz with fractional bandwidth of 4% and an insertion loss of 3.54 dB. The proposed filter has narrow bandwidth and high insertion loss [11]. J. D. Baena (2005) et al. studied the electromagnetic behaviour of split ring and complementary split ring structures, as well as their coupling to the coplanar waveguide transmission line. A bandpass filter designed using SRRs resulted in a passband frequency range from 7.8 GHz - 8.2 GHz. The attained fractional bandwidth is 5% and maximum insertion loss is 4 dB, a bandpass filter using complementary SRRs has frequency range from 3.2 GHz - 3.8 GHz, fractional bandwidth of 17%, insertion loss less than 4dB [12]. Shikhar Chandra (2021) designed a bandpass filter composed of split ring resonators and complementary split ring resonators (CSRR). The filter's frequency range is 8.98 GHz- 9.278 GHz with fractional bandwidth of 3.11%, insertion loss and return loss are 0.005 dB and 37.29 dB respectively, but the filter has less fractional bandwidth [13]. But the narrow bandwidth is not sufficient for some applications.

Bandwidth improvement can be obtained using fractal structures and complementary metamaterials. Fractal structures are implemented in many published works resulting in a wide bandwidth. D. Oloumi (2009) et al. designed and fabricated a novel waveguide filter with Koch geometry as a periodic structure results in fractional bandwidth of 8.6% with a compact size [14]. Rana Sadaf Anwar (2019) et al. implemented minkowski fractal islands on a three-layer frequency selective surface to reduce the size and improve bandwidth using a novel approach

resulting in fractional bandwidth of 87.4% [15]. He-Xiu Xu (2012) et al. investigated single negative metamaterial transmission lines consisting of a host transmission line in the conductor strip and a moore and Hilbert fractal-shaped complementary ring resonator etched in the ground plane. The proposed filter has fractional bandwidth of 32% at resonant frequency of 3.5 GHz, insertion loss less than 1 dB and return loss of 30 dB. The application of fractals improves bandwidth compared to a conventional design by 30.2% for the first iteration and 47.7 % for the second iteration [16].

Wide bandpass filters can be designed using complementary metamaterial structures. Mahmoud Abu Hussain (2020) et al. presented double symmetric unit cells with electric coupling between CSRRs which has resonating frequency at 10 GHz to design a bandpass filter. The fractional bandwidth of the filter is 15%, but the filter is large [17]. Badr Nasiri (2020) et al. designed a bandpass filter using low-impedance feed lines and CSRR structures. The designed filter operates at 4 GHz with fractional bandwidth of 62%, but the filter is large [18]. Kada becharaf (2020) et al. published an article to design a wide bandpass filter using circular complementary split ring resonators. The proposed filters operate with a center frequency of around 6.8 GHz, with a bandwidth of 3.4 GHz – 9.3 GHz, a return loss greater than 17 dB, minimum insertion loss of 2 dB. The proposed filter has high insertion loss [19]. Rasool Keshavarz (2020) et al. introduced a four-turn complementary spiral resonator to design a miniaturized bandpass filter. The fractional bandwidth of the proposed filter is 8.2% at a center frequency of 0.73 GHz [20].

S. Moitra (2019) et al. proposed a substrate-integrated waveguide bandpass filter using circular CSRR structures. The designed bandpass filter has fractional bandwidth of 24.2% at center frequency 10 GHz, maximum insertion loss is 3.05 dB [21]. W. Yuan (2019) et al. proposed a bandpass filter using CSRR-defected ground structures (DGS), dumbbell-shaped DGS structures, interdigital coupling structures, open stubs and short stubs resulting in fractional bandwidth of 63% at a resonant frequency of 5.5 GHz. The insertion loss obtained is greater than 1 dB [22]. Y. Cheng (2015) et al. presented a dual-mode bandpass filter using CSRR split as a square patch resonator. The designed filter resonates at 3.42 GHz with fractional bandwidth of 3.5%. The insertion loss obtained is less than 1 dB [23]. Yan Zheng (2020) et al. proposed a four-stage bandpass filter using substrate-integrated waveguide cavities with complementary split ring resonators. The proposed design has a frequency range from 9.4 GHz – 10.6 GHz with fractional bandwidth of 12%. The insertion loss of 1.59 dB [24].

Bandstop filters can be designed using resonant metamaterial structures and complementary resonant structures. Mustafa K. Taher Al-Nuaimi (2010) et al. used sub-wavelength split ring

resonators and complementary split ring resonators (CSRRs) to design compact microstrip bandstop filters. A sharp bandstop is achieved at 5.41 GHz with 50 dB stopband attenuation using split ring resonators. But with complementary metamaterial resonators, a rejection of 50 dB is attained around 4 GHz – 5.8 GHz with sharp cut-offs. Complementary metamaterial structures result in wide bands and are compact using same structures [25]. Badr Nasiri (2018) et al. proposed microstrip band-stop filter using complementary split ring resonator attached to the microstrip feed line. The proposed structure results in a rejection bandwidth of 1.2 GHz – 2 GHZ with FBW of 50% with 30 dB attenuation [26].

Multi-bandpass filters are playing a significant role nowadays to meet the increasing demands of satellite and modern communication systems. Bukola Ajewole (2022) et al. proposed an I-shape design with three SSRRs on the outmost part that are etched onto the FR-4 dielectric substrate material to design multi-bandpass filter results in high insertion loss, large size due to usage of array structure [27]. Manoj Prabhakar Mohan (2018) et al. designed a triple band filter based on double periodic CRLH structure resulting in insertion loss of 3.06 dB, 2.71 dB and 3.16 dB at resonant frequencies 3.3 GHz, 6 GHz and 9 GHz, respectively. The fractional bandwidths are 3 %, 4.7 % and 3.5 %, respectively for all three bands, but the filter is large [28].

Another approach to designing compact bandpass filters is by using microstrip coupled metamaterial resonators. Ria Lovina Defitri (2016) et al. proposed an SRR structure circle-shaped coupled to a microstrip line to obtain a compact size narrow bandpass filter for X-band applications at an operating frequency of 9 GHz. The fractional bandwidth obtained is 2.3%. The insertion loss is 2.242 dB. The proposed filter is large [29]. Ahmed A. Ibrahim (2018) et al. presented second and third-order microstrip coupled SRR resonators using optimization techniques. The obtained fractional bandwidth is 13% at the center frequency 2.3 GHz and the insertion loss attained is 0.7 dB. The size of the filter is large [30]. D. Bukuru (2017) et al. proposed a compact quad bandpass filter by using two coupled half-wavelength quad mode stepped impedance resonators and two open-loop stepped impedance resonators. The proposed filter has fractional bandwidth of 3 %, 6.41 %, 3.7 % and 4.56 % at center frequencies 2.4 GHz, 3.3 GHz, 5.38 GHz, 6.48 GHz respectively, but the filter has high insertion loss of 1.9 dB, 1.6 dB, 3.5 dB, 3.2 dB [31].

In the published literature narrow bandwidth is obtained using sub-wavelength split ring resonator structures. Wide bandwidth is obtained using fractal structures, but with large size. Compactness and wide bandwidth are the basic requirement for communication systems. These can be achieved by applying fractals on the sub-wavelength resonant structures. For the first

time symmetrical ring resonators are loaded on either side of transmission lines to design wide bandpass filters for mid-band 5G applications. Moore fractal is applied to the symmetrical ring resonator metamaterial structures providing the advantage of getting wide bandwidth with compact size for C band applications.

Compactness and wide stop band can be obtained using complementary metamaterial structures for Ku band applications. The multi-bandpass filter is designed using metamaterial and slotted stubs for fixed/ mobile satellite services. Multi-bandpass filters are designed using metamaterial spiral resonators, complementary SRRs, stubs and stepped impedance resonators for GPS, WLAN and Wi-Fi applications. Microstrip coupled metamaterial resonators are used to design compact dual bandpass filters. For the first time compact dual bandpass filter is designed using microstrip technology useful for Upper Microwave Flexible Use services.

2.5 Conclusion

Microstrip technology is vital for filter design at microwave and millimeter wave frequencies. The literature survey for compact designs and improvement of bandwidth is studied. From the literature survey, it is obvious that the compact wideband filter design is a well-researched topic. However, there is still more research must be done to design simple single and multiple wide bandpass/bandstop filters with small sizes and low insertion loss. So, this thesis presents a simple, compact, wideband microstrip filter design.

Chapter 3

Bandpass filters with single and multiple pass bands using metamaterials

3.1 Introduction

In microwave and millimeter wave applications, bandpass filters are used to select the desired frequency range for efficient use of spectrum. Weather radar systems, terrestrial microwave links, 802.11 a version of Wi-Fi devices are some of the applications in C-band frequency range which lies from 4 GHz to 8 GHz. Remote sensing satellites, fixed and mobile satellites for communications, meteorological satellites for weather monitoring applications are in X band from 8 GHz to 12 GHz frequency range. Ku band frequency range is used for fixed satellite broadcast services, aviation and cable TV relay. Fixed satellite services fixed wireless access applications comes under Upper Microwave Flexible Use Services. All the above-mentioned applications need bandpass filters at many stages of the transmitter and receiver.

Compact, wide bandpass filters operating in microwave and millimeter wave frequencies are in demand for many communication systems. Several techniques are reported in the literature for realising microstrip bandpass filters. Researchers have reported design of bandpass filters using concepts of substrate-integrated waveguide techniques, stubs, open loop uniform impedance resonators and coupled resonators along the transmission line.

Qing Liu (2016) et al. presented elliptic single cavity and dual cavity bandpass filters based on dual mode resonators. A non-degenerate dual mode resonator is developed from circular substrate integrated waveguide cavity. Single cavity bandpass filter has fractional bandwidth of 7.6% at 5.21 GHz center frequency with minimum insertion loss of 0.87 dB. But, the size of the single cavity filter is large. Dual cavity bandpass filter has fractional bandwidth of 9.57% at 5.22 GHz center frequency. The obtained insertion loss is 1.62 dB. But, the dual cavity filter has high insertion loss and also large in size [32].

M. Amirian (2019) et al. proposed a microstrip bandpass filter using a transmission line with two identical open-ended stubs on both sides. The passband frequency range of the filter is 1.68 GHz-1.82 GHz with fractional bandwidth of 8%. The insertion loss of the designed filter is 4 dB and return loss is 23 dB. But, the insertion loss of the filter is high [33].

Wenjie Feng (2020) et al. investigated a bandpass filter using intercoupled short and open-ended resonators which interact through adjacent coupling. The bandpass filter frequency range is 1.79 GHz – 2.2 GHz with a fractional bandwidth of 8.5% at 2 GHz resonant frequency. An insertion loss of 1.43 dB is obtained, but the filter has high insertion loss and the structure of the filter is complex [34].

Min-hang weng (2020) et al. proposed a triple bandpass filter using two pairs of open loop uniform impedance resonators. Three passbands are obtained for the filter by selecting the lengths of two pairs of resonators. The bandpass filter operates at 1.93 GHz, 2.6 GHz and 3.9 GHz with fractional bandwidth of 5%, 11%, 3% respectively. The obtained insertion loss is 1.5 dB, 0.6 dB and 1.83 dB respectively for the above mentioned three bands. But the size of the filter is large [35].

Muhib Ur Rahman (2017) et al. presented a triband bandpass filter using two stub-loaded dual-mode resonators and coupled resonators. The fractional bandwidths of the filter are 12.6 %, 6.25 % and 14.49% at 1.575 GHz, 2.4 GHz and 3.45 GHz center frequencies, respectively. The measured insertion loss is 0.7 dB, 1.14 dB and 0.3 dB, but the size of the filter is large [36].

W. Wang (2005) et al. investigated different metamaterial structures such as split ring, symmetrical ring, omega and S shaped resonators. In the presented structures, symmetrical ring resonators have 12% fractional bandwidth which is large when compared with other structures [37].

Y.S. Mezaal (2015) et al. presented a microstrip bandpass filter using dual edge coupled resonators designed in the form of moore fractal geometries up to third order iteration. Both the second and third iteration levels resonates at a center frequency of 2.4 GHz with insertion loss less than 0.2 dB. The size of the filter is 0.026 λ_g^2 and 0.015 λ_g^2 for second and third iterations, respectively. Size reduction of 43% is observed from second iteration to third iteration [38]. From the literature it is observed that the reported filters have wide bandwidth but have high insertion loss.

Published metamaterial bandpass filters have narrow band and high insertion loss [7,8]. To obtain compact filters the number of resonators should be kept minimum. Fractal structures can be applied to filters to get wide bandwidth. Insertion loss can also be reduced by decreasing the

number of resonators in the design. By combining all the above techniques compact, wideband, low insertion loss bandpass filters can be designed.

In the proposed chapter, symmetrical ring metamaterial resonator and moore fractal structures are used for the bandpass filter design in the C and X bands. An EI shaped resonator is used to design bandpass filter for upper microwave flexible use services applications. Slotted stubs are implemented in between EIE shaped resonators to design triple bandpass filters which lies in C, X and Ku bands.

Metamaterial structures varies permittivity and permeability of the medium. The possible structures which cause these effects are symmetrical ring resonators and vias which are discussed below. Further, structure modifications of the resonator with fractals are also discussed.

3.2 Symmetrical ring resonator

Symmetrical ring resonator structure is novel example of metamaterial resonators as shown in Fig 3.1. Symmetrical ring resonator is a metallic ring that has been split symmetrically and two rings are placed adjacent to each other. This structure can concentrate the energy of the coupled field between adjacent arms of the rings. As there is a less fringing effect with this structure, it tends to yield accurate response [37].

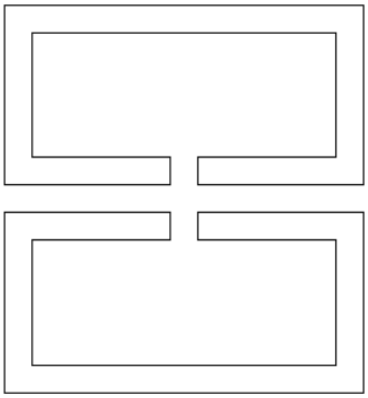

Fig 3.1 Symmetrical ring resonator

3.3 Metallic vias

Metallic vias are used to connect the transmission line to the ground plane as shown in Fig 3.2. Vias provide resistance and capacitance. These vias produce a negative dielectric constant

that can be used to control wave propagation along the transmission line. To control pass and stop bands, the spacing ‘s’ and diameter ‘d’ of vias are changed.

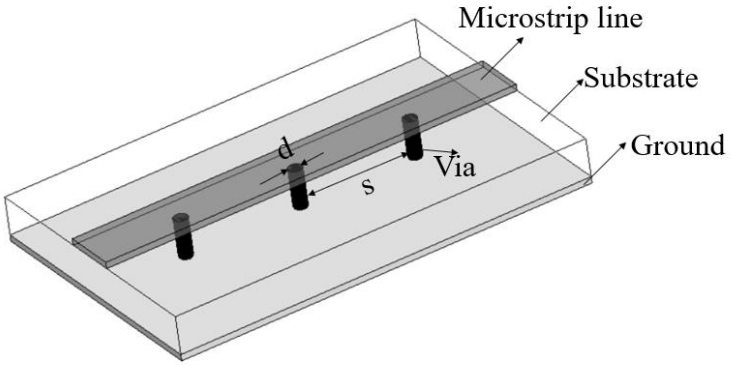

Fig 3.2 Metallic via

3.4 Fractals

Benoit Mandelbrot derived the term fractal from the Latin word ‘fractus’ means fragmented or broken. Fractal is geometric shape in which each side is repeated statistically along the structure which has the property of self-similarity.

3.4.1 Moore fractal

The Moore curve, which is similar to the Hilbert curve, is a continuous fractal space-filling curve. It is a loop version of the Hilbert curve with a unique recursive process that makes the moore curve's ends converge. Hilbert and moore fractal curves for second, third and fourth iterations are shown in Fig 3.3 and Fig 3.4, respectively.

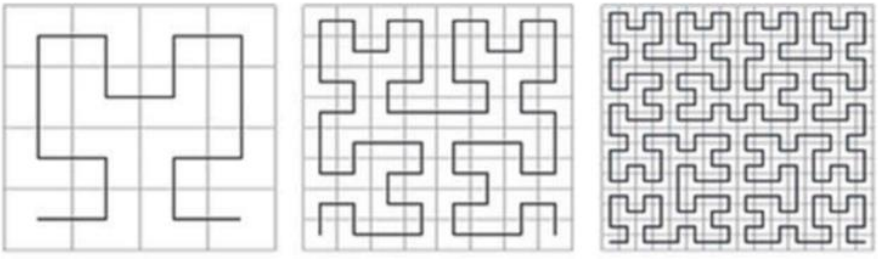

Fig 3.3 Hilbert fractal curve

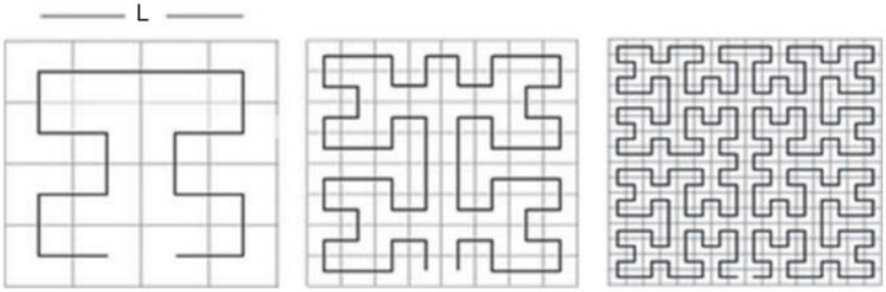

Fig 3.4 Moore fractal curve

3.5 Stubs

A stub is a length of microstrip line that is connected to the line as shown in Fig 3.5.a & Fig 3.5.b. The stub connected to the microstrip line can be left open or shorted to the ground using via. As a result, standing waves are formed on the stub. The length of the stub determines the impedance offered on the line at the location of stub. The impedance offered can be either a capacitive, inductive, open circuit or short circuit. A quarter wavelength of the stub is used for impedance transformation. Stubs are employed on the transmission line for impedance matching. Stubs can also be used as series or shunt resonant circuits.

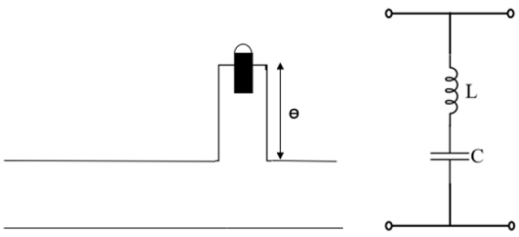

Fig 3.5 Short circuit stub, its equivalent circuit

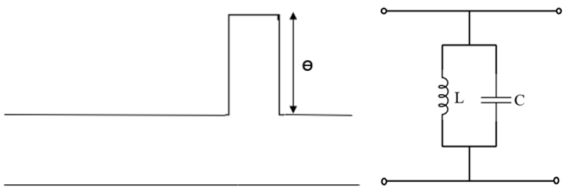

Fig 3.6 Open circuit stub, its equivalent circuit

3.6 Metamaterial filters

The combination of split ring resonators and vias are incorporated along the microstrip line to control the wave propagation along the transmission line. Microstrip line acts as all pass

filter. To obtain bandpass filter, frequencies above and below the passband have to be stopped. A significant portion of electric flux lines are induced between microstrip line and ground when vias are connected through the substrate along the microstrip line. This electric field produces a negative-ε effect over a band of frequency which introduce stop bands. Split ring resonators are placed on either side of the microstrip line to have better coupling between the microstrip line and split ring resonators. A significant portion of the magnetic field lines is expected to cut the split ring resonators. This magnetic field gives rise to a negative-μ effect over a band of frequencies which stops signal propagation. Thus, over a band of frequencies when negative μ and ε occurs, signal propagation happens along the line.

3.7. Design of bandpass filter using symmetrical ring resonator for C-band applications

Bandpass filters with wide bandwidth using symmetrical ring resonators and vias along microstrip line is proposed to lie in the frequency range of C-band. The specifications of the filter are given in Table 3.1. The center frequency of the bandpass filter is selected as 5.75 GHz. A conventional high-frequency material, RT Duroid 3010 substrate is selected for the design. The dimensions of the microstrip line used in the bandpass filter is realised using equations [2.4-2.6] for 50 Ω feed impedance. The width of the microstrip line is obtained as 2.11 mm.

Table 3.1. Design specifications of symmetrical ring resonator BPF

Parameter	Value
Frequency band of operation	C-band
Bandwidth	0.53 GHz
Center frequency	5.75 GHz
Feed impedance	50 Ω
Substrate material	RT Duroid 3010
Dielectric constant	10.2
Substrate thickness	0.13mm
Copper laminate thickness	35 μm
Order of the filter	1 and 2
Insertion loss	1.2 dB
Return loss	29 dB
Q-factor	10.9

The unit cell of the symmetrical ring resonator is taken to satisfy the homogeneity condition i.e, larger dimension of the unit cell is less than or equal to $\lambda_g/4$, where λ_g is the guided wavelength. At $f_0 = 5.75$ GHz and $\varepsilon_r = 10.2$, the guided wavelength is obtained as

$$\lambda_g = \frac{C}{f_0\sqrt{\varepsilon_r}} = 16.19 \text{ mm}$$

Symmetrical ring resonator unit cell is shown in Fig 3.7. The dimensions of the symmetrical ring resonator are shown in Table 3.2. The dimensions of the symmetrical ring resonator are optimized to get better performance.

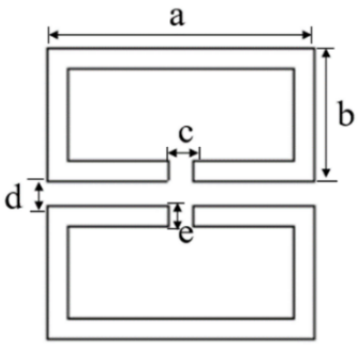

Fig 3.7 Symmetrical ring resonator unit cell

Table 3.2 Dimensions of symmetrical ring resonator unit cell

Parameter	**a**	**b**	**c**	**d**	**e**
Value (mm)	3.12	1.56	0.3	0.295	0.24

Initially, the bandpass filter is designed with single symmetric ring resonator which corresponds first order filter. Later, two resonators are placed along the microstrip line which corresponds to second order filter. First order and second order bandpass filters are realised using symmetrical ring resonators and vias on microstrip line as shown in Fig 3.8 and 3.9 respectively. Length of microstrip line is taken as 8.12 mm and 16.12mm for first order and second order bandpass filter respectively. The diameter of metallic via as 0.4 mm and the gap between vias as 8.08 mm is chosen for better performance characteristics. The size of the first order and second order filters are 8.12 mm × 10.84 mm and 16.12 mm × 10.84 mm respectively.

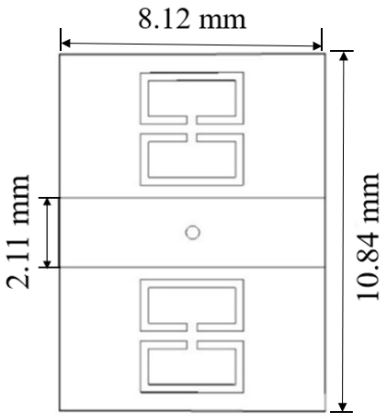

Fig 3.8 Top view of first order symmetrical ring resonator bandpass filter using single resonator

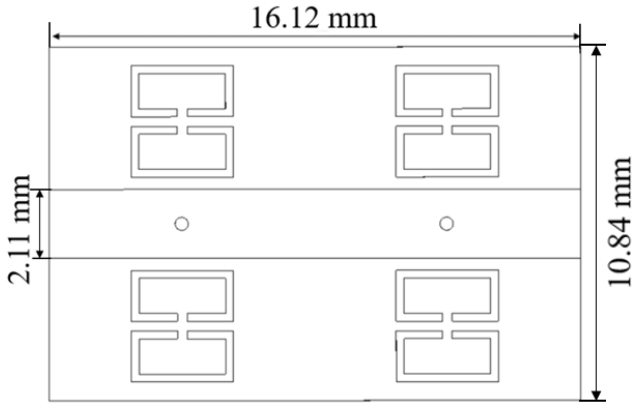

Fig 3.9 Top view of second order symmetrical ring resonator bandpass filter using double resonators

3.7.1 Equivalent circuit realization

Equivalent circuit of the proposed bandpass filter is represented using the T circuit model for second order symmetrical ring resonator bandpass filter is shown in Fig 3.10. The lumped inductance and capacitance values of the second order symmetrical ring resonator bandpass filter are given below

L_1 = 30 nH, C_1=0.0257 pF, L_2=0.064 nH, C_2= 12 pF

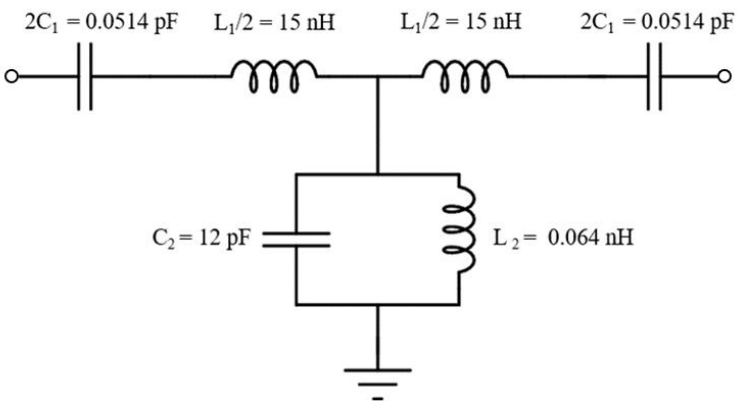

Fig 3.10 Equivalent circuit of second order symmetrical ring resonator bandpass filter

3.7.2 Results and discussion

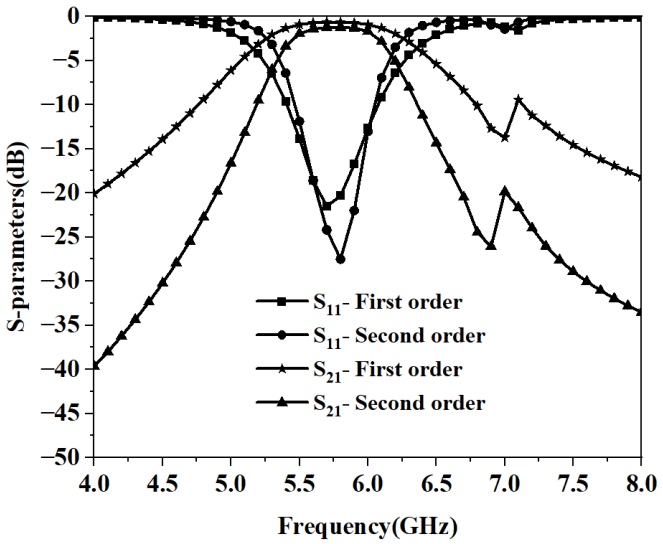

Fig 3.11 Comparison of S-parameters of first order and second order symmetrical ring resonator bandpass filter

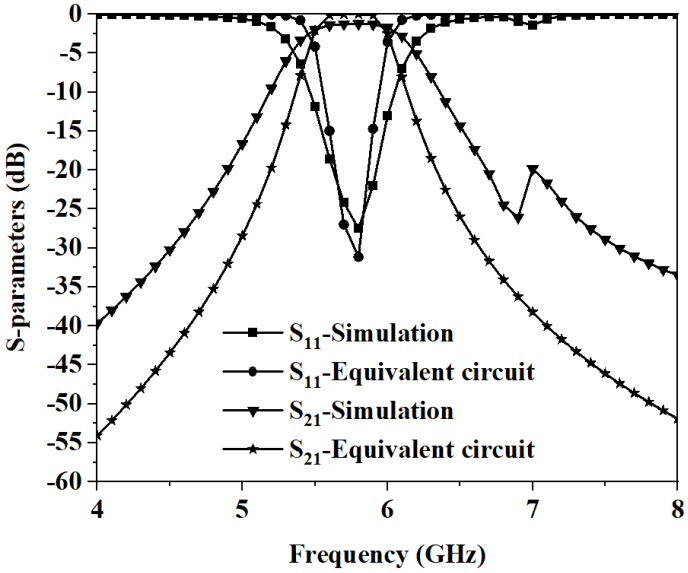

Fig 3.12 Comparison of simulation and equivalent circuit results of second order symmetrical split ring resonator bandpass filter

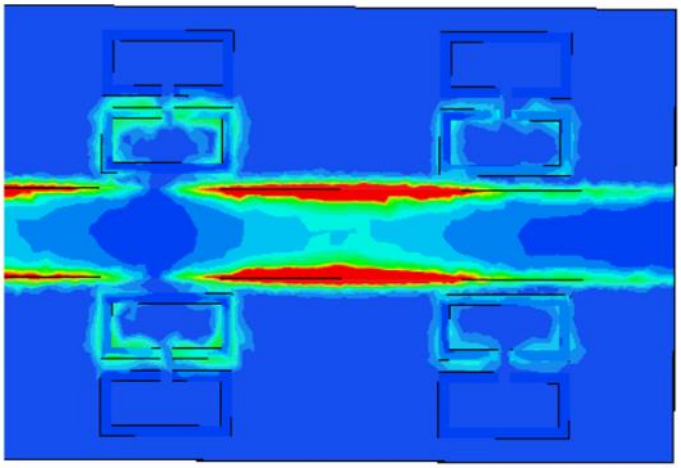

Fig 3.13 The electric field distribution of second order symmetrical ring resonator bandpass filter at 5.7 GHz frequency in the passband

The designed bandpass filters are simulated using Ansys HFSS and simulation results are presented in the following Fig 3.11. The second order filter has better performance when compared to first order. Hence, equivalent circuit is represented for second order filter. From Fig 3.11, an improvement in the roll-off rate from first order bandpass filter to second order bandpass filter is observed. An equivalent circuit is designed from the simulation results of HFSS and the circuit is simulated using an AWR design environment to determine S_{11} and S_{21} response. The HFSS simulation results and equivalent circuit simulation results are compared in Fig 3.12. for the second order symmetrical ring resonator bandpass filter. The passband

frequency range of the symmetrical ring resonator bandpass filter designed using lumped equivalent circuit is 5.55 GHz – 5.95 GHz. The fractional bandwidth is 6.9% with an insertion loss of 0.1 dB. The return loss of the filter is 27 dB. The frequency range of the simulated bandpass filter is 5.47 GHz – 6 GHz which lies in C-band with fractional bandwidth of 9.25%. The insertion loss of the simulated filter is 1.2 dB. The return loss is 32 dB. The electric field distribution of the proposed bandpass filters is shown in Fig 3.13. in which transmission of current from port 1 to port 2 illustrates the passband characteristic.

3.8. Design of bandpass filter using moore fractal symmetrical ring resonator for C-band applications

Moore fractal is applied to the symmetrical ring resonator unit cell as shown in Fig 3.14. The vertical side of symmetrical ring resonator unit cell is folded to one third of the total length. The total length of the vertical side of moore fractal applied symmetrical ring resonator is same as that of symmetrical split ring resonator. As a result, the size of moore fractal symmetrical ring resonator unit cell is reduced and also the capacitance effect of the moore fractal resonator is increased with resultant increase in bandwidth. The design specifications of the moore fractal symmetric ring resonator BPF are shown in Table 3.3.

Table 3.3. Design specifications of moore fractal symmetrical ring resonator BPF

Parameter	Value
Frequency band of operation	C-band
Center frequency	7.36 GHz
Feed impedance	50 Ω
Substrate material	RT Duroid 3010
Dielectric constant	10.2
Substrate thickness	0.13mm
Copper thickness	35 µm
Order of the filter	2
Bandwidth	0.85 GHz
Insertion loss	0.4 dB
Return loss	29 dB
Q-factor	8.6

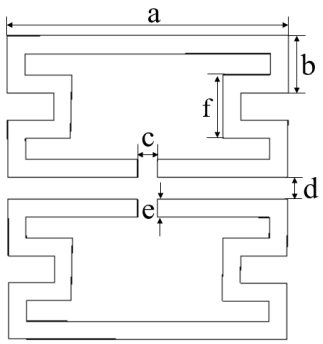

Fig 3.14 The unit cell of the moore fractal symmetrical ring resonator

Table 3.4 Dimensions of moore fractal symmetrical ring resonator unit cell

Parameter	**a**	**b**	**c**	**d**	**e**	**f**
Value (mm)	3.12	0.63	0.22	0.24	0.2	0.7

The dimensions of the unit cell are shown in Table 3.4. Moore fractal symmetrical ring resonators are placed on either side of the microstrip line at the same location on the microstrip line where via is placed. To improve the performance two sets of via and unit cell are used. Initially, a microstrip line is designed at the center frequency for 50 **Ω** feed impedance. The width of the line is obtained as 1.95mm and a length of 12.2mm is considered to accommodate the two-unit cell resonators for second order filter. The size of the filter is obtained as 12.2 mm × 10.84mm (0.97 λ_g × 0.78 λ_g). The top view of moore fractal symmetrical ring resonator bandpass filter is shown in Fig 3.15.

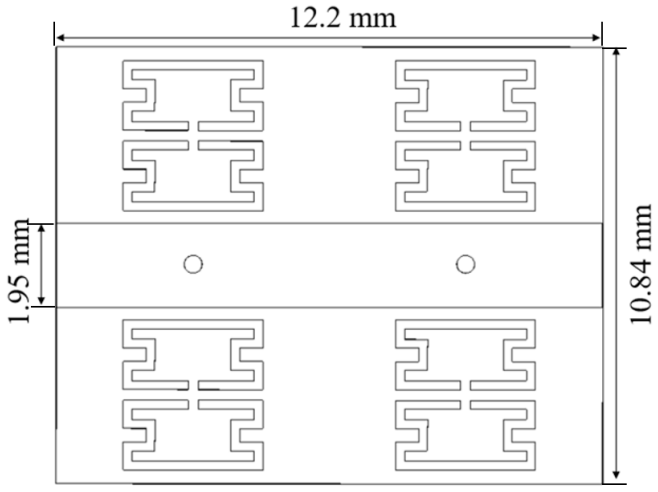

Fig 3.15 Top view of moore fractal symmetrical ring resonator bandpass filter

3.8.1 Equivalent circuit realization

The equivalent circuit of the moore fractal symmetrical ring resonator bandpass filter is shown in Fig 3.16. The lumped inductance and capacitance values of the moore fractal symmetrical ring resonator bandpass filter are L_1 = 17.69 nH, C_1=0.024 pF, L_2=0.06 nH, C_2 = 7 pF, where L_1 and C_1 are series inductance and capacitance L_2 and C_2 are shunt elements.

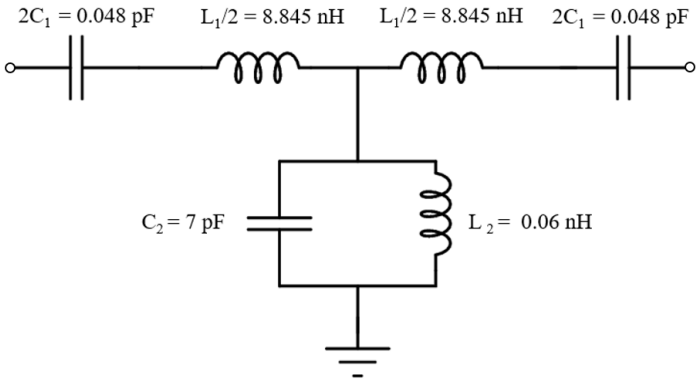

Fig 3.16 Equivalent circuit of moore fractal symmetrical ring resonator bandpass filter

3.8.2 Results and discussion

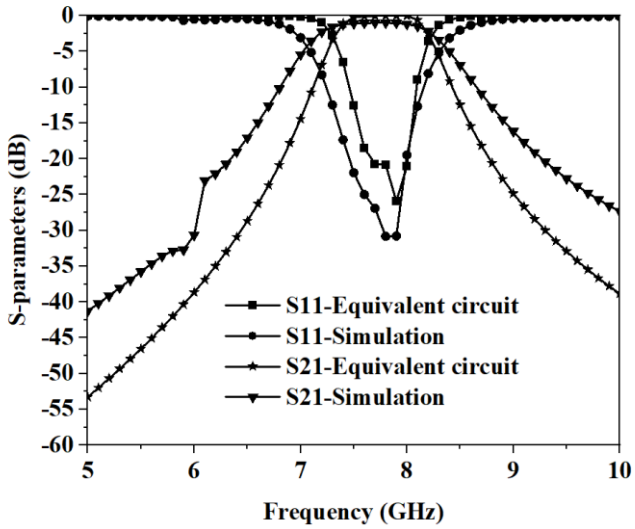

Fig 3.17 Comparison of S-parameters of moore fractal symmetrical ring resonator bandpass filter for simulation and equivalent circuit

The S-parameters of the moore fractal symmetrical ring resonator bandpass filter using HFSS simulation and equivalent circuit simulation are shown in Fig 3.17. The passband frequency using lumped equivalent circuit is 7.45 GHz – 8.05 GHz with fractional bandwidth of 7.74% at the center frequency 7.75 GHz. From the simulation results, the passband frequency

range is 7.15 GHz - 8.15 GHz with fractional bandwidth of 13.1% at the center frequency 7.63 GHz. A good similarity is obtained between equivalent circuit results and HFSS simulation results. The electric field distribution of the proposed bandpass filter is shown in Fig 3.18. which represents signal flow from input port to output port.

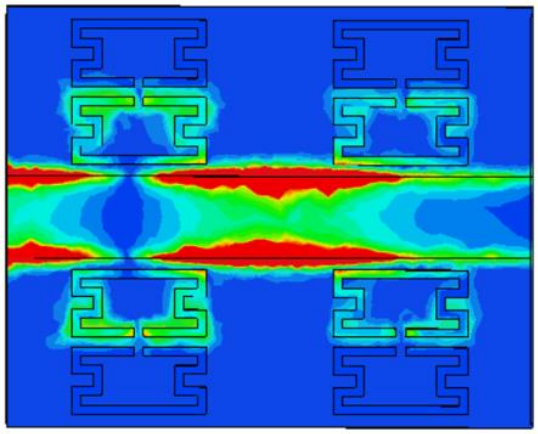

Fig 3.18 The electric field distribution of moore fractal symmetrical ring resonator bandpass filter at 7.8 GHz frequency in the passband

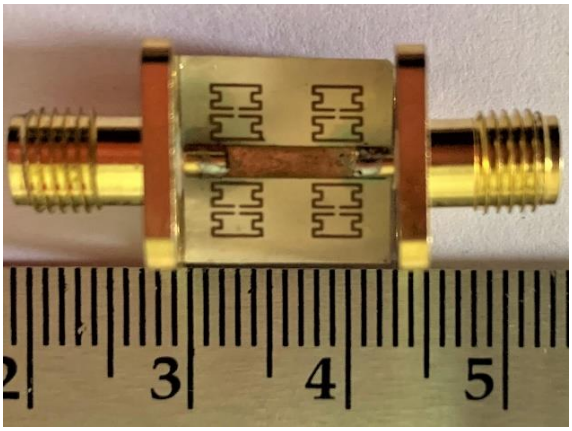

Fig 3.19 Top view of fabricated moore fractal symmetrical ring resonator bandpass filter

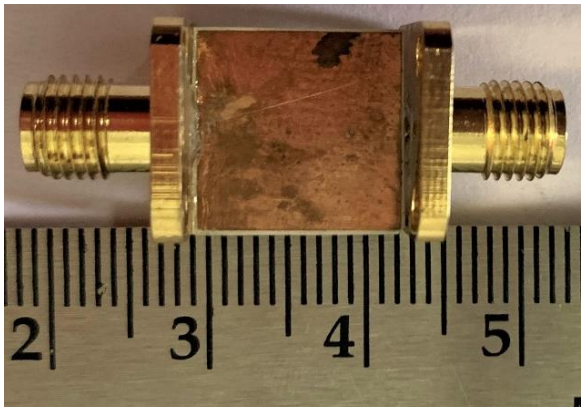

Fig 3.20 Bottom view of fabricated moore fractal symmetrical ring resonator bandpass filter

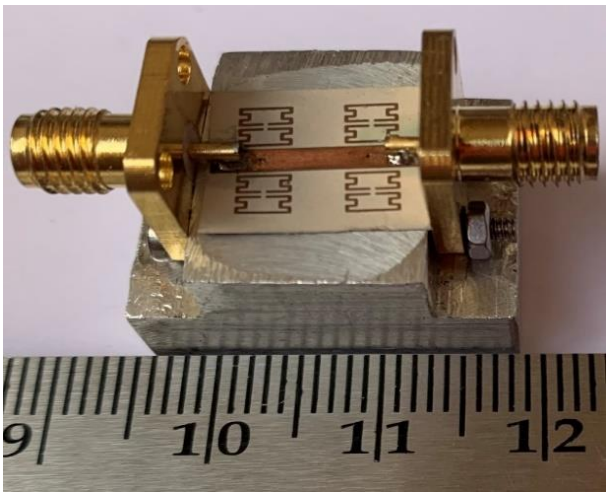

Fig 3.21 Top view of fabricated moore fractal symmetrical ring resonator bandpass filter with mounting box

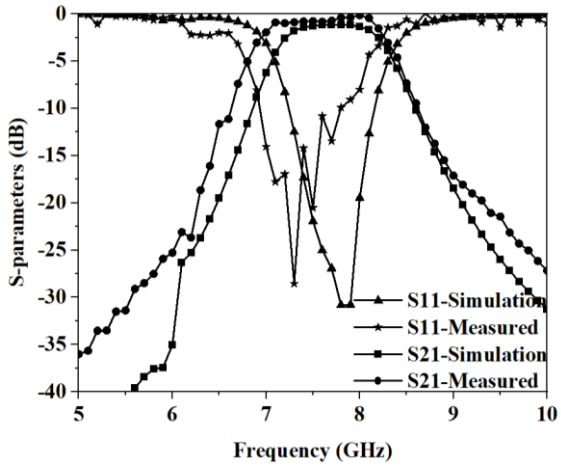

Fig 3.22 HFSS simulation and measurement S-parameters comparison for moore fractal symmetrical ring resonator bandpass filter

The top view, bottom view and with mounting box of fabricated prototype of moore fractal symmetrical ring resonator BPF are shown in Fig 3.19, Fig 3.20 and Fig 3.21. The measured and simulation results are compared in Fig 3.22. The frequency range of passband from the measurement results is from 6.95 GHz - 7.8 GHz which lies in C-band with fractional bandwidth of 11.54% at the center frequency of 7.36 GHz and insertion loss is 0.4 dB.

The shift in the passband frequency may be due to dimensional tolerances during etching of the copper material at the time of fabrication. The variations in the S21 are due to SMA connector and cable losses.

Bandwidth enhancement and compact size are observed by using moore fractal on a symmetrical ring resonator bandpass filter.

Table 3.5 Comparison of symmetrical ring resonator BPF with published works

References	**Center frequency (GHz)**	**Fractional Bandwidth (%)**	**Insertion Loss (dB)**	**Size (λ_g^2)**
[32]	5.22	7.6	1.62	3.36
[33]	1.75	8	4	0.042
[34]	2	8.5	1.43	0.25
[39]	5.25	9.5	<1	1.08
[2]	6	9	3.5	1.3
Symmetrical ring resonator BPF	5.75	9.25	1.2	0.64
Moore fractal symmetrical ring resonator BPF	7.36	11.5	0.4	0.75

The proposed bandpass filter parameters are compared with published bandpass filters in Table 3.5. As compared to published work, moore fractal BPF has low insertion loss and large bandwidth useful for C band applications.

3.9 Design of bandpass filter using symmetrical ring resonator for X-band applications

The dimensions of the symmetrical ring resonator and gaps in between resonators are modified to realize bandpass filters for X-band applications. The number of resonators is increased to improve the selectivity of the filter. The design specifications of the X-band bandpass filter are shown in Table 3.6. A microstrip line of width 1.46 mm is designed based on equations [2.4-2.6] for impedance matching for 50 Ω feed line. To accommodate the unit cell resonators the length of the microstrip line is considered as 23.88mm. The structure of the symmetrical ring resonator unit cell is shown in Fig 3.23 and dimensions for the proposed filter are listed in Table 3.7.

Table 3.6 Design specifications of fourth order symmetrical ring resonator BPF

Parameter	Value
Frequency band of operation	X-band
Center frequency	10.75 GHz
Feed impedance	50 Ω
Substrate material	RT Duroid 3010
Dielectric constant	10.2
Substrate thickness	1.27mm
Copper laminate thickness	35 µm
Order of the filter	4
Bandwidth	2.5 GHz
Insertion loss	< 1 dB
Return loss	> 12 dB
Q-factor	4.3

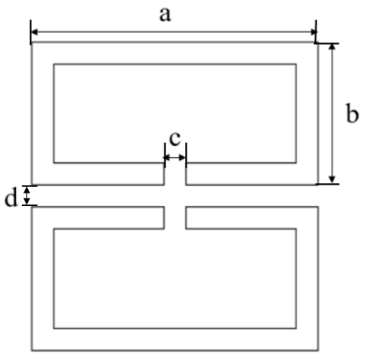

Fig 3.23 Symmetrical ring resonator unit cell

Table 3.7 Unit cell dimensions of symmetrical ring resonator

Parameter	a	b	c	d
Value (mm)	3.12	1.56	0.24	0.24

Four vias of diameter 0.4mm are placed at a distance of 3.52mm in between them. The top view of the proposed filter is shown in Fig 3.24. The size of the proposed filter is 10 mm × 23.88 mm, which is approximately 2.6 λ_g × 1.1 λ_g, where λ_g is the guided wavelength.

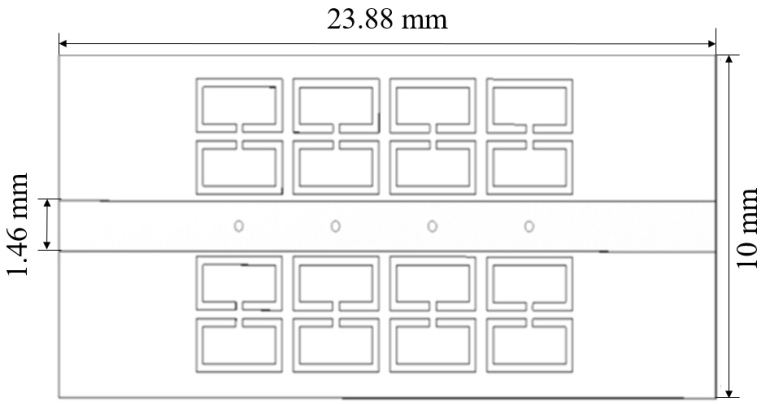

Fig 3.24 Top view of the fourth order symmetrical ring resonator bandpass filter

3.9.1 Results and discussion

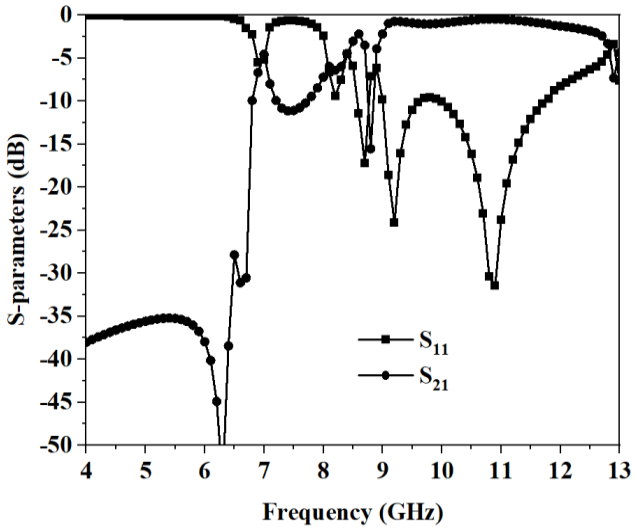

Fig 3.25 Simulation results of fourth order symmetrical ring resonator bandpass filter

Simulation results are shown in Fig 3.25. The proposed filter has a wide pass band extended from 9.2 GHz to 11.7 GHz which lies in X-band. The fractional bandwidth is 23.8%. The insertion loss is 0.5 dB to 1 dB. The return loss is greater than 12 dB in the passband.

3.10 Design of EI-shaped metamaterial bandpass filter for higher 5G applications

EI-shaped unit cell behaves as an LC resonant circuit to resonate at higher frequencies. The inductance is inversely related to length of the line and capacitance is inversely proportional to spacing between the lines. EI shaped unit cells are designed to resonate at high frequencies resulting in design of bandpass filter at millimeter wave frequencies. The EI-shaped unit cells and vias are proposed along the microstrip line to design a bandpass filter useful for higher 5G applications. The design specifications of the filter are listed in table 3.8.

Table 3.8. Design specifications of EI shaped metamaterial BPF

Parameter	Value
Frequency band of Operation	Higher 5G
Center frequency	40 GHz
Feed impedance	50 Ω
Substrate material	RT Duroid 4003C
Dielectric constant	3.55
Substrate thickness	0.813 mm
Copper laminate thickness	35 µm
Order of the filter	3
Bandwidth	0.8 GHz
Insertion loss	2.5 dB
Return loss	>10 dB
Q-factor	50

The width of the microstrip line calculated using equations [2.4-2.6] is obtained as 1.1mm for 50Ω feed impedance. The length of the microstrip line is taken as 14mm to accommodate the unit cells on both sides of the line. EI-shaped unit cell is shown in Fig 3.26. and its dimensions are mentioned in Table 3.9. The vias are placed with a spacing of 3.7 mm along the microstrip line, which have a diameter of 0.4 mm. The top view of the EI shaped metamaterial bandpass filter is shown in Fig 3.27.

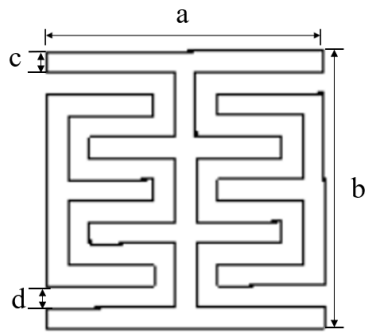

Fig 3.26 EI-shaped unit cell structure

Table 3.9 Dimensions of EI-shaped unit cell

Parameter	a	b	c	d
Value (mm)	2.6	2.6	0.2	0.2

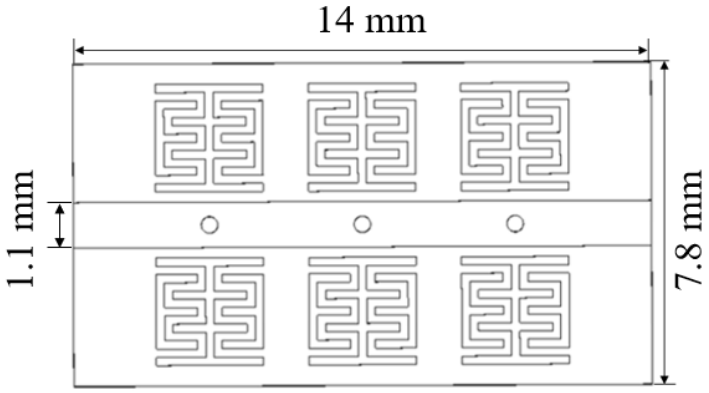

Fig 3.27 Top view of the EI-shaped unit cell bandpass filter

3.10.1 Results and discussion

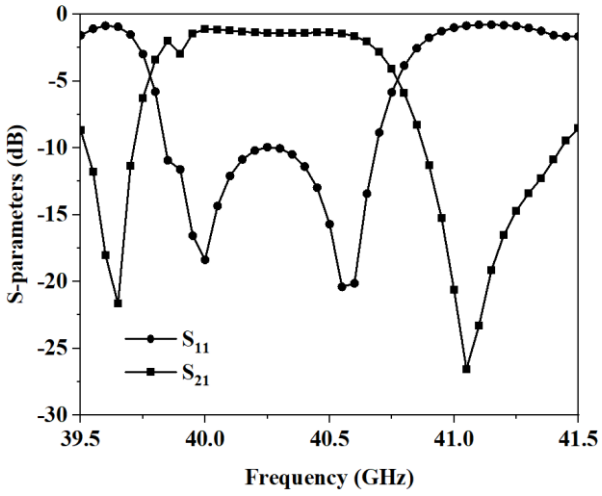

Fig 3.28 S-parameters of EI-shaped unit cell bandpass filter

S-parameters of the simulated filter are shown in Fig 3.28. The passband range of the proposed filter is 39.7 GHz - 40.5 GHz lies in higher 5G band at the central frequency 40.1 GHZ. The fractional bandwidth of the filter is 2%. The insertion loss of the proposed filter is less than 2.5 dB within the pass band range. The proposed bandpass filter has a sharp roll-off of 66 dB/GHz and 186 dB/GHz on both sides with 21 dB attenuation in both stopbands. Simulation results of the proposed filter are compared with published works in Table 3.10. But, the size of the filter is large when compared with published literature.

Table 3.10 Comparison of EI shaped metamaterial BPF with published works

References	**Frequency Range (GHz)**	**Fractional Bandwidth (%)**	**Insertion Loss (dB)**	**Size (λ_g^2)**
[40]	31- 32.42	4.5	1.19	-
[41]	29-30.6	5.3	1.6	3.39
[42]	34.2-35.8	4.28	3	0.11
EI shaped BPF	39.7-40.5	2	2.5	7

3.11 Design of EIE-shaped metamaterial and slotted stubs-based triple passbands filter

The EI shaped unit cell is modified to EIE shaped structure with reduced dimensions of 'I' in the unit cell. A microstrip line of width 1.75mm and length of 19.95mm is obtained to get impedance matching with a 50Ω feed line.

The EIE-shaped metamaterial unit cell is shown in Fig 3.29 and dimensions are shown in Table 3.11. EIE-shaped metamaterial and vias are placed along the microstrip line. Open circuit stubs of length 2.085 mm approximately λ_g /8, a width of 1.05 mm nearly λ_g /4 are introduced to the microstrip line in between the EIE shaped resonator as shown in Fig 3.30. The spacing between the stubs is taken as 5 mm. Slots are introduced in the stubs to improve the performance. Vias are placed along the microstrip line to obtain better stopband attenuation. The diameter of the vias is chosen as 0.4mm with spacing between them as 3.7 mm. The combination of metamaterial structures, vias and slotted stubs resulted in a triple bandpass filter

with good performance characteristics. The top view of the proposed bandpass filter is shown in Fig 3.31. The dimensions of the structure are optimised to achieve a compact triple pass bands bandpass filter.

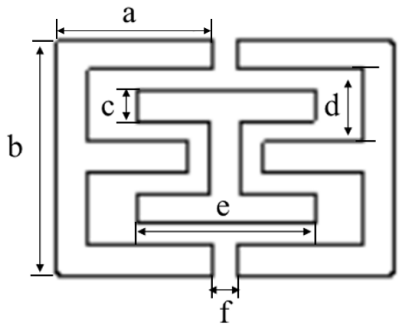

Fig 3.29 Structure of EIE-shaped metamaterial unit cell

Table 3.11 Dimensions of EIE-shaped metamaterial unit cell

Parameter	**a**	**b**	**c**	**d**	**e**	**f**
Value (mm)	1.22	1.84	0.24	0.56	1.4	0.2

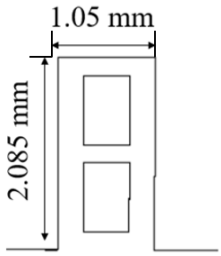

Fig 3.30 Open circuit slotted stub

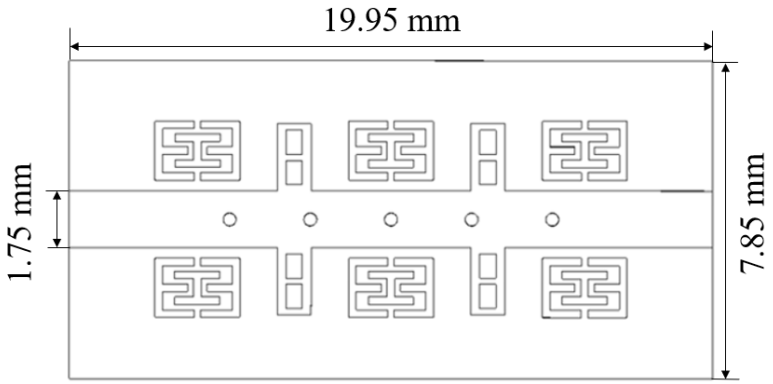

Fig 3.31 Top view of EIE-shaped metamaterial triple bandpass filter

3.11.1 Results and discussion

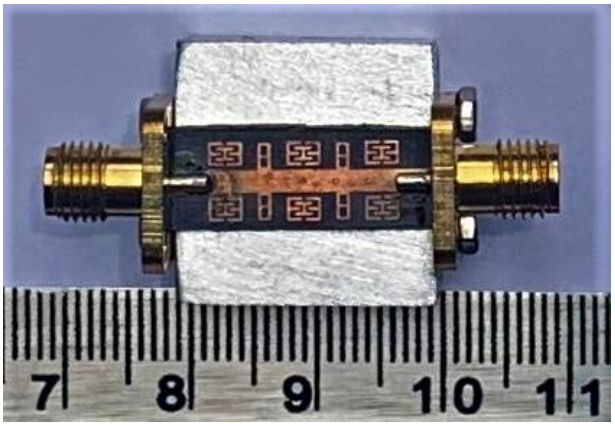

Fig 3.32 Top view of fabricated prototype of triple bandpass filter

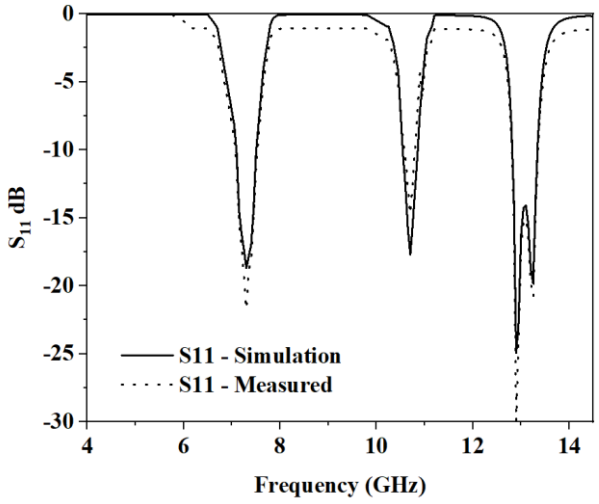

Fig 3.33 Simulation and measured S_{11} for the triple bandpass filter

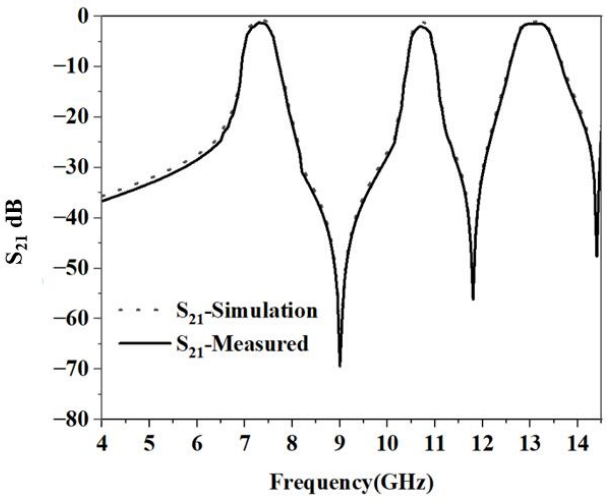

Fig 3.34 Simulation and measured S_{21} of the triple bandpass filter

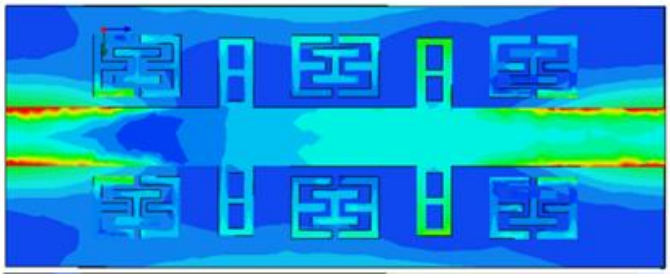

(a)

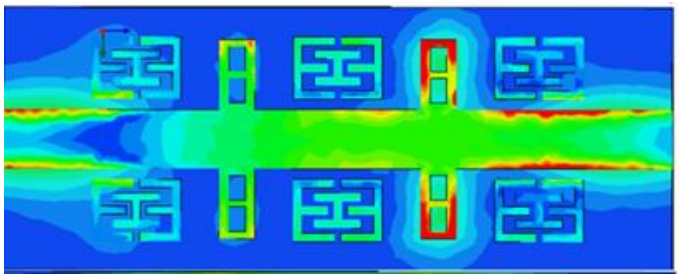

(b)

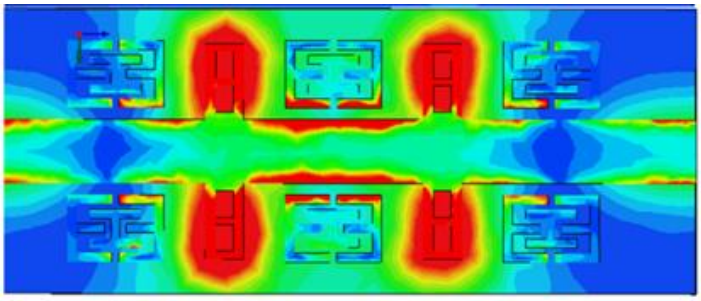

(c)

Fig 3.35 Electric field distributions of the triple bandpass filter at pass bands frequencies (a) 7.3 GHz, (b) 10.7 GHz and (c) 13 GHz respectively

The top view of the fabricated prototype is shown in Fig 3.32. The overall dimensions of the proposed filter are 7.85 mm × 19.95 mm, which are approximately 0.36 λ_g × 0.91 λ_g, where λ_g is the guided wavelength. The simulation and measured results are compared in Fig 3.33 & Fig 3.34. The passbands of the bandpass filter are 7.1 GHz - 7.5 GHz, 10.57 GHz - 10.78 GHz and 12.8 GHz -13.4 GHz lies in C-band, X-band and Ku-band respectively. The fractional bandwidth is 5.4%, 2.5% and 4.58% for both simulation and measured results. The minimum insertion losses are 1.3 dB, 1.9 dB and 1.5 dB for measurement whereas for simulation are 0.8 dB, 1 dB and 1.2 dB in the three passbands respectively. The maximum measured return losses

are 23 dB, 13 dB and 30 dB whereas simulation return losses are 20 dB, 19 dB and 25 dB for the three bands respectively. The transmission zeros are at 9 GHz, 11.8 GHz and 14.3 GHz in both measured and simulated results. The electric field distributions of the pass bands of the triple bandpass filter are shown in Fig 3.35. The transmission of the signal from input port to output port is observed at 7.3 GHz, 10.7 GHz and 13 GHz. The measured and simulated results are in good agreement. In Table 3.12, triple bandpass filter is compared with published works which shows that proposed triple bandpass filter is compact.

Table 3.12 Comparison of EIE shaped metamaterial BPF with published works

References	**Central frequencies (GHz)**	**Fractional Bandwidth (GHz)**	**Insertion loss (dB)**	**Size (λ_g^2)**
[35]	1.93,2.6,3.9	5,11,3	1.5,0.6,1.83	0.41
[36]	1.575,2.4,3.45	12.6,6.25,14.49	0.7,1.14,0.3	0.48
[43]	9.15,9.6,10.3	<1,1.2,3.8	<1, <1, <1	1.18
EIE metamaterial and slotted stubs BPF	7.29, 10.67,13	5.4,2.5, 4.58	1.3,1.9,1.5	0.32

3.12 Conclusion

In this chapter single and multi-passbands bandpass filters are designed. Bandpass filters are designed by loading metamaterial resonators on either side of the microstrip line and vias are placed from microstrip line to ground. Symmetrical ring resonators are used to design compact single bandpass filters for C band and X band applications. Moore fractal symmetrical ring resonators have given compact and wide pass passband for C band applications. Metamaterial resonators are also attempted for 5G applications. Consideration of metamaterial unit cells and stubs resulted in multiple passbands bandpass filters in C, X and Ku bands respectively.

Chapter 4

Bandpass and Bandstop filter using complementary metamaterials

4.1 Introduction

In filter design, the usage of complementary metamaterial resonators provides compactness of the design and also wide bandwidth. Communication devices are in great need of compact filters operating in microwave and millimeter wave bands. Radio location and maritime radio navigation applications operate in the S-band require compact bandpass filter.

Several papers are published on design of compact bandpass filters using complementary split ring resonators (CSRR). Benzerga Fellah (2021) et al. proposed X band bandpass filter based on half-mode substrate integrated waveguide. Complementary split ring resonators are used as defected ground structures in the design. The bandpass filter frequency range is 13.2 GHz – 14.8 GHz with fractional bandwidth of 11.4% at a center frequency of 14 GHz. An insertion loss of 2.6 dB and a return loss of 14 dB are realised. But, the filter has high insertion loss [44]. Snezana Lj. Stefanovski (2013) et al. presented X-band bandpass waveguide filters, utilizing CSRR structures as single and dual-mode resonators. The filter's pass band frequency range is 11.82 GHz – 12.18 GHz. A fractional bandwidth of 3% is obtained at 12.037 GHz center frequency. The bandpass filter has return loss of 32 dB and insertion loss of 0.1 dB , but do not have sharp roll-off [45]. Hailin Cao (2013) et al. designed a bandpass filter using back-to-back triangular complementary split-ring resonators engraved on the waveguide surface with a quarter-mode substrate integrated waveguide resonator. At the center frequency of 3.7 GHz, the designed filter attains a wideband with a fractional bandwidth of 24.3%. The measured insertion loss is 1.8 dB at 3.7 GHz and the return loss is better than 10 dB from 3.4 to 4.2 GHz but the filter has high insertion loss [46].

Bandstop filters are also required at many stages of communication systems and healthcare applications. Fixed-Satellite broadcast services, Aviation, Cable TV relay applications comes under Ku band. Compact wideband bandstop filters are to be designed in the Ku band to meet the present-day requirements.

Many papers are published to design compact bandstop filters. Hicham Lalj (2013) et al. proposed a design of compact microstrip bandstop filters based on complementary split ring resonators using an array of miniaturized loaded CSRRs etched below the microstrip line on

the ground plane. The filter has a stop band from 5 GHz – 6.8 GHz with stopband attenuation of 43 dB at center frequency [47]. S. Thomas Niba (2020) et al. presented a bandstop filter using half-wavelength transmission lines which is based on the design and optimization technique. The designed filter stop band frequency range is 6 GHz – 7 GHz with stopband attenuation of 25 dB at center frequency [48].

In the proposed work, complementary triple concentric split ring resonators are employed for the first time on both sides of the gaps of the microstrip line and vias are used to short the microstrip line and ground plane resulting in a bandpass filter useful for radar applications. Complementary symmetrical ring resonators are loaded in the ground plane just beneath the microstrip line, resulting in a compact bandstop filter with high stopband attenuation and wide stopband in the Ku band.

4.2 Complementary split ring resonator

The structure that results from removing the split ring resonator topology from a metallic sheet can be considered as the SRR's complementary structure known as a complementary split ring resonator (CSRR). It can be excited using either a magnetic field applied to the structure plane or with axial electric field. CSRR exhibits negative permittivity for a certain frequency band. A well-known method to realize filters is to have CSRR etched on the ground plane below the microstrip line. Good in-band and out-of-band performance are offered by filters with CSRRs. The structure of complementary split ring resonator is shown in Fig 4.1.

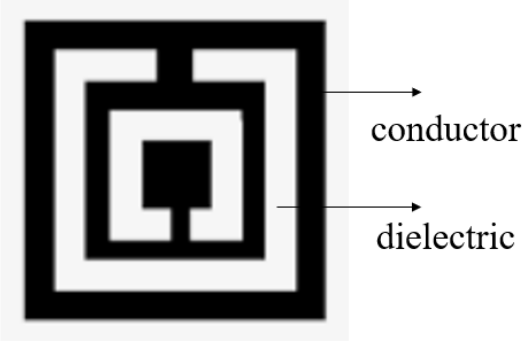

Fig 4.1. Complementary split ring resonator unit cell

4.3 Design of bandpass filter using complementary split-ring resonators for S-band applications

A novel compact triple complementary resonant metamaterial structures, gaps, vias are implemented for S-band filter applications. Gaps are introduced along the microstrip line. Via filled with copper is placed along the microstrip line in between the microstrip line and ground plane. Triple concentric split ring resonators consist of three concentric square rings are etched from the ground plane. The design specifications of the proposed filter are listed in Table 4.1.

Novelty: The gaps and vias are used with in a design for the first time. A single via introduces a pass band with the proposed design dimensions at lower frequencies. The coupling effect of triple concentric split ring resonator improves return loss of the bandpass filter.

Table 4.1 Design specifications of complementary triple concentric split ring resonator BPF

Parameter	Value
Frequency band of operation	S-band
Center frequency	3 GHz
Feed impedance	50 Ω
Substrate material	RT Duroid 3010
Dielectric constant	10.2
Substrate thickness	0.13mm
Copper laminate thickness	35 µm
Order of the filter	2
Bandwidth	0.3 GHz
Insertion loss	1.5 dB
Return loss	16 dB
Q-factor	10

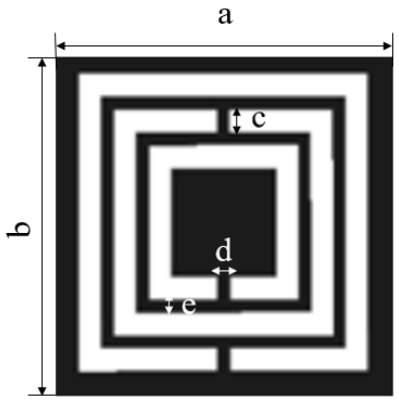

Fig 4.2 Triple concentric split ring resonator unit cell

Table 4.2 Dimensions of the triple concentric split ring resonator unit cell

Parameter	**a**	**b**	**c**	**d**	**e**
Value (mm)	5	5	0.4	0.2	0.2

The triple concentric split ring resonator unit cell is shown in Fig 4.2. and its dimensions are mentioned in Table 4.2. The consideration of three rings increases the greater flexibility for the design by incorporating additional inductance and capacitance effect. In addition, the size of the unit cell is also reduced to realise a compact filter.

A microstrip line of length of 17.5 mm and width of 2.25 mm is designed based on equations [2.4-2.6] for impedance matching with a 50Ω feed line. Gaps of length 0.15mm are placed along the microstrip line and via with diameter of 0.4 mm is placed through the substrate from the microstrip line to the ground plane to lie midway in between the gaps. The top and bottom views of the realised filter are shown in Fig 4.3 and Fig 4.4. respectively. The dimensions of the proposed filter are 17.5 mm×7.81 mm (0.55 λg ×0.25 λg).

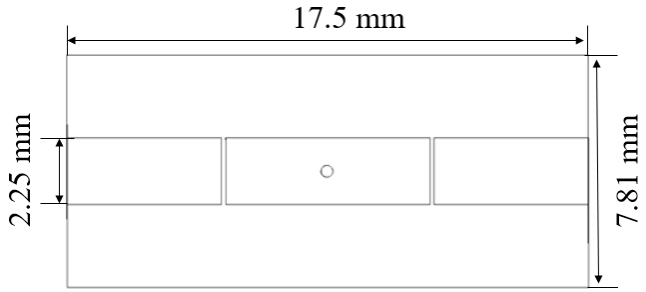

Fig 4.3 Top view of the triple concentric split ring resonator bandpass filter

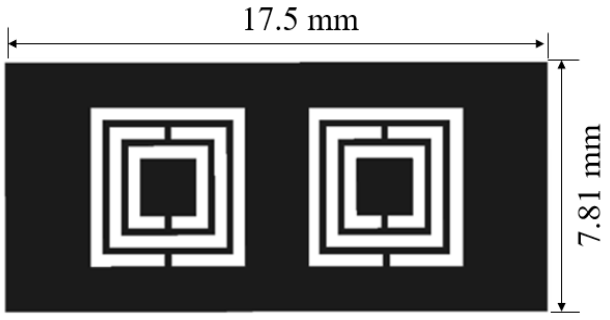

Fig 4.4 Bottom view of the triple concentric split ring resonator bandpass filter

4.3.1 Results and discussion

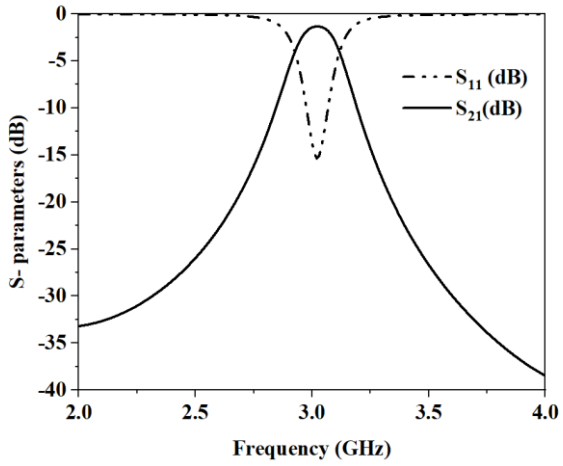

Fig 4.5 S-parametrs of triple concentric split ring resonator bandpass filter

The simulation results are shown in Fig 4.5. The proposed filter has a passband from 2.85 GHz-3.15 GHz lies in S-band with center frequency at 3 GHz and fractional bandwidth of 3%. The insertion loss of the filter is 1.5 dB at the center frequency. The roll-off rate of the filter is 58.8 dB/GHz on the lower side and 67.8 dB/GHz on the upper side. From Table 4.3, it can be concluded that the proposed filter is compact and also has low insertion loss. The proposed design is useful for S-band applications.

Table 4.3 Comparison of complementary triple concentric split ring resonator BPF with published works

References	**Center frequency (GHz)**	**Fractional Bandwidth (%)**	**Stop band**	**Rejection over stopband**	**Insertion loss (dB)**	**Size (λ_g^2)**
[49]	5	7.6	5.2 GHz-50 GHz	> 20 dB	1.8	0.1
[23]	3.41	3.5	3.7 GHz-4.5 GHz	> 20 dB	<1	0.38
[24]	10	12	10.6 GHz -16.3 GHz	> 37 dB	1.59	0.39
Triple concentric CSRR BPF	3 (2.85-3.15)	3	3.15 GHz-11.5 GHz	> 20dB	1.5	0.13

Compared to the results of [49] the proposed filter has better insertion loss and the design is complex compare to the proposed design.

4.4 Design of compact complementary symmetrical ring resonator bandstop filter for Ku band applications

A bandstop filter is proposed using complementary symmetrical ring resonator structures which are periodically etched in the ground plane along the microstrip line for Ku band applications in the frequency range 12 GHz – 18 GHz. The design specifications are shown in Table 4.4.

Table 4.4 Design specifications of complementary symmetrical ring resonator BSF

Parameter	Value
Frequency band of operation	Ku band
Center frequency	12.87 GHz
Feed impedance	50 Ω
Substrate material	RT Duroid 4003C
Dielectric constant	3.55
Substrate thickness	0.813mm
Copper laminate thickness	35 µm
Order of the filter	4
Bandwidth	1.6
Stopband attenuation	31 dB
Q-factor	8

The microstrip line is designed for 50 Ω feed impedance. All pass filter is designed by choosing a microstrip line width of 2.06 mm on RT Duroid 4003C substrate material considering substrate height of 0.813 mm and dielectric constant of 3.55 based on the equations [2.4-2.6]. The length of the microstrip line is taken as 19.23 mm.

The design of the bandstop filter is proposed initially by designing an all-pass filter with the microstrip line. Complementary resonant structures are incorporated in the ground plane for the bandstop filter. The magnetic field is induced around the microstrip line. The presence of a dielectric substrate makes the field lines to be tightly concentrated just below the central conductor and the electric flux density reaches its maximum value in the vicinity of this region. If an array of complementary symmetrical ring resonator structures which act as LC resonators are etched on the ground plane aligned with the microstrip line, strong coupling with the desired polarization is expected, which results in a single negative medium with a negative permittivity. Therefore, the previously propagating waves in the absence of complementary symmetrical ring resonators become evanescent waves. Consequently, the signal propagation is inhibited over a

certain band of frequencies. Thus, the use of resonators along the microstrip line forms a bandstop filter.

The structure of unit cell of the complementary symmetrical ring resonator is shown in Fig 4.6. The dimensions of the unit cell are shown in Table 4.5.

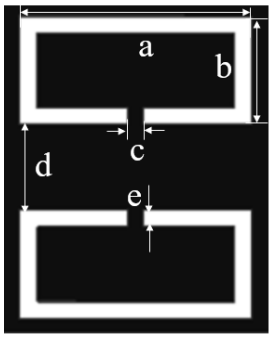

Fig 4.6 Structure of complementary symmetrical ring resonator unit cell

Table 4.5 Unit cell dimensions of complementary symmetrical ring resonator

Parameter	**a**	**b**	**c**	**d**	**e**
Value (mm)	3.12	1.56	0.2	1.24	0.24

The top view and bottom view of the proposed filter are shown in Fig 4.7 and Fig 4.8 respectively. The total size of the proposed filter is 19.23×4.78 mm^2, which is approximately 1.5 λg by 0.37 λg, where λg is the guided wavelength at the center frequency.

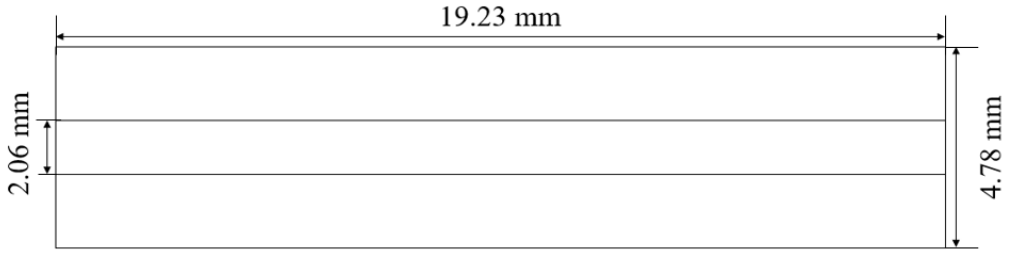

Fig 4.7 Top view of complementary symmetrical ring resonator bandstop filter

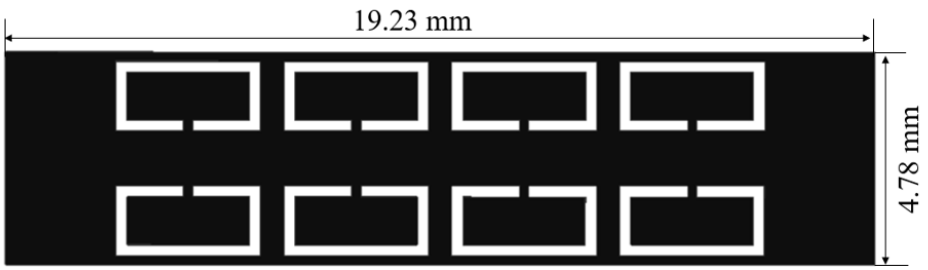

Fig 4.8 Bottom view of complementary symmetrical ring resonator bandstop filter

4.4.1 Equivalent circuit realization

The lumped element equivalent circuit of the proposed bandstop filter is represented using the T circuit model as shown in Fig 4.9. The microstrip line consists of series inductance and shunt capacitance. The series inductance 'L' is calculated using the equations [4.1- 4.2],

$$L = \frac{60l}{v_0} ln[\frac{8h}{w} + \frac{w}{4h}] \quad for \quad \frac{w}{h} \leq 1 \tag{4.1}$$

$$L = \frac{120\pi l}{v_0}\left[\frac{1}{\frac{w}{h} + 1.393 + 0.667\ln\left(\frac{w}{h} + 1.444\right)}\right] for \ \frac{w}{h} > 1 \tag{4.2}$$

The coupling between the microstrip line and complementary symmetrical ring resonator structures is represented by C_C. L_r and C_r represent the equivalent inductance and capacitance of resonant structures used in the proposed design. The inductance and capacitance values are determined using equation 4.3 where f_r represents the resonant frequency of the proposed bandstop filter determined from the simulation results.

$$f_r = \frac{1}{2\pi\sqrt{L_r(C_r + C_c)}} \tag{4.3}$$

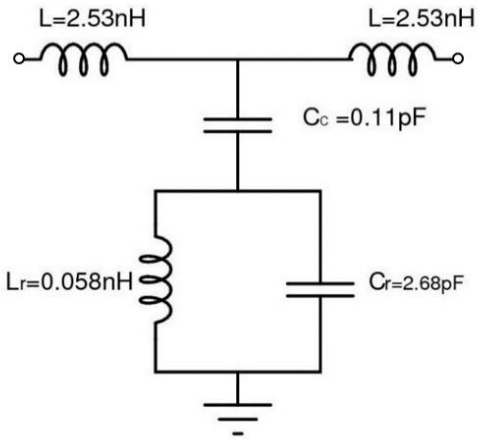

Fig 4.9 Equivalent circuit model for the complementary symmetrical ring resonator bandstop filter

4.4.2 Results and discussion

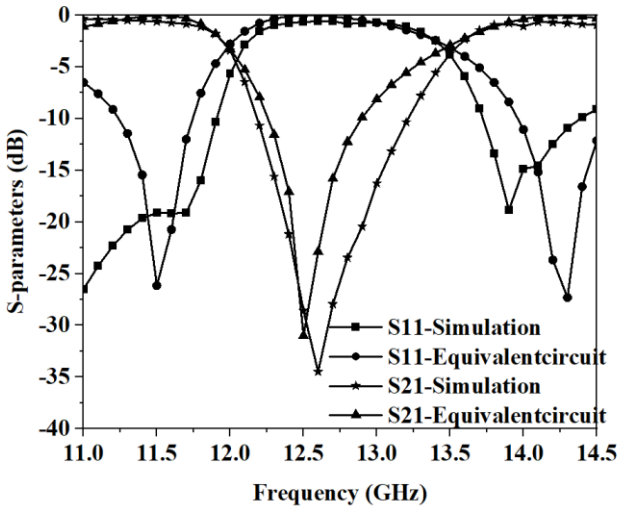

Fig 4.10 Comparison of S-parameters of complementary symmetrical ring resonator bandstop filter from simulation and equivalent circuit

Labels represented are for a bandstop filter. Out of band responses are different for simulation and equivalent circuit results may be due to the different analysis techniques such as Finite element method in HFSS and Method of moments in AWR. The variations are resulted in the simulation results.

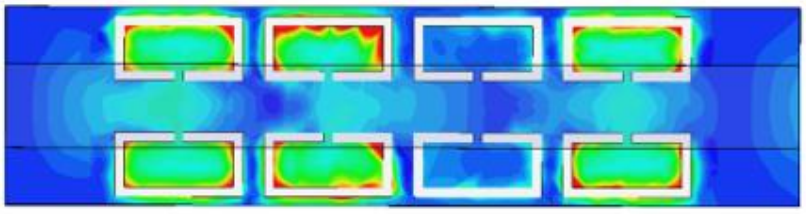

Fig 4.11 Electric field distribution for a complementary symmetric ring resonator bandstop filter at 11.5 GHz frequency in the passband

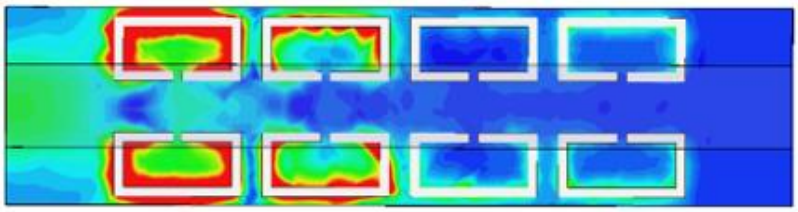

Fig 4.12 Electric field distribution for a complementary symmetric ring resonator bandstop filter at 12.6 GHz frequency in the stopband

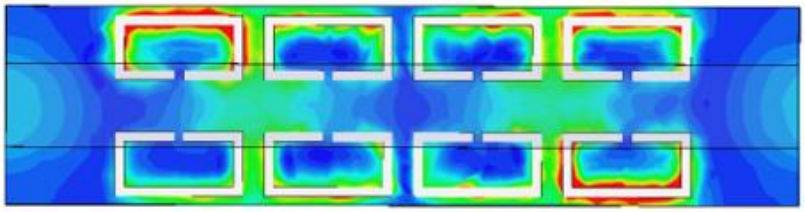

Fig 4.13 Electric field distribution for a complementary symmetric ring resonator bandstop filter at 14 GHz frequency in the passband

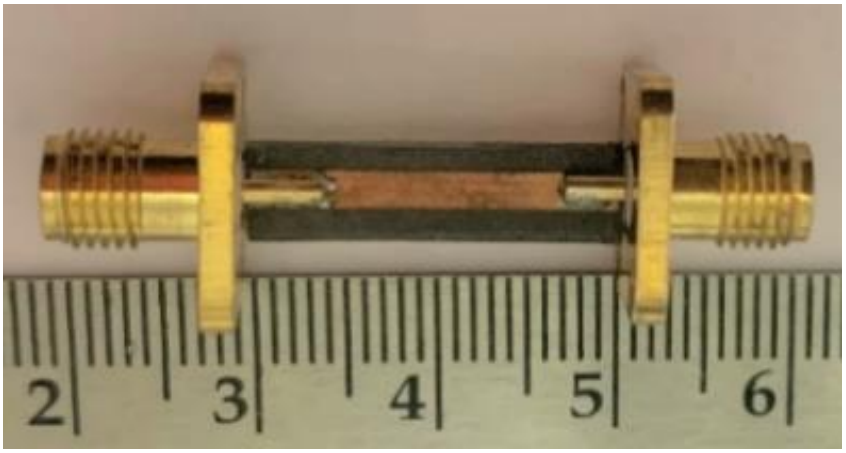

Fig 4.14 Top view of fabricated complementary symmetrical ring resonator bandstop filter

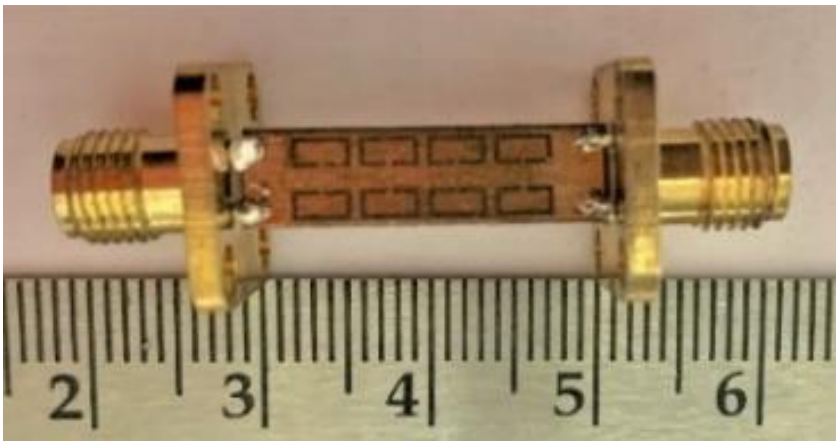

Fig 4.15 Bottom view of fabricated complementary symmetrical ring resonator bandstop filter

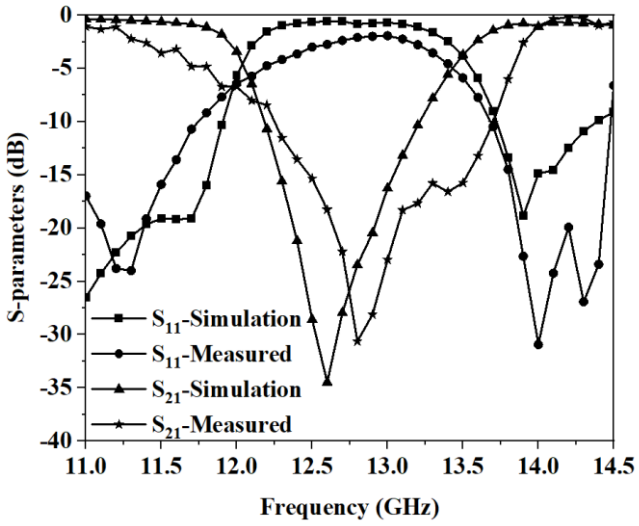

Fig 4.16 Simulation and measured S-parameters of complementary symmetrical ring resonator bandstop filter

The variations in the S21 are due to dielectric losses, SMA connector and cable losses. The shift in the passband frequency may be due to dimensional tolerances during etching of the copper material at the time of fabrication.

The designed complementary symmetrical ring resonator bandstop filter is simulated with an Ansys HFSS simulator using the finite element method. The equivalent circuit is determined from the simulation results of HFSS and the circuit is simulated using AWR design to determine the S_{11} and S_{21} response. The comparison of S_{11} and S_{21} simulation results is shown in Fig 4.10. The fractional bandwidth of the simulated bandstop filter is 11.9% with stopband from 12 GHz - 13.5 GHz. The proposed filter has a center frequency of 12.72 GHz. The maximum attenuation obtained is nearly 39 dB in the stopband.

The fractional bandwidth obtained for the equivalent circuit is 11.2% at center frequency 12.58 GHz with stopband from 11.9 GHz - 13.3 GHz. The maximum attenuation obtained through electrical simulation is nearly 36 dB. The simulation and equivalent circuit results have a good agreement. The electric field distribution for the bandstop filter at 11.5 GHZ, 12.6 GHz and 14 GHz are shown in Fig 4.11 to Fig 4.13. The signal propagation from input port to output port is observed in Fig 4.11 and Fig 4.13. The signal inhibition is observed in Fig 4.12.

The fabricated top and bottom views of the proposed bandstop filters are shown in Fig 4.14 and Fig 4.15 respectively. The measured and simulation results are compared in Fig 4.16. The frequency range of the bandstop filter is 12.1 GHz - 13.7 GHz lies in Ku-band from the measurement results. The fractional bandwidth is 12.4%. The maximum stopband attenuation is nearly 31 dB. An insertion loss of nearly 4 dB is obtained in the passband with measurement. The performance of the designed bandstop filter is compared with published work in Table 4.6.

The designed filter is compact and has high stopband attenuation when compared with published work.

Table 4.6 Comparison of complementary symmetrical ring resonator BSF with published works

References	**Center frequency (GHz)**	**Fractional Bandwidth (%)**	**Stopband Attenuation (dB)**	**Size (λ_g^2)**
[50]	11.4	9.6	35	0.75
[51]	3.5	9.2	21.6	3.2
[52]	2.4	8.3	24	2.13
[22]	3.7	53	27	0.28
[53]	3.33	3	12.08	0.72
[54]	10.74	14.7	20	2.77
Complementary symmetrical ring resonator BSF	12.87	12.4	31	0.55

4.5 Conclusion

In this chapter, compact bandpass and bandstop filters are designed using complementary resonators. For bandpass filter, gaps and vias are also introduced for realising the desired passbands for S-band applications, whereas for bandstop filter only complementary structures are able to give the desired stopbands for Ku band applications. Both filters have shown good performance characteristics with complementary metamaterial structure. Compactness is achieved for bandpass filters by using complementary structure. Compactness and wide stopband are obtained for bandstop filter by using complementary structures.

Chapter 5

Multiband bandpass filters using a combination of metamaterials and complementary metamaterials

5.1 Introduction

For multiband operations filters are significant components in microwave and millimeter wave transceivers. In upcoming applications, several communication standards are provided for operation especially in mobile terminals also the size of the filter needs to be reduced to meet the mass and volume requirements of the entire system particularly for satellite system and mobile devices. Multiband bandpass filters are an attractive solution to select multiple bands using single filter with a relatively compact circuit size. To incorporate two or more desired communication bands in a single unit and to filter unwanted frequencies, filters with a multi-band response have attracted more and more interest in modern devices implemented for different applications. Many applications are emerging in millimeter wave region like broadcasting, mobile phone and remote sensing. GPS application falls in L band and WLAN and Wimax applications are in the C band. All the above-mentioned applications need multiband bandpass filter.

Several design methods are proposed for multiband bandpass filters in published literature. D.C.H. Bong (2019) et al. synthesized a dual bandpass filter using a chained response method which has multiple passbands at center frequencies of 26.1 GHz and 27.9 GHz with fractional bandwidth of less than 1% for both bands and with insertion loss of 1 dB, 1.4 dB respectively, but the designed filter is large in size [55]. D. Bukuru (2017) et al. presented a compact quad bandpass filter by using two coupled half-wavelength quad mode stepped impedance resonators. The filter has passband center frequencies at 2.4 GHz, 3.3 GHz, 5.38 GHz and 6.48 GHz with fractional bandwidth of 3%, 6.41%, 3.7 %, 4.56 % and insertion loss of 1.9 dB, 1.6 dB, 3.5 dB, 3.2 dB respectively. But, the filter has high insertion loss [31]. C.F. Chen (2012) et al. designed a bandpass filter using a coupling technique which has passbands at 1.55 GHz, 2.79 GHz, 3.29 GHz, 4.47 GHz with fractional bandwidth of 3.1 %, 3.22 %, 2.79 %, 2.23 % and insertion loss of 2.8 dB, 2.9 dB, 2.6 dB and 2.3 dB respectively. But this design has high insertion loss [56]. Y. Guo (2018) et al. proposed a quint bandpass filter using a two-layer PCB manufacturing technique, EBG material and lumped capacitors that have center frequencies at 1.53 GHz, 1.9 GHz, 2.35 GHz, 2.86 GHz and 3.3 GHz with fractional bandwidth of 1.91%, 1.31%, 1.62%, 1.05% and 0.97% and insertion loss of 2.2 dB, 3.6 dB, 2.5 dB, 2.6 dB and 5.4

dB respectively, but the size of the filter is large due to periodic structure [57]. J. Ai (2016) et al. designed a multiband bandpass filter using three quarter wave stepped impedance resonators with a common short point to the ground that has center frequencies at 2.1 GHz, 3 GHz, 4 GHz, 4.7 GHz, 7.2 GHz with fractional bandwidth of 13.7%, 5.6%, 10.5%, 5.1% and 2.9% and insertion loss of 0.98 dB, 1.78 dB, 1.22 dB, 1.77 dB and 2.39 dB respectively, but this design has high insertion loss at lower frequencies [58].

H. Y. Gao (2016) et al. proposed two dual bandpass filters one using complementary split ring resonators, complementary spiral resonators (CSR) on tapered substrate integrated waveguide. The designed filter pass bands have center frequencies at 4.32 GHz and 5.52 GHz with fractional bandwidth of 5.76% and 4.98% and insertion loss of 2.79 dB and 2.92 dB respectively. Second filter is proposed with substrate integrated waveguide has passband center frequencies at 3.84 GHz and 4.96 GHz with fractional bandwidth of 6.69% and 5.28% and insertion loss of 1.65 dB and 3.33 dB respectively. But the filter has high insertion loss [59]. A. Rouabhi (2022) et al. developed a filter with dual passbands using tapered SRRs which consist of asymmetric shaped square rings with interlinking has center frequencies at 5.02 GHz and 8.92 GHz with fractional bandwidth of less than 1% for both bands. The insertion loss is 6.22 dB and 5.23 dB respectively. But the filter has high insertion loss and low fractional bandwidth [60].

H. Fabian Gongora (2021) et al. presented a tunable triband frequency selective surface unit cell based on varactor diode loaded split ring slots. When the varactor diode is reverse biased, capacitance is introduced between the split rings then the resonant frequencies are at 8.74 GHz, 10.03 GHz and 11.77 GHz with insertion loss of 0.8 dB, 1.4 dB and 1.7 dB respectively, when diode is off, the resonant frequencies are at 8.53 GHz, 9.7 GHz and 11.47 GHz with insertion loss of 1.1 dB, 2.3 dB and 2.4 dB respectively [61]. A. Kumar (2017) et al. proposed a compact tri-band bandpass metamaterial filter based on a meander line with a rectangular stub that has center frequencies at 2.1 GHz, 5.7 GHz and 7.3 GHz with fractional bandwidth of 57.1%, 8.7% and 4.1%, insertion loss of 0.8 dB, 1.6 dB and 2.4 dB respectively [62].

M. U. Rahman (2018) et al. designed a bandpass filter for three bands using resonators and stub loading on line. The resonators are further coupled with internal resistors for dual-mode operation, but the size of the filter is large [36] . N. Kumar (2014) et al. presented a compact three stubs loaded open-loop resonator-based triple bandpass filters, one filter has passband center frequencies at 1.59 GHz, 3.12 GH and 4.02 GHz with fractional bandwidth of 15.7%, 12.7% and 5.71%, another one has passband center frequencies at 1.93 GHz, 3.6 GHz and 4.89 GHz with fractional bandwidth of 19.2%, 11.6% and 2.86% respectively [63].

Designing a multiband bandpass filter is complex as all the passbands must have good performance. Several techniques are to be involved in the design, to get better performance for all bands. Metamaterials, complementary metamaterials, gaps, vias, stubs and stepped impedance resonators are employed to improve stop band attenuation for stop bands in between passbands and to improve return loss for pass bands. Novel structures like EI coupling structures are used for filter design at higher 5G band application. Stepped impedance resonators are also employed in the design of filters.

5.2 Stepped impedance resonators

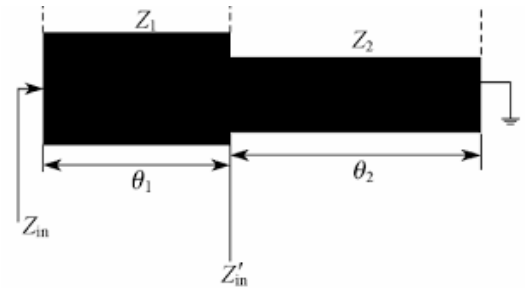

Fig 5.1 Stepped impedance resonator

Stepped impedance is realized with transmission lines of low and high impedances. Stepped impedance resonator is made up of two transmission lines with different lengths and characteristic impedance as shown in Fig 5.1. The resonant frequency of stepped impedance resonator is realized by adjusting the high and low impedance of the lines. These resonators when applied to filters suppress spurious frequencies and also control the insertion loss.

5.3 Design of EI-shaped metamaterial and complementary split ring resonator based multiband bandpass filter for higher 5G applications

EI-shaped metamaterial structure and vias are proposed along the microstrip line to design a bandpass filter. EI-shaped unit cell is designed as LC resonant circuit to resonate at higher frequencies. CSRRs are placed beneath the microstrip line in the proposed design to generate multiple bands at higher 5G frequency bands. The design specifications are listed in Table 5.1.

Table 5.1 Design specifications of EI shaped metamaterial and CSRR BPF

Parameter	Value
Frequency band of operation	Higher 5G
Center frequency	38.75 GHz, 39.08 GHz, 40.02 GHz, 42.02 GHz and 42.93 GHz
Feed impedance	50 Ω
Substrate material	RT Duroid 4003C
Dielectric constant	3.55
Substrate thickness	0.813mm
Copper laminate thickness	35 µm
Order of the filter	3
Bandwidth	0.2 GHz, 0.04 GHz, 0.35 GHz,0.11 GHz, 0.1 GHz.
Isolation	24 dB, 30 dB,32 dB,48 dB, 23 dB
Insertion Loss	1.67 dB, 2 dB, 1.54 dB, 2.45 dB, 2 dB
Return Loss	18 dB, 17 dB, 20 dB,13.7 dB, 21.5 dB.
Q-factor	977

The width of the microstrip line for the multi-bandpass filter is 0.95mm and the length of the microstrip line is 14mm using equations [2.4-2.6] for 50Ω feed impedance. The diameter of the vias is 0.4mm and the spacing between them is 3.7mm. EI-shaped unit cell is shown in Fig 5.2. and its dimensions are mentioned in Table 5.2. Complementary split ring resonator is shown in Fig 5.3 and its dimensions are listed in Table 5.3. The layout of the EI shaped metamaterial quint bandpass filter is shown in Fig 5.4.

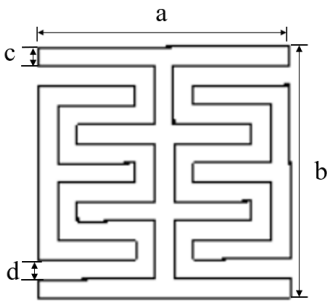

Fig 5.2 Structure of EI-shaped metamaterial unit cell

Table 5.2 Dimensions of EI shaped metamaterial unit cell

Parameter	**a**	**b**	**c**	**d**
Value (mm)	2.6	2.6	0.2	0.2

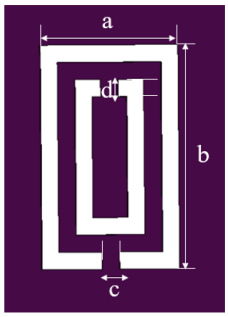

Fig 5.3 Structure of complementary split ring resonator

Table 5.3 Dimensions of complementary split ring resonator

Parameter	**a**	**b**	**c**	**d**
Value (mm)	0.8	1.3	0.1	0.1

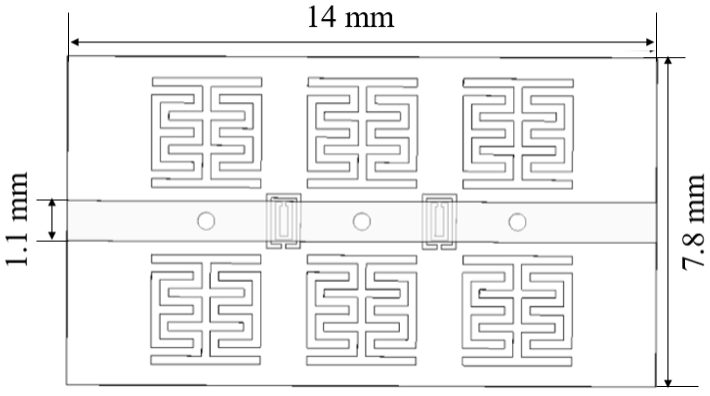

Fig 5.4 Layout of the EI-shaped metamaterial quint bandpass filter

5.3.1. Results and discussion

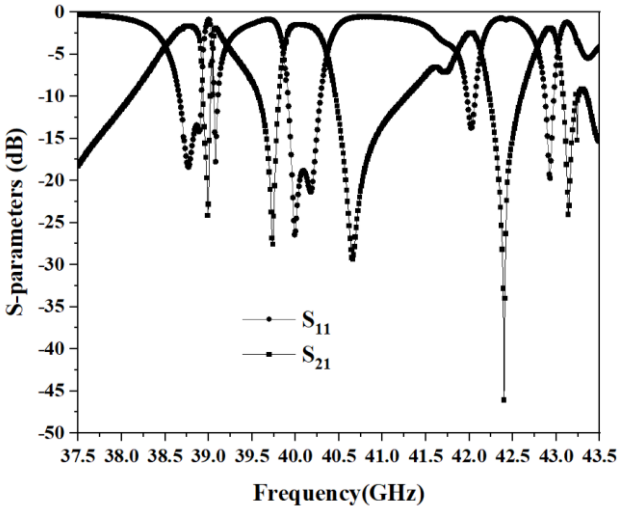

Fig 5.5 S-parameters of the simulated EI-shaped metamaterial quint bandpass filter

The proposed bandpass filters are simulated by the finite element method (FEM) using the software package ANSYS's HFSS. The S-parameters of the simulated quint passband filter is shown in Fig 5.5. The response of the quint bandpass filter has a frequency range from 38.65 GHz-38.85 GHz, 39.06 GHz-39.1 GHz, 39.9 GHz-40.25 GHz, 41.96 GHz-42.07 GHz, 42.87 GHz-42.97 GHz. The proposed quint bandpass filter has fractional bandwidth of 0.5%, 0.1%, 0.94%, 0.23% and 0.23% at the respective frequency bands. The insertion loss of the quint bandpass filter is 1.67 dB, 2 dB, 1.54 dB, 2.45 dB and 2 dB respectively at the center frequencies. The return loss is greater than 13.7 dB all over the passbands and band-to-band isolation is better than 24 dB. The electric field distribution of quint passbands is shown in Fig 5.6 to Fig 5.10. The signal propagation from input port to output port is observed at all pass band frequencies. The proposed quint bandpass filter is compared with published works in Table 5.4.

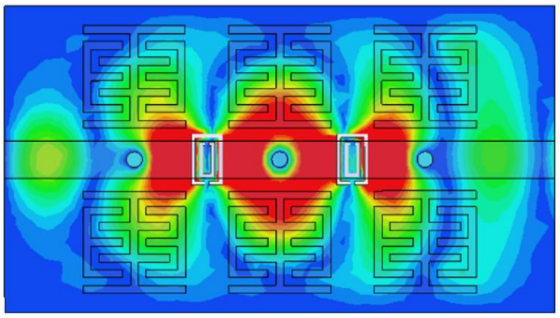

Fig 5.6 Electric field distribution of the passband at 38.75 GHz of quint bandpass filter

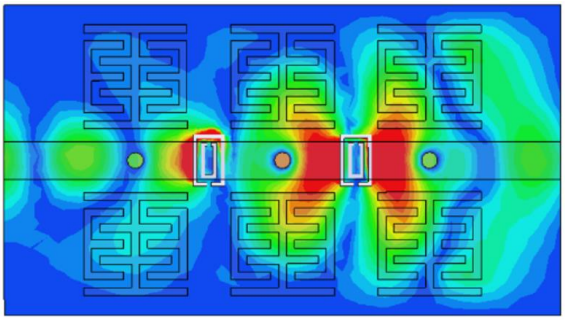

Fig 5.7 Electric field distribution of the passband at 39.08 GHz of quint bandpass filter

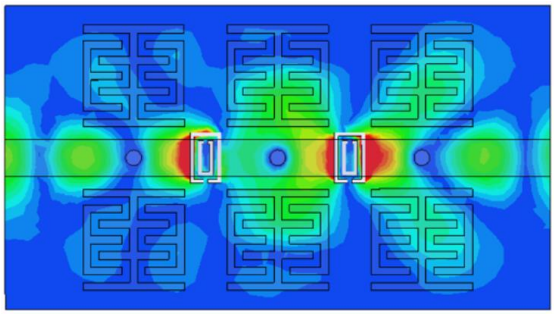

Fig 5.8 Electric field distribution of the passband at 40.02 GHz of quint bandpass filter

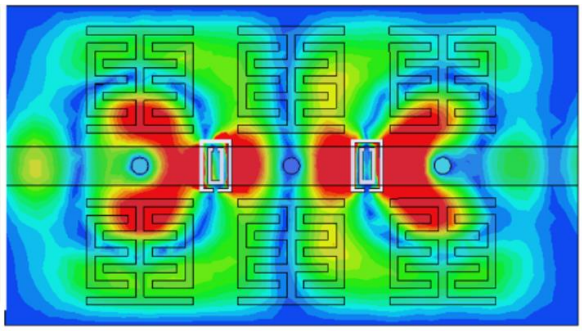

Fig 5.9 Electric field distribution of the passband at 42.02 GHz of quint bandpass filter

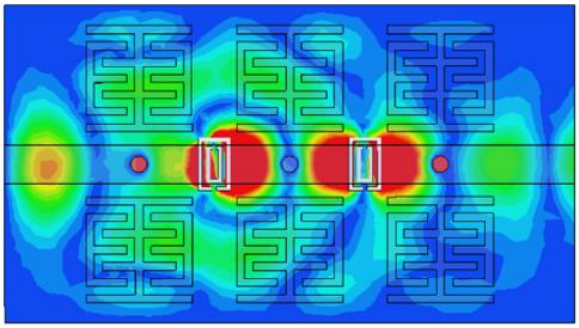

Fig 5.10 Electric field distribution of the passband at 42.93 GHz of quint bandpass filter

Table 5.4 Comparison of EI shaped metamaterial and CSRR BPF with published works

References	**Frequency range (GHz)**	**FBW (%)**	**IL (dB)**	**Size (λ_g^2)**
[64]	4.22-4.38,4.59-4.61, 4.88-4.93	3.7, 0.4, 1	<1, <1, <1	0.48
[65]	0.5-1.03,2-3.41, 3.18-3.8,4.05-4.9,5.2-6.25	10.6, 33.5, 17.6, 16, 20	0.12, 0.68, 0.28, 0.65, 0.57	0.01
[66]	0.43-0.68, 1.5-1.54, 3.64-3.91,4.69-4.72, 4.2-5.6	50, 1.4, 5.8, 1.2, 5.5	0.1, 0.2, 0.2, 0.25, 0.15	0.01
[67]	2.31-2.46, 3.35-3.68, 5.1-5.4, 6.63-6.91	6.4, 9.4, 3.8, 4.9	0.5, 1.3, 1.3, 1	0.09
[57]	1.52-1.54, 1.8-1.85, 2.3-2.35, 2.8-2.84, 3.3-3.32	1.91, 1.13, 1.62, 1.05, 0.97	2.2, 3.6, 2.5, 2.6, 5.4	0.21
[58]	1.97-2.28, 2.92-3.1, 3.7-4.1, 4.55-4.8, 7.12-7.36	13.7, 5.6,10.5, 5.1, 2.9	0.98, 1.78, 1.22, 1.77, 2.39	0.1
Quint band pass filter	38.65-38.85, 39.06-39.1, 39.9-40.28, 41.96-42.06, 42.87-42.97.	0.5, 0.1, 0.94, 0.23, 0.23	1.67, 2, 1.54, 2.45, 2	7

5.4 Design of dual band bandpass filters using metamaterials and spiral resonators for L band and S band applications

Bandpass filter is designed with gaps, vias and complementary split ring resonators [4.3]. A dual bandpass filter is designed by modifying the gap on the microstrip line as spiral resonator. The design specifications are shown in Table 5.5.

Microstrip line has a width of 2.25 mm for impedance matching with 50Ω feed line. Gaps along the microstrip line are 0.15 mm while via filled with copper has a diameter of 0.4 mm and placed through the substrate from the microstrip line to the ground plane. Complementary triple concentric split ring resonators are etched on the ground plane beneath the microstrip line.

Table 5.5 Design specifications of dual bandpass filter

Parameter	Value
Frequency band of operation	L band, S band
Center frequency	1.32 GHz, 2.47 GHz
Feed impedance	50 Ω
Substrate material	RT Duroid 3010
Dielectric constant	10.2
Substrate thickness	0.13mm
Copper laminate thickness	35 µm
Order of the filter	2
Bandwidth	0.1 GHz, 0.2 GHz
Isolation	20 dB
Insertion loss	1.3 dB, 1.8 dB
Return loss	15 dB, 16 dB
Q-factor	13

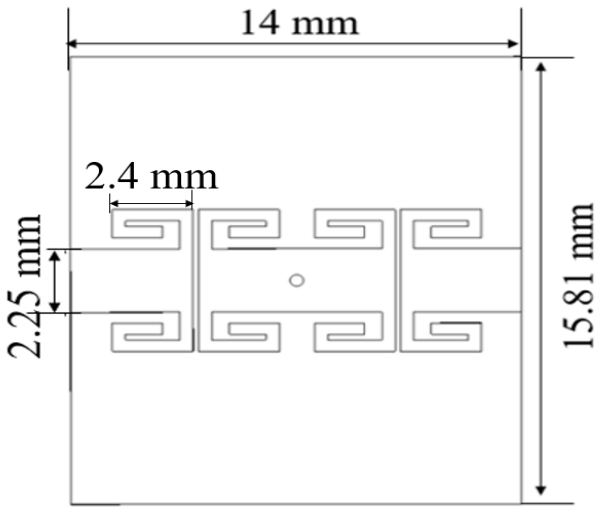

Fig 5.11 Top view of the dual bandpass filter

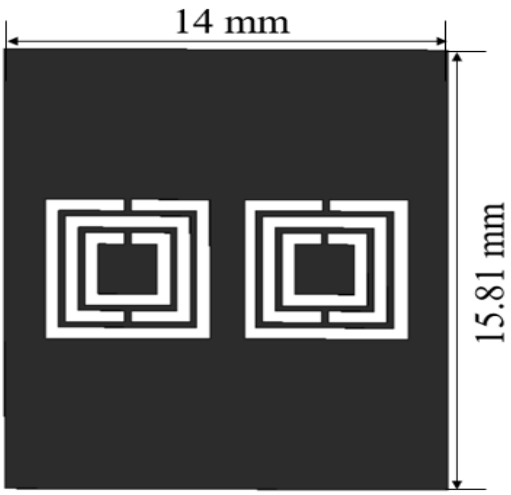

Fig 5.12 Bottom view of the dual bandpass filter

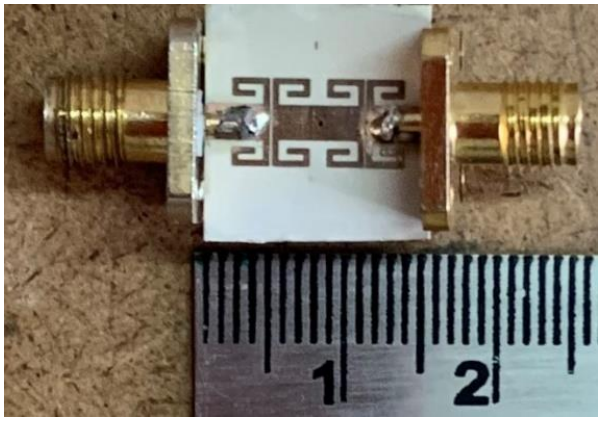

Fig 5.13 Fabricated top view of the dual bandpass filter

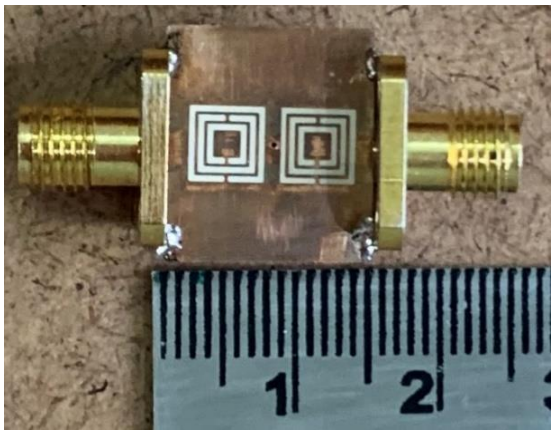

Fig 5.14 Fabricated bottom view of the dual bandpass filter

The gaps along the microstrip line are modified as spiral resonator to have the effect of coupled lines. The dimensions of the filter are 14 mm × 15.81mm which is approximately 0.19

$\lambda_g \times 0.21\ \lambda_g$, where λ_g is the guided wavelength at the lowest center frequency. The top and bottom views of the simulated dual bandpass filter are shown in Fig 5.11 and Fig 5.12, respectively while that of fabricated prototypes are shown in Fig 5.13 and Fig 5.14, respectively.

5.4.1 Results and discussion

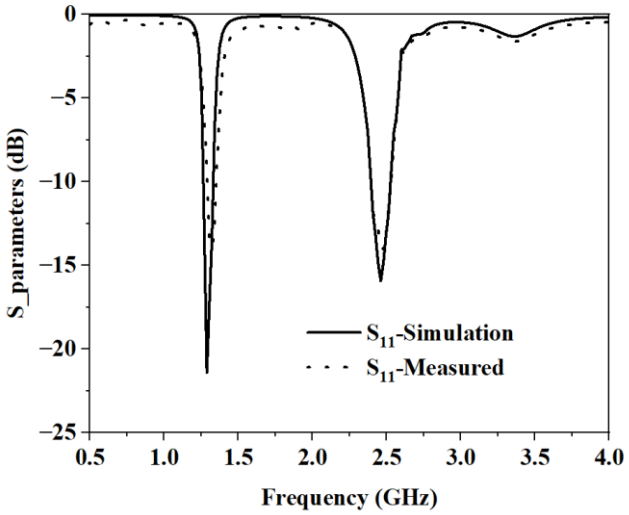

Fig 5.15 Simulation and measured return loss S_{11} of the dual bandpass filter

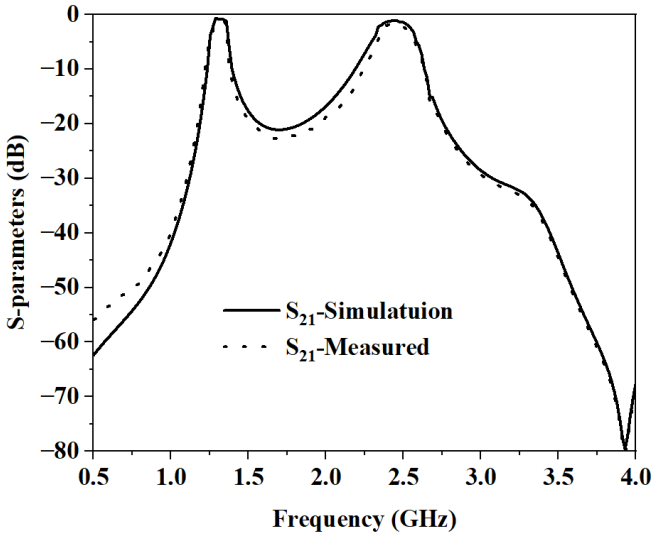

Fig 5.16 Simulation and measured insertion loss S_{21} of the dual bandpass filter

The simulation and measured S_{11} and S_{21} results for the dual bandpass filter are shown in Fig 5.15 & Fig 5.16, respectively. The simulated dual bandpass filter has center frequencies at 1.3 GHz and 2.46 GHz with fractional bandwidth of 8% and 4.85% for first and second band respectively. The minimum insertion loss obtained is 1.15 dB and 1.7 dB for first and second bands respectively. The return loss is 21 dB for the first band and 17 dB for the second band. The measured dual bandpass filter has passband center frequencies at 1.32 GHz and 2.47 GHz lies in L-band and S-band respectively. The fractional bandwidth of the proposed filter is 7.5%

for the first band and 4.85% for the second band. The minimum insertion loss obtained is 1.3 dB for the first band and 1.8 dB for the second band. The return loss is 15 dB for the first band and 16 dB for the second band. The roll-off rate for the first band is 203 dB/GHz on the lower side, 64 dB/GHz on the upper side, for the second band 35 dB/GHz on the lower side and 94.6 dB/GHz on the upper side. The dual bandpass filter is of size 0.039 λ_g^2 and is compact and useful for GPS and WLAN applications. From Table 5.6. it is observed that the dual bandpass filter is compact.

Table 5.6 Dual bandpass filter comparison table

References		**Center frequency (GHz)**	**Fractional bandwidth (%)**	**Insertion loss (dB)**	**Size (λ_g^2)**
[59]	**Type 1**	4.32,5.52	5.76,4.98	2.79,2.92	0.22
	Type 2	3.84,4.96	6.69,5.28	1.65,3.33	0.07
[60]		8.89,11.04	<1, <1	2.68,2.61	3.3
[68]		5.57,7.84	6.8,4.1	1.8,2	0.22
[69]		5.02,8.92	<1, <1	6.22,5.23	0.17
Dual bandpass filter		1.32, 2.47	7.5,4.85	1.3,1.8	0.039

5.5 Design of triple band bandpass filters using metamaterials, stepped impedance resonators and stubs for L-band and S-band applications

Triple bandpass filter is realised from dual bandpass filter [5.4] by introducing T-shaped stubs on the microstrip line to lie between the spiral resonators. The T-shaped stubs with optimum dimensions are added in between spiral resonators to improve the return loss and to generate triple pass bands. Further stepped impedance resonators are introduced along the microstrip line at the input and output ports. The design specifications of triple bandpass filter are listed in Table 5.7.

Table 5.7 Design specifications of triple bandpass filter

Parameter	Value
Frequency band of operation	L band, S band
Center frequency	1.29 GHz, 2.27 GHz, 3.21 GHz
Feed impedance	50 Ω
Substrate material	RT Duroid 3010
Dielectric constant	10.2
Substrate thickness	0.13mm
Copper laminate thickness	35 µm
Order of the filter	2
Bandwidth	0.15 GHz, 0.32 GHz, 0.1 GHz
Isolation	20 dB for both bands
Insertion loss	1.6 dB, 1.3 dB, 1.8 dB
Return loss	17 dB, 13 dB, 18 dB
Q-factor	32

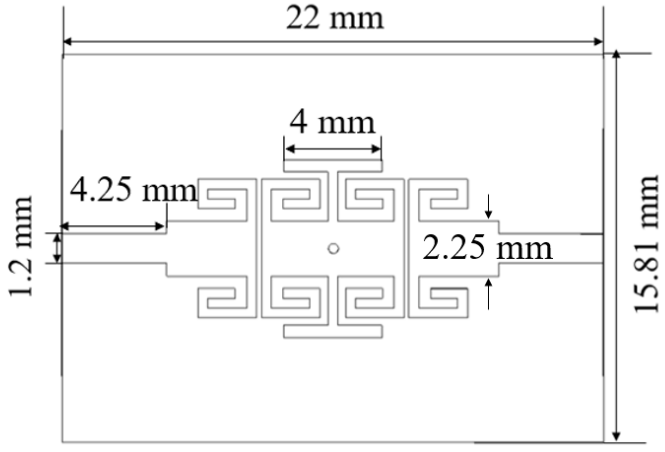

Fig 5.17 Top view of the triple bandpass filter

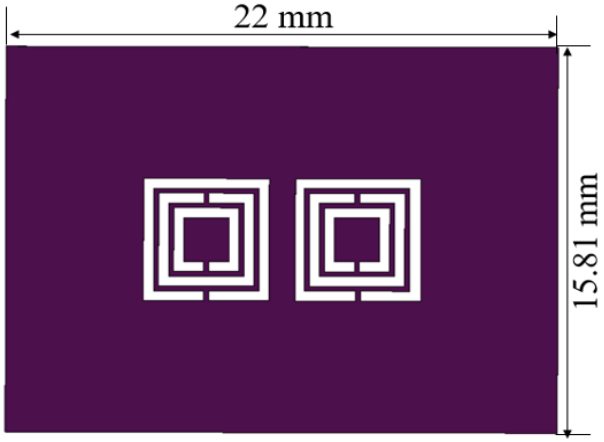

Fig 5.18 Bottom view of the triple bandpass filter

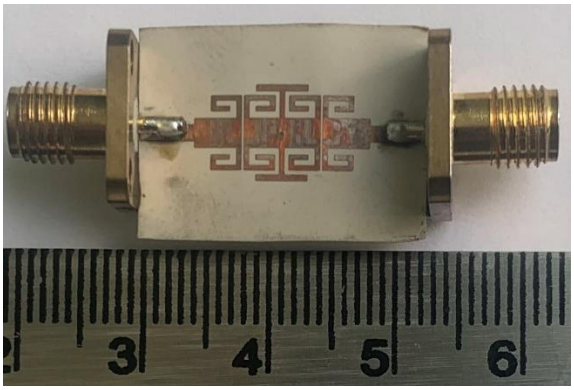

Fig 5.19 Fabricated top view of Triple bandpass filter

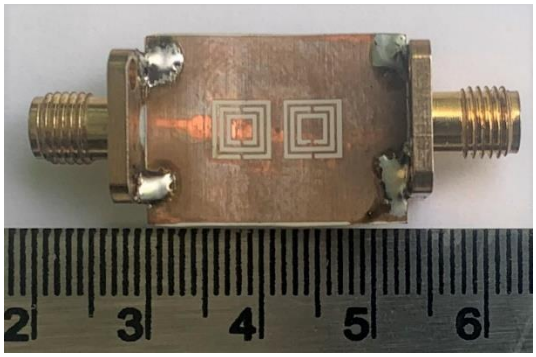

Fig 5.20 Fabricated bottom view of Triple bandpass filter

The dimensions of the designed filter are 22mm × 15.81mm which can also be represented as 0.3 λ_g × 0.2 λ_g, where the guided wavelength (λ_g) is calculated at the lowest center frequency. The top and bottom views of the triple bandpass filter are shown in Fig 5.17 and 5.18, while that of the fabricated filters are shown in Fig 5.19 and 5.20, respectively.

5.5.1 Results and discussion

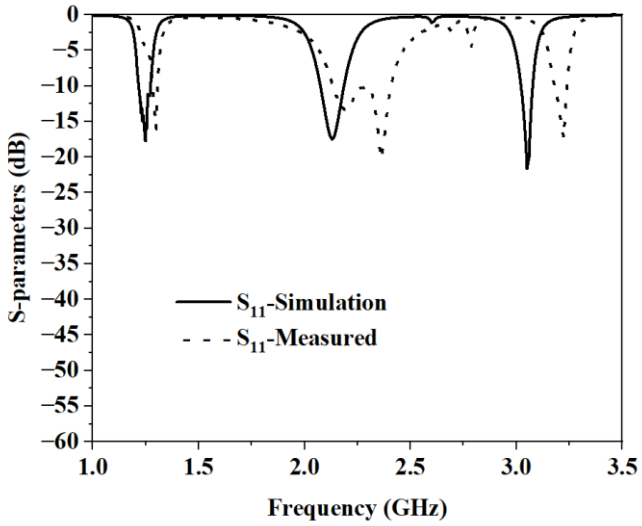

Fig 5.21 Simulation and measured return loss S_{11} of the triple bandpass filter

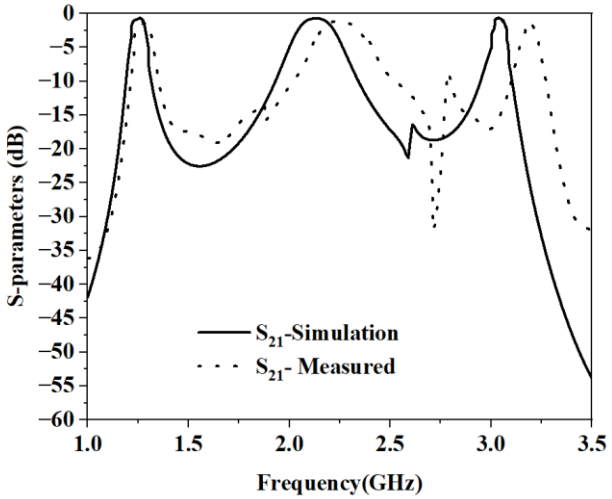

Fig 5.22 Simulation and measured insertion loss S_{21} of the triple bandpass filter

The simulation and measurement results for S_{11} and S_{21} of the triple bandpass filter are shown in Fig 5.21 & Fig 5.22, respectively. The simulated triple bandpass filter has center frequencies at 1.27 GHz, 2.2 GHz and 3 GHz lies in L-band and S-band. The fractional bandwidth for the first band is 1%, for the second band is 6% and for the third band is 1.8%. The minimum insertion loss obtained is 1.2 dB, 0.99 dB and 1.5 dB respectively. The return loss is 18 dB,17 dB and 22 dB respectively. The measured triple bandpass filter have center frequencies at 1.29 GHz, 2.27 GHz and 3.21 GHz. The fractional bandwidth is 1.16%, 11.4% and 1.86% for all three bands respectively. The minimum insertion loss obtained is 1.6 dB, 1.3 dB and 1.8 dB respectively in the passband. The return loss is 17 dB,13 dB and 18 dB respectively. The roll-off rate for the first band is 262 dB/GHz on the lower side and 115 dB/GHz on the upper side, for the second band it is 56 dB/GHz on the lower side, 49 dB/GHz

on the upper side, for the third band it is 47 dB/GHz on the lower side and 180 dB/GHz on the upper side.

The triple bandpass filter size is 0.06 λ_g^2 which is compact and useful for GPS, WLAN, WiMAX applications. The right shift in frequency response of return loss is observed may be due to dimensional tolerances at the time of fabrication. The variations in S21 may be due to cable losses, SMA connector losses. From Table 5.8. it is observed that the triple bandpass filter is compact.

Table 5.8 Triple bandpass filter comparison table

References	**Center frequency (GHz)**	**Fractional bandwidth (%)**	**Insertion loss (dB)**	**Size (λ_g^2)**
[61]	8.63,9.86,11.62	2.4,3.3,2.5	0.8,1.4,1.7	0.97
[36]	1.575,2.4,3.45	10,5,11	0.7,1.14,0.3	0.54
[63]	1.93,3.6,4.89	19.2, 1.6, 2.86	-	0.076
[35]	1.96,2.6,3.9	5,11,3	1.5,0.6,1.83	0.41
[62]	2.1,5.7,7.3	57.1,8.7,4.1	0.8,1.6,2.4	0.073
Triple bandpass filter	1.29,2.27,3.21	1.16,11.4,1.86	1.6,1.3,1.8	0.06

5.6 Conclusion

A Quint bandpass filter is designed using EI-shaped resonators and complementary split ring resonators for higher 5G applications. Spiral resonators and T shaped stubs are applied for compact design. A compact dual bandpass filter is designed for GPS and WLAN applications. A compact triple bandpass filter is designed using complementary triple concentric split ring resonators, spiral resonators and T shaped stubs for GPS, WLAN and Wimax applications.

Chapter 6

Bandpass filters using microstrip coupled resonators

6.1 Microstrip coupled resonators

Coupled resonator circuits are used for the design of compact microwave/millimeter wave filters. Coupled resonator circuits can be applied for the design of waveguide filters, dielectric resonator filters, ceramic combline filters and microstrip filters. The coupling between the microstrip line and resonators, among resonators is based on the proximity and the associated fringe fields. Resonators can be coupled directly or in proximity to the microstrip line. Different types of coupling configurations like electric coupling, magnetic coupling and mixed-coupling are shown in Fig 6.1.

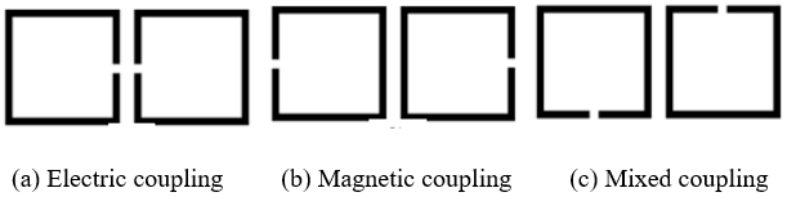

Fig 6.1 Types of coupling

Commercial applications like fixed-satellite, mobile satellite, remote sensing applications comes under Upper Microwave Flexible Use Services. Several papers are published to design bandpass filters at higher frequencies using different waveguide technologies. H. Hanen (2012) et al. designed a bandpass filter at 28 GHz frequency with dielectric waveguide which has fractional bandwidth of 5.14% and insertion loss of 0.15 dB. But the size of the filter is large [70]. K. Onaka (2017) et al. proposed a bandpass filter using a quartz crystal waveguide at 28 GHz band which has fractional bandwidth of 10.4% and insertion loss of 1.2 dB. But the filter size is large [71]. D. C. Bong (2019) et al. used waveguide topology to design a dual bandpass filter at 26 GHz and 28 GHz which has fractional bandwidth less than 1% for both bands and insertion loss is 1 dB and 1.4 dB for first and second bands respectively. Size of the filter is large [55].

Coupled transmission lines are proposed in the literature for design of filters [72]. Metamaterial structures can exhibit novel electromagnetic properties at microwave and millimeter wave frequencies that cannot be obtained using conventional materials. By employing metamaterial units as coupled resonators, it is possible to achieve good miniaturization in filters. A.A. Ibrahim (2018) et al. designed a bandpass filter using microstrip

coupled split-ring resonators that have a center frequency at 2.4 GHz with fractional bandwidth of 12.5%. The insertion loss and return loss are 0.7 dB and 15 dB respectively [30]. Ghaith Mansour et.al. proposed a cross-coupled microstrip bandpass filter composed of C-shaped square resonators and tapped feed lines. The proposed bandpass filter resonates at 2GHz with fractional bandwidth of about 5%. The return loss is 25 dB, insertion loss is 6 dB in the passband which is high [73].

Mohammed Chetioui et.al. presented a cross-coupled trisection bandpass filter using open-loop resonators. The simulated trisection filter with a passband center frequency of 1.025 GHz exhibits an insertion loss of 0.6 dB, a return loss of 20 dB and fractional bandwidth of 10%. The rejection is larger than 30 dB at 1.09 GHz, but the filter size is large [74]. Rohit. et al. proposed a method to design a bandpass filter using a dual feed line and microstrip open-loop resonator structure. The proposed filter response produces passband frequency range of 5.3-5.4GHz, stopband attenuation of 50dB, return loss above 25dB. The fractional bandwidth of the filter is 1.86 % which is less [75]. A.J. Salim et.al. presented a bandpass filter using two open-loop resonators with polygonal structures. The fractional bandwidth is 10% at the center frequency of 2.4 GHz, with a return loss of about 26 dB and an insertion loss of 0.8 dB [76].

Mudrik Alaydrus et.al. proposed a four-pole bandpass filter using square open-loop resonators. The center frequency of the passband is located at about 2.45 GHz with fractional bandwidth of 4.89% and an insertion loss of 6.64 dB. But the filter has high insertion loss [77]. Nikita. V. Ivanov proposed an approach to define coupling characteristics of coupled resonators. The proposed bandpass filter resonates at 2.9 GHz with fractional bandwidth of 6.8%, return loss of 25 dB and insertion loss of 2dB. But filter size is large [78]. Ahmed. A. Ibrahim et.al presented a compact bandpass filter using microstrip coupled resonators. The proposed filter resonates at 3 GHz with FBW of 6.6%, insertion loss less than 1 dB and return loss of 25 dB [79].

Keeping the above techniques into consideration, a compact microstrip coupled metamaterial dual bandpass filter is proposed for Upper microwave flexible use services. A bandpass filter using EC-shaped coupled line resonators is designed for 37 GHz band for higher 5G mobile communications.

6.2 Compact dual bandpass filter using dual split rings resonator for upper microwave flexible use services

A dual bandpass filter is designed with dual split rings resonator unit cell. The unit cell is incorporated to the gaps on the microstrip line as coupled lines. The design specifications are listed in Table 6.1.

Table 6.1 Design specifications of dual split rings resonator BPF.

Parameter	Value
Frequency band of operation	Higher 5G
Center frequency	24.79 GHz, 28.37 GHz
Feed impedance	50 Ω
Substrate material	RT Duroid 4003
Dielectric constant	3.55
Substrate thickness	0.813mm
Copper laminate thickness	35 µm
Bandwidth	2.18 GHz, 0.65 GHz
Isolation	24 dB
Insertion loss	< 4.2. < 4.2
Return loss	>10 dB, 20 dB
Q-factor	43

A dual-split rings resonator dimensions are optimized to obtain better performance of the bandpass filter. The metamaterial structure homogeneity condition of a unit cell size less than one-fourth of the guided wavelength is considered for the design as shown in Fig 6.2. The dimensions of the dual-split ring resonator are shown in Table 6.2.

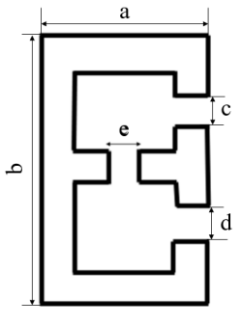

Fig 6.2 Dual-split rings resonator unit cell

Table 6.2 Dimensions of dual-split rings resonator unit cell

Parameter	**a**	**b**	**c**	**d**	**e**
Value (mm)	1.17	1.8	0.2	0.2	0.2

The microstrip line is coupled through dual split rings resonators. The dual split rings resonators are coupled through fringe fields due to proximity placement. The strength of coupling depends on the fringe fields. The dual split rings resonators have maximum electric field intensity at the open gaps of the resonator at resonance condition. Electric coupling is obtained as the open sides of the two coupled resonators are placed closely. The fringe fields are stronger near the gaps and decay outside the region. The top view of the proposed filter is shown in Fig 6.3. The main design occupies the area of 2.6 mm × 1.8 mm, which is $0.4\lambda_g \times 0.27\lambda_g$, where λ_g is the guided wavelength at a center frequency of the first band. The overall circuit size of the filter is 14 mm × 10.75 mm. The width of 14mm is chosen to match to the SMA connector size.

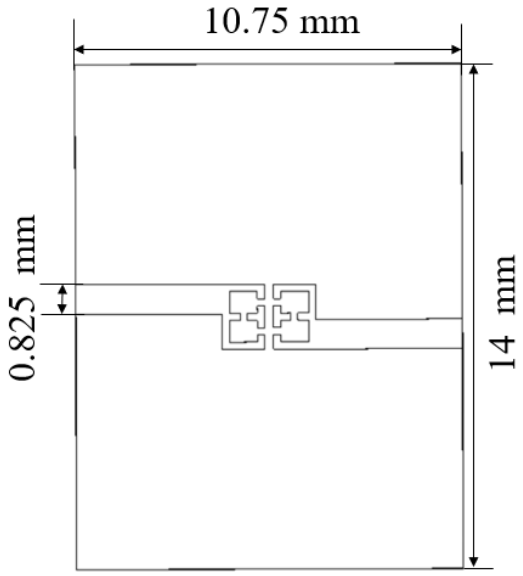

Fig 6.3 Top view of the dual-split ring resonator dual bandpass filter

6.2.1 Equivalent circuit realization

The lumped element equivalent circuit of the proposed dual split rings resonator dual bandpass filter is shown in Fig 6.4.

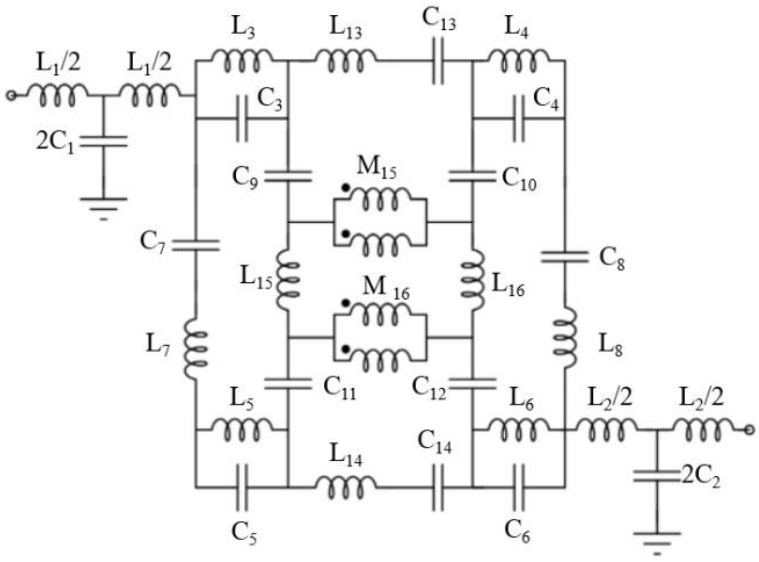

Fig 6.4 Equivalent circuit for dual split rings resonator bandpass filter

The T-circuit of $L_1/2$, $L_2/2$ and $2C_1$ and $2C_2$ represents the microstrip line on each side. L_3C_3, L_4C_4, L_5C_5 and L_6C_6 resonators represent equivalent dual split rings resonators. The coupling of microstrip line and resonators is represented using C_7 and C_8 and Inductance is represented using L_7 and L_8. Open slit gaps are represented using C_9, C_{10}, C_{11} and C_{12}. The coupling gaps are represented using C_{13} and C_{14}. Mutual inductance between coupling gaps is represented using L_{13} and L_{14}. Inductance and mutual inductance due to a T-shaped patch between open slits of proximately coupled resonators are represented using L_{15}, L_{16}, M_{15} and M_{16}.

The equivalent lumped element values of the proposed dual split rings resonator dual bandpass filter are $L_1 = L_2 = 0.0004$ nH, $C_1 = C_2 = 0.0375$ pF, $L_3 = L_4 = L_5 = L_6 = 0.8$ nH, $C_3 = C_4 = C_5 = C_6 = 0.02115$ pF, $C_7 = C_8 = 0.029$ pF, $L_7 = L_8 = 0.85$ nH, $C_9 = C_{10} = C_{11} = C_{12} = 0.02115$ pF, $L_{13} = L_{14} = 1.9$ nH, $C_{13} = C_{14} = 0.008$ pF, $L_{15} = L_{16} = 0.65$ nH and $M_{15} = M_{16} = 0.707$ nH.

6.2.2 Results and discussion

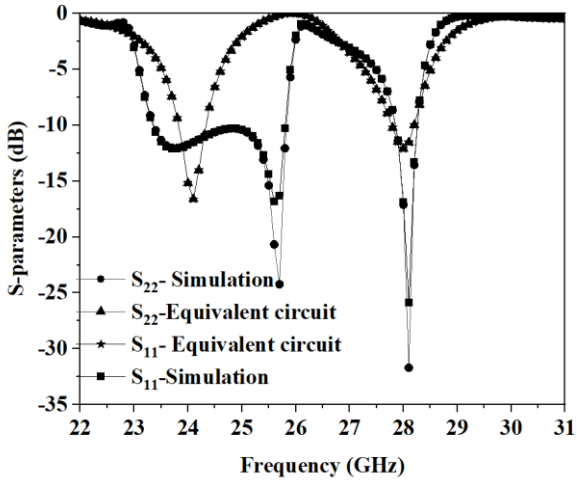

Fig 6.5 Comparison of S_{11} and S_{22} for simulation and equivalent circuit of dual split rings resonator dual BPF

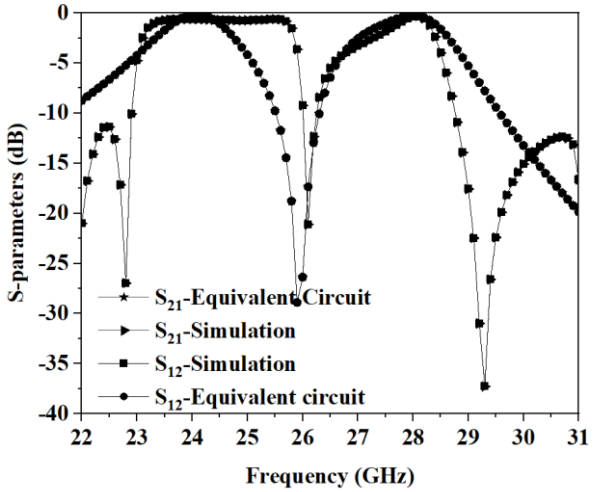

Fig 6.6 Comparison of S_{12} and S_{21} for simulation and equivalent circuit of dual split rings resonator dual BPF

The proposed dual-split ring resonator dual bandpass filter is simulated using the HFSS simulator and the finite element method. The equivalent circuit of the proposed dual-split ring resonator dual bandpass filter is simulated using an AWR design environment. The comparison of S-parameters S_{11}, S_{21}, S_{22} and S_{12} for HFSS simulation and lumped element equivalent circuits are shown in Fig 6.5 and Fig 6.6, respectively. The proposed design resonated in the frequency range from 23.6 to 25.6 GHz and 27.9 to 28.25 GHz from simulation results with pass band center frequency 24.6 GHz and 28 GHz respectively. The frequency of the lumped equivalent circuit ranged from 23.8–24.35 GHz and 27.7–28.2 GHz with pass band center frequencies at 24.075 GHz and 27.95 GHz. The fractional bandwidth of the proposed design is 8.1% and 1.1% for both bands and 2.28% and 1.78% from HFSS simulation and AWR simulation respectively. The insertion loss is less than 1 dB in both bands for the HFSS simulation and less than 0.5 dB in the AWR simulation

for lumped element equivalent circuits. In the proposed design, S_{12} and S_{22} are measured to verify the reciprocity of the design.

Fig 6.7 Top view of fabricated prototype for dual-split ring resonator dual bandpass filter

Fig 6.8 Bottom view of fabricated prototype for dual-split ring resonator dual bandpass filter

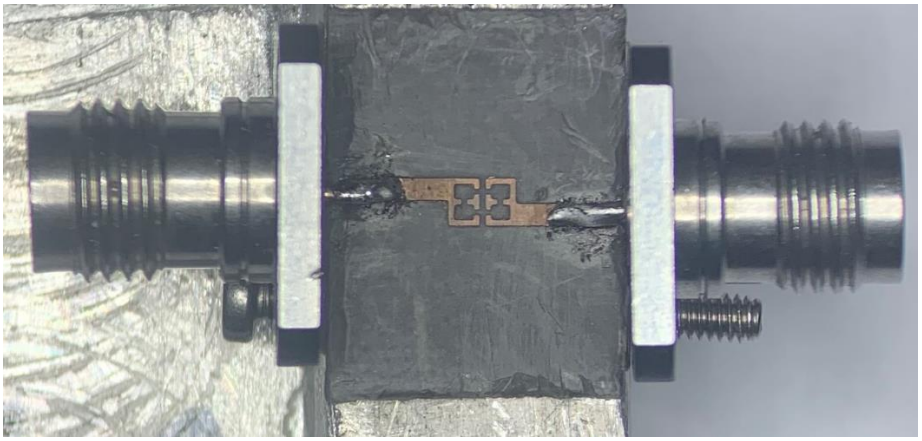

Fig 6.9 Top view of fabricated prototype along with an aluminum mounting box for dual-split ring resonator dual bandpass filter

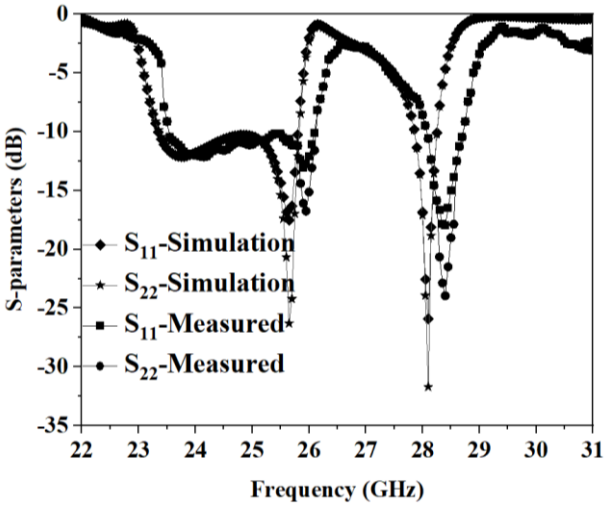

Fig 6.10 Comparison of S_{11} and S_{22} of dual split rings resonator dual bandpass filter for simulation and measurement

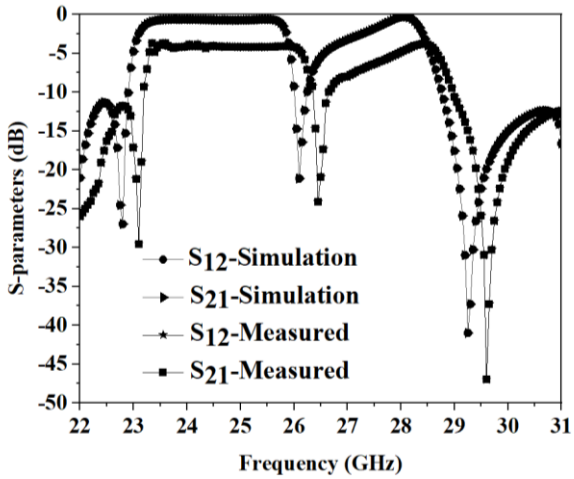

Fig 6.11 Comparison of S_{21} and S_{12} of dual split rings resonator dual bandpass filter for simulation and measurement

The proposed dual-split rings resonator dual bandpass filter is fabricated and measured to validate its performance using the network analyser N5222A. The fabricated prototypes of the

proposed dual-split ring resonator dual bandpass filter are shown in Fig 6.7 to Fig 6.9. The comparison of S-parameters S_{11}, S_{21}, S_{22} and S_{12} for HFSS simulation and measurement are shown in Fig 6.10 and 6.11 respectively. The frequency range for the measurement results is 23.8 GHz–25.98 GHz and 28.05 GHz–28.7 GHz with pass band center frequencies 24.79 GHz and 28.37 GHz lies in higher 5G band. The fractional bandwidth of the proposed design is 8.8% and 2.2% for the first band and second band, respectively from the measurement results. The insertion loss is less than 4.2 dB from the measurement results. From the comparison table 6.3, it can be concluded that the proposed design is compact, dual bands are observed using microstrip technology, which is compact. The variations are high in S21 may be due to more dielectric losses, SMA connectors losses, calibration losses in vector network analyser at higher frequencies.

Table 6.3 Comparison of dual split rings resonator BPF with published works

References	**Center frequency (GHz)**	**Fractional bandwidth (%)**	**Insertion loss (dB)**	**Size**
[80]	28	11	2.7	23×10 mm^2 3.19×1.38 λ_g^2
[70]	28	5.14	0.15	60 ×40 mm^2
[71]	27.95	10.4	1.2	33.7×3.4 mm^2 0.47×4.68 λ_g^2
[55]	26.1,27.9	<1	1, 1.4	30×18 mm^2 45×18 mm^2
[81]	33	18	2.6	0.3×0.126 mm^2
[82]	30	23.4	1.66	0.11×0.086 mm^2
[83]	28	9	1.6	16.8×12 mm^2 2.97×2.13 λ_g^2
Dual split rings resonator dual BPF	24.79,28.37	8.8, 2.2	<4.2	2.6×1.8 mm^2 0.1 λ_g^2

6.3. EC-shaped resonator microstrip coupled based bandpass filter for 37 GHz band 5G mobile communications

A microstrip coupled resonator bandpass filter is designed for upper microwave flexible-use services. The microstrip line is designed to match feed line of 50 Ω, which leads to a microstrip line width of about 1.2 mm (for the relative permittivity of 3.55). The E-shaped resonator is formed by using C shaped line of length λ_g and a line of length $\lambda_g/4$ to enhance coupling. To improve coupling between two E-shaped resonators, C-shaped resonators of length nearly $\lambda_g/2$ are placed facing each other and located in between two E-shaped resonators facing each other. The design specifications are mentioned in Table 6.4.

Table 6.4 Design specifications of EC shaped resonator BPF

Parameter	**Value**
Frequency band of operation	Higher 5G
Center frequency	38 GHz
Feed impedance	50 Ω
Substrate material	RT Duroid 4003 C
Dielectric constant	3.55
Substrate thickness	0.813mm
Copper laminate thickness	35 µm
Bandwidth	2 GHz
Insertion loss	0.37 dB
Return loss	37 dB
Q-factor	19

The proposed filter is designed on Rogers RT Duroid 4003C substrate material with a permittivity of 3.55, having a thickness of 0.813mm. The length and width of the proposed design are 13 mm and 9 mm respectively. The electrical size of the filter excluding input and output ports is $1.7\ \lambda_g \times 0.57\ \lambda_g$ where λ_g is the guided wavelength at the resonant frequency. The top view of the EC-shaped resonator microstrip coupled bandpass filter is shown in Fig 6.12.

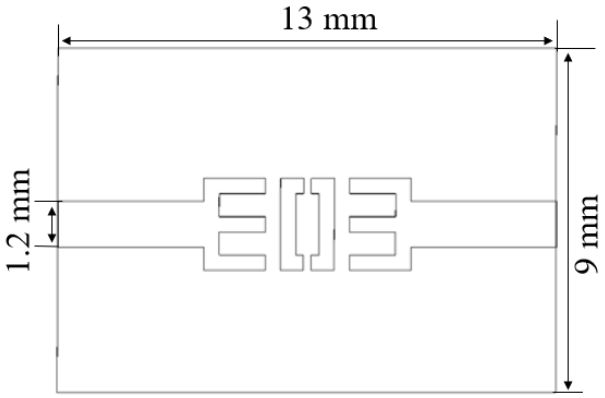

Fig 6.12 Top view of the microstrip coupled EC-shaped resonator bandpass filter

6.3.1 Results and discussion

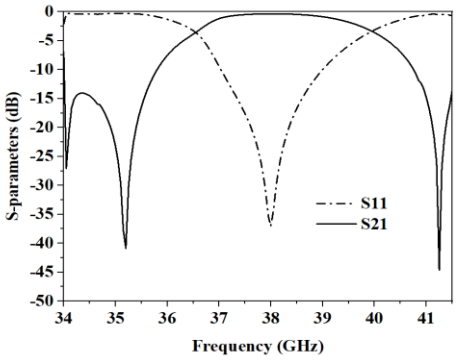

Fig 6.13 S-parameter of the simulated EC-shaped resonator microstrip coupled bandpass filter

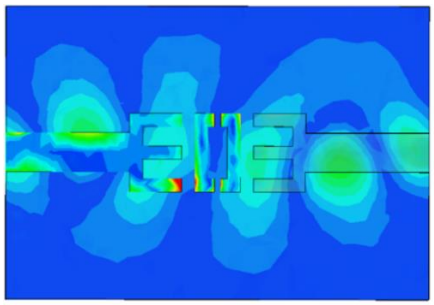

Fig 6.14 Electric field distribution of the EC-shaped resonator microstrip coupled bandpass filter for the pass band at 38 GHz frequency

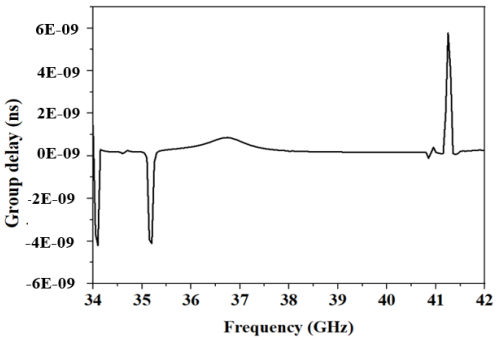

Fig 6.15 The group delay of the EC-shaped resonator microstrip coupled bandpass filter

The proposed design is simulated using Ansys HFSS simulator, a finite element method mesh analysis solver. The proposed EC-shaped resonator bandpass filter resonates at 38GHz frequency. The S-parameter of the simulated EC-shaped resonator microstrip coupled bandpass filter is shown in Fig 6.13. The proposed filter has a frequency range from 37 GHz - 39 GHz lies in higher 5G band. The fractional bandwidth of the filter is 5.26% at 38 GHz center frequency. The insertion loss realized for the filter is 0.37 dB. The return loss obtained for the filter is 37 dB. The EC-shaped resonator filter has transmission zeros at 35.2 GHz and 41.2 GHz respectively. The electric field distribution is shown in Fig 6.14. shows the electric field distribution from input port to output port is shown in Fig 6.14. The group delay of the filter is a measure of the average time delay of the filter as a function of frequency. The group delay is a convenient measure of the linearity of the phase to frequency. Flat group delay shows good filter response in passband. A group delay of nearly 0.25 ns is there in the entire passband as shown in Fig 6.15. Flat group delay is observed over the pass band frequencies. From the comparison table 6.5., it can be concluded that the designed bandpass filter is compact and has low insertion loss.

Table 6.5 Comparison of EC shaped resonator BPF with published works

References	**Center frequency (GHz)**	**Fractional Bandwidth (%)**	**Insertion loss (dB)**	**Circuit size (λ_g^2)**
[41]	29.8	4.76	1.4	1.14
[4]	36.51	9.1	3.37	2.34
[84]	38.2	8.4	2	2.74
EC shaped resonator BPF	38	5.26	0.37	0.96

6.4 Conclusion

In this chapter, bandpass filters are designed using microstrip coupled resonators. Coupled resonators are directly connected to the microstrip line to achieve compactness and low insertion loss. A compact dual bandpass filter is designed using dual split rings resonator for upper microwave flexible use services. A wide bandpass filter is designed using EC shaped microstrip coupled resonator for 37 GHz band 5G mobile applications.

Chapter 7

Overall conclusions and future scope

7.1. Research findings of the thesis

The literature published on microstrip filters is explored and the gaps are identified. Research objectives are framed to design microstrip filters at microwave and millimeter wave frequencies. The research work is focused on exploring single, multiple pass bands bandpass filters, bandstop filter design using metamaterials, complementary metamaterials and microstrip coupled resonators. The designed filters have potential applications such as GPS, WLAN, Wimax, radar, mid-band 5G, fixed/mobile satellite and upper microwave flexible use services applications for trans-receive roles.

In chapter 3, Symmetrical ring metamaterial resonators are loaded on either side of the microstrip line along with vias to design a single bandpass filter. The passband frequency range of the filter is from 5.47 GHz to 6 GHz. The obtained insertion loss is 1.2 dB. The fractional bandwidth is 9.8% at the center frequency of 5.73 GHz. The size of the filter is 0.64 λ_g^2. The realized filter is useful for C-band applications. Moore fractal is applied on the boundary of the symmetrical ring resonator resulting in a wide bandpass filter. The filter's operating frequency is from 6.95 GHz to 7.8 GHz with fractional bandwidth of 11.5%. The attained insertion loss is 0.4 dB. The area occupied by the filter is 0.75 λ_g^2. The moore fractal symmetrical ring resonator bandpass filter is useful for C band applications. The spacing between resonators is changed and the thickness of the RT Duroid 3010 substrate is changed from 0.13 mm to 1.28 mm, the resulting filter works in the X-band. The operating frequency range is from 10 GHz to 11.8 GHz with fractional bandwidth of 19.3%. The insertion loss obtained is less than 0.6 dB and return loss is 13 dB. The area of the filter is 2.8 λ_g^2.

EI-shaped unit cell is designed and loaded on either side of the microstrip line along with vias to design a bandpass filter. The frequency range of the filter is from 39.7 GHz to 40.7 GHz. The insertion loss and fractional bandwidth obtained are 2.5 dB and 2% respectively. The size of the filter is 7 λ_g^2. The filter is useful for higher 5G applications. The outer I shape is removed to reduce operating frequency leading to EIE shaped resonator. These resonators are loaded on either side of the microstrip line. Stubs placed in between resonators improved the return loss. The slots are placed within the stubs to improve stopband attenuation. Thus, a triple bandpass filter is designed. The triple bandpass filter has fractional bandwidth of 5.4 %, 2.5% and 4.58% at central frequencies at 7.29 GHz, 10.67 GHz and 13 GHz respectively. The realized insertion

loss is 1.2 dB, 1 dB and 1.4 dB. The area occupied by the filter is 0.32 λ_g^2. The designed triple bandpass filter is useful for fixed/mobile satellite communications.

In chapter 4, a bandpass filter is designed by employing complementary triple concentric split ring resonators at the gaps in addition to vias. The bandpass filter has a frequency range from 2.85 GHz to 3.15 GHz. The insertion loss is obtained as1.5 dB. The fractional bandwidth is 3% at the center frequency 3 GHz with filter size of 0.13 λ_g^2. The filter is compact and useful for S-band applications. A bandstop filter is designed by placing complementary symmetrical ring resonators on the ground plane along the transmission line and has fractional bandwidth of 11.9 % at a center frequency of 12.6 GHz. The maximum stopband attenuation obtained is 31 dB. The area occupied by the filter is 0.55 λ_g^2. The compact bandstop filter is useful for Ku band applications.

In chapter 5, the EI-shaped unit cell quint band bandpass filter is designed by placing unit cell structure on either side of the microstrip line in addition to complementary symmetrical ring resonators. The quint bandpass filter has frequency ranges from 38.65-38.85 GHz, 39.06-39.1 GHz, 39.9-40.28 GHz,41.96-42.06 GHz and 42.87-42.97 GHz, insertion loss of 1.67 dB, 2 dB, 1.54 dB, 2.45 dB and 2 dB, respectively. The size of the filter is 7 λ_g^2. The filter is useful for higher 5G applications. A dual bandpass filter is designed by placing the complementary triple concentric split ring resonators in the ground plane. The spiral resonators are attached to the transmission line and placed in between the complementary structures. The dual bandpass filter has center frequencies at 1.32 GHz and 2.47 GHz. The minimum insertion loss obtained is 1.3 dB and 1.8 dB. The fractional bandwidth is 7.5 % and 4.85 % for both bands. The area of the filter is 0.039 λ_g^2. The compact dual bandpass filter is useful for GPS and WLAN applications. A stepped impedance microstrip line is introduced to generate additional passband and stubs are added in between spiral resonators on either side of the transmission line for the dual bandpass configuration resulting in a triple bandpass filter. The bandpass filter has fractional bandwidth of 1.16%, 11.4% and 1.86% at center frequencies 1.29 GHz, 2.27 GHz and 3.21 GHz respectively. The obtained insertion loss is 1.6 dB, 1.3 dB and 1.8 dB. The size of the filter is 0.06 λ_g^2. The triple bandpass filter is useful for GPS, WLAN and WiMAX applications.

In chapter 6, dual split rings resonators are coupled to the microstrip line to design a dual bandpass filter. The bandpass filter has fractional bandwidth of 8.8 % and 2.2 % at center frequencies at 24.79 GHz and 28.37 GHz, with an insertion loss of less than 4.2 dB for both bands. The size of the dual bandpass filter is 0.1 λ_g^2. The dual bandpass filter is useful for Upper microwave flexible use services. A bandpass filter is designed using EC-shaped coupled lines

coupled to the microstrip line. The bandpass filter has an insertion loss of 0.4 dB at a center frequency of 38 GHz. The fractional bandwidth obtained is 5.26%. The occupied area of the filter is 0.96 λ_g^2 useful for 37 GHz band 5G mobile communications.

7.2. Future scope of work

Compact single and multi-bandpass filters, bandstop filters using different metamaterial and complementary metamaterial resonators useful for higher 5G applications can be explored. Additive manufacturing can be applied which can improve the design freedom and productivity of compact designs required at the millimeter wave frequencies.

7.2.1 Design of diplexers using microstrip bandpass filters

The design of diplexers involves combining two or more bandpass filters on the same PCB to create a device that can separate or combine multiple frequency bands. First identify the frequency bands required to separate or combine. Select appropriate microstrip bandpass filter types for each frequency band. The filters should be designed to have passbands that match the desired frequency ranges. For combing the signals, connect the input signals of the two frequency bands to the input ports of the respective bandpass filters. Connect the output ports of both bandpass filters together to form the combined output of the diplexer. Multiplexers can also be designed in the same process.

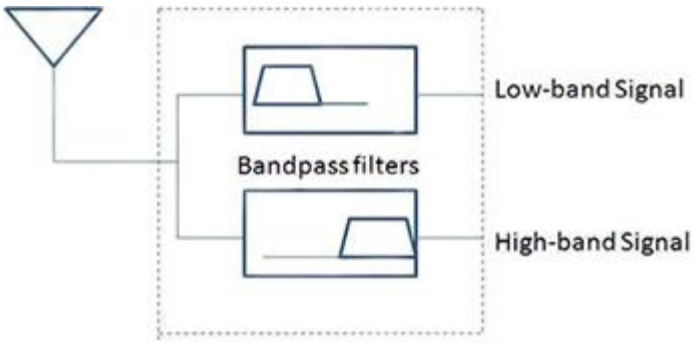

Fig 7.1 Diplexer using bandpass filters

References

[1] J.S. Hong and M. J. Lancaster, "Microstrip Filters for RF/Microwave Applications". *Wiley interscience publications*, 2001, ISBN 0-471-38877-7.

[2] D. S. Sreenath Kashyap, K. M.V.V. Prasad and D. Vipul, "Novel Microstrip Band Pass Filter for C- Band Wireless Applications," *Int. J. Eng. Technol.*, vol. 7, no. 4.6, pp. 227–229, 2018, doi: 10.14419/ijet.v7i4.6.20481.

[3] R. A. Maulidini, M. R. Hidayat and T. Praludi, "Band-Pass Filter Microstrip at 3 GHz Frequency Using Square Open-Loop Resonator for S-Band Radar Applications," *J. Elektron. dan Telekomun.*, vol. 20, no. 2, p. 53, 2020, doi: 10.14203/jet.v20.53-59.

[4] M. Mbeutcha, T. K. Johansen, Y. Dong, B. Cimoli and V. Krozer, "Replicability of a Millimeter-Wave Microstrip Bandpass Filter using Parallel Coupled Lines," *2018 IEEE MTT-S Lat. Am. Microw. Conf. LAMC 2018 - Proc.*, pp. 2–4, 2018, doi: 10.1109/LAMC.2018.8699012.

[5] N. Han, Y. L. Dong and M. Y. Wang, "A dual-band bandpass filter using parallel doubly coupled structure with loading capacitance," *2010 Int. Conf. Microw. Millim. Wave Technol. ICMMT 2010*, pp. 1849–1851, 2010, doi: 10.1109/ICMMT.2010.5524872.

[6] C. Caloz and T. Itoh, "Electromagnetic Metamaterials: Transmission Line Theory and Microwave Applications, The Engineering Approach", 2005. doi:10.1002/0471754323.

[7] R. Mittra and Y. Hao, " FDTD Modelling of Metamaterials: Theory and Applications", *Artech house*, 2009. ISBN:9781596931602.

[8] M. Gil, J. Bonache and F. Martín, "Metamaterial filters: A review," *Metamaterials*, vol. 2, no. 4, pp. 186–197, 2008, doi: 10.1016/j.metmat.2008.07.006.

[9] R. Bojanic, V. Milosevic, B. Jokanovic, F. Medina-Mena and F. Mesa, "Enhanced modelling of split-ring resonators couplings in printed circuits," *IEEE Trans. Microw. Theory Tech.*, vol. 62, no. 8, pp. 1605–1615, 2014, doi: 10.1109/TMTT.2014.2332302.

[10] M. Syahral and A. Munir, "Effect of elements number of SRR-based BPF to its characteristics," *Proc. - 2016 3rd Int. Conf. Inf. Technol. Comput. Electr. Eng. ICITACEE 2016*, pp. 1–4, 2017, doi: 10.1109/ICITACEE.2016.7892489.

[11] I. Gil, J. Bonache, J. Garcia-Garcia, F. Falcone and F. Martin, "Metamaterials in Microstrip Technology for Filter Applications," no. 1, pp. 668–671, 2005.

[12] J. D. Baena. J. Bonache, R.Marques and F.Falcone, "Equivalent-circuit models for split-ring resonators and complementary split-ring resonators coupled to planar transmission lines," *IEEE Trans. Microw. Theory Tech.*, vol. 53, no. 4, pp. 1451–1460, 2005, doi: 10.1109/TMTT.2005.845211.

[13] S. Chandra, "X-Band Metamaterial Bandpass Filter Design," *Int. J. Eng. Res. Technol.*, vol. 10, no. 05, pp. 1004–1006, 2021. ISSN: 2278-0181.

[14] D. Oloumi, A. Kordzadeh and A. A. L. Neyestanak, "Size reduction and bandwidth enhancement of a waveguide bandpass filter using fractal-shaped irises," *IEEE Antennas Wirel. Propag. Lett.*, vol. 8, pp. 1214–1217, 2009, doi: 10.1109/LAWP.2009.2035648.

[15] R. S. Anwar, Y. Wei, L. Mao and H. Ning, "Miniaturised frequency selective surface based on fractal arrays with square slots for enhanced bandwidth," *IET Microwaves, Antennas Propag.*, vol. 13, no. 11, pp. 1811–1819, 2019, doi: 10.1049/iet-map.2018.5224.

[16] H. X. Xu, G. M. Wang and C. X. Zhang, “Fractal-shaped metamaterials and applications to enhanced-performance devices exhibiting high selectivity,” *Int. J. Antennas Propag.*, pp. 1–14, 2012, doi: 10.1155/2012/515167.

[17] M. Abuhussain and U. C. Hasar, “Design of X-bandpass waveguide Chebyshev filter based on CSRR metamaterial for telecommunication systems,” *Electron.*, vol. 9, no. 101, pp. 1–16, 2020, doi: 10.3390/electronics9010101.

[18] B. Nasiri, A. Ennajih, A. Errkik, J. Zbitou and M. Derri, “Band-pass filter based on complementary split ring resonator,” *Telkomnika (Telecommunication Comput. Electron. Control.*, vol. 18, no. 3, pp. 1145–1149, 2020, doi: 10.12928/TELKOMNIKA.v18i3.13929.

[19] K. Becharef, K. Nouri, H. Kandouci, B. S. Bouazza, M. Damou and T. H. C. Bouazza, “Design and Simulation of a Broadband Bandpass Filter Based on Complementary Split Ring Resonator Circular ‘CSRRs,’” *Wirel. Pers. Commun.*, vol. 111, no. 3, pp. 1341–1354, 2020, doi: 10.1007/s11277-019-06918-6.

[20] R. Keshavarz and N. Shariati, “Low profile metamaterial band-pass filter loaded with 4-turn complementary spiral resonator for WPT applications,” in *ICECS 2020 - 27th IEEE International Conference on Electronics, Circuits and Systems, Proceedings*, 2020, pp. 50–53, doi: 10.1109/ICECS49266.2020.9294811.

[21] S. Moitra, S. Nayak, R. Regar, S. Kumari, K. Kumari, F. Parween and F. Naseem “Circular complementary split ring resonators (CSRR) based SIW BPF,” in *2019 2nd International Conference on Advanced Computational and Communication Paradigms, ICACCP 2019*, 2019, pp. 1–5, doi: 10.1109/ICACCP.2019.8883003.

[22] W. Yuan, X. Liu, H. Lu, W. Wu and N. Yuan, “Flexible Design Method for Microstrip Bandstop, Highpass and Bandpass Filters Using Similar Defected Ground Structures,” *IEEE Access*, vol. 7, pp. 98453–98461, 2019, doi: 10.1109/ACCESS.2019.2928816.

[23] Y. Cheng, L. Zeng and W. Lu, “A compact CSRR- based dual-mode patch bandpass filter,” *2015 IEEE MTT-S Int. Microw. Work. Ser. Adv. Mater. Process. RF THz Appl. IEEE MTT-S IMWS-AMP 2015 - Proc.*, pp. 3–5, 2015, doi: 10.1109/IMWS-AMP.2015.7325010.

[24] Y. Zheng, Y. Zhu and Y. Dong, “Compact Hybrid Bandpass Filter Using SIW and CSRRs with Wide Stopband Rejection,” *Asia-Pacific Microw. Conf. Proceedings, APMC*, pp. 767–769, 2020, doi: 10.1109/APMC47863.2020.9331361.

[25] M. K. T. Al-Nuaimi and W. G. Whittow, “Compact microstrip band stop filter using SRR and CSSR: Design, simulation and results,” *EuCAP 2010 - 4th Eur. Conf. Antennas Propag.*, pp. 0–6, 2010, ISBN: 9788476534724.

[26] B. Nasiri, A. Errkik, J. Zbitou, A. Tajmouati, L. El Abdellaoui and M. Latrach, “A miniature microstrip BSF using complementary split ring resonator,” *Int. J. Intell. Eng. Syst.*, vol. 11, no. 3, pp. 29–36, 2018, doi: 10.22266/IJIES2018.0630.04.

[27] B. Ajewole, P. Kumar and T. Afullo, “I-Shaped Metamaterial Using SRR for Multi-Band Wireless Communication,” *Crystals*, vol. 12, no. 4, 2022, doi: 10.3390/cryst12040559.

[28] M. P. Mohan, A. Alphones and M. F. Karim, “Triple Band Filter Based on Double Periodic CRLH Resonator,” *IEEE Microw. Wirel. Components Lett.*, vol. 28, no. 3, pp. 212–214, 2018, doi: 10.1109/LMWC.2018.2804171.

[29] R. L. Defitri and A. Munir, “X-band microstrip narrowband BPF composed of split ring resonator,” *2016 Prog. Electromagn. Res. Symp. PIERS 2016 - Proc.*, pp. 3468–3471,

2016, doi: 10.1109/PIERS.2016.7735347.

[30] A. A. Ibrahim, M. A. Abdalla and A. B. Abdel-Rahman, “Wireless bandpass filters build on metamaterials,” *Microwaves RF*, vol. 57, no. 5, pp. 1–7, 2018, ISSN:07452993.

[31] D. Bukuru, K. Song, F. Zhang, Y. Zhu and M. Fan, “Compact Quad-Band Bandpass Filter Using Quad-Mode Stepped Impedance Resonator and Multiple Coupling Circuits,” *IEEE Trans. Microw. Theory Tech.*, vol. 65, no. 3, pp. 783–791, 2017, doi: 10.1109/TMTT.2016.2638814.

[32] Q. Liu, D. Zhou, S. Wang and Y. Zhang, “Highly-selective pseudoelliptic filters based on dual-mode substrate integrated waveguide resonators,” *Electron. Lett.*, vol. 52, no. 14, pp. 1233–1235, 2016, doi: 10.1049/el.2016.1517.

[33] M. Amirian, G. Karimi, B. D. Wiltshire and M. H. Zarifi, “Differential Narrow Bandpass Microstrip Filter Design for Material and Liquid Purity Interrogation,” *IEEE Sens. J.*, vol. 19, no. 22, pp. 10545–10553, 2019, doi: 10.1109/JSEN.2019.2932693.

[34] W. Feng, X. Ma, Y. Shi, S. Shi and W. Che, “High-Selectivity Narrow- A nd Wide-band Input-Reflectionless Bandpass Filters with Intercoupled Dual-Behavior Resonators,” *IEEE Trans. Plasma Sci.*, vol. 48, no. 2, pp. 446–454, 2020, doi: 10.1109/TPS.2020.2968481.

[35] M. H. Weng, C. W. Hsu, Y. Lin, C. Y. Tsai and R. Y. Yang, “A simple method to design a tri-bandpass filter using open-loop uniform impedance resonators,” *J. Electromagn. Waves Appl.*, vol. 34, no. 1, pp. 103–115, 2020, doi: 10.1080/09205071.2019.1689181.

[36] M. U. Rahman and J. D. Park, “A compact tri-band bandpass filter using two stub-loaded dual mode resonators,” *Prog. Electromagn. Res. M*, vol. 64, pp. 201–209, 2018, doi: 10.2528/pierm17120404.

[37] B. I. Wu, W. Wang, J. Pacheco, X. Chen, T. M. Grzegorczyk and J. A. Kong, “A study of using metamaterials as antenna substrate to enhance gain,” *Prog. Electromagn. Res.*, vol. 51, pp. 295–328, 2005, doi: 10.2528/PIER04070701.

[38] Y. S. Mezaal, J. K. Ali and H. T. Eyyuboglu, “Miniaturised microstrip bandpass filters based on moore fractal geometry,” *Int. J. Electron.*, vol. 102, no. 8, pp. 1306–1319, 2015, doi: 10.1080/00207217.2014.971351.

[39] O. Yeşilyurt, M. Köksal and T. Imeci, “Microstrip band pass filter design,” *2015 23rd Signal Process. Commun. Appl. Conf. SIU 2015 - Proc.*, pp. 379–382, 2015, doi: 10.1109/SIU.2015.7129838.

[40] S. W. Sattler ,A. B. A. Alterkawi, F. Gentili, R. Teschl, E. Schlaffer, B. Reitmaier, W. Bosch, “Embedded Suspended Stripline Substrate Technology (ESSS) as a Catalyst for Low-loss PCB Structures in the Ka-Band,” *IMWS-AMP 2019 - 2019 IEEE MTT-S Int. Microw. Work. Ser. Adv. Mater. Process. RF THz Appl.*, pp. 154–156, 2019, doi: 10.1109/IMWS-AMP.2019.8880129.

[41] M. D. Li, J. Ma and A. Y. Ma, “Ka band orthogonal dumbbell groove substrate integrated waveguide filter,” *2018 12th Int. Symp. Antennas, Propag. EM Theory, ISAPE 2018 - Proc.*, pp. 18–21, 2018, doi: 10.1109/ISAPE.2018.8634079.

[42] N. Han, Y. L. Dong and M. Y. Wang, “A dual-band bandpass filter using parallel doubly coupled structure with loading capacitance,” *2010 Int. Conf. Microw. Millim. Wave Technol. ICMMT 2010*, pp. 1849–1851, 2010, doi: 10.1109/ICMMT.2010.5524872.

[43] B. P. Rao and V.M. Rao, “Design Of Triple Band Pass Filters Using Three-Coupled Finline And Metamaterials 1,” *Int. J. Eng. Res.*, vol. 6, no. 3, pp. 149–153, 2017, ISSN:

2347-5013.

[44] B. Fellah, N. Cherif, M. Abri and H. Badaoui, “CSRR-DGS bandpass filter based on half mode substrate integrated waveguide for X-band applications,” *Adv. Electromagn.*, vol. 10, no. 3, pp. 39–42, 2021, doi: 10.7716/aem.v10i3.1782.

[45] D. V. T. Snezana Lj. Stefanovski, Milka M. Potrebic, “Design and Analysis of Bandpass Waveguide Filters Using Novel Complementary Split Ring Resonators,” *11 th Int. Conf. Telecommun. Mod. Satell. cable Broadcast. Serv.*, pp. 16–19, 2013, doi: 10.1109/TELSKS.2013.6704929.

[46] H. Cao, S. He, H. Li and S. Yang, “A compact wideband bandpass filter using novel CSRR loaded QMSIW resonator with high selectivity,” *Prog. Electromagn. Res. C*, vol. 41, pp. 239–254, 2013, doi: 10.2528/PIERC13053006.

[47] H. Lalj, H. Griguer and M. Drissi, “Very Compact Bandstop Filters Based on Miniaturized Complementary Metamaterial Resonators,” *Wirel. Eng. Technol.*, vol. 04, no. 02, pp. 101–104, 2013, doi: 10.4236/wet.2013.42015.

[48] S. T. Niba and A. S. A. Nisha, “Design and Analysis of Microstrip Band Stop Filter Using Complementary Split Ring Resonator,” *Wirel. Pers. Commun.*, vol. 111, no. 3, pp. 1899–1907, 2020, doi: 10.1007/s11277-019-06963-1.

[49] Q. L. Zhang, B. Z. Wang, D. S. Zhao and K. Wu, “A Compact Half-Mode Substrate Integrated Waveguide Bandpass Filter with Wide Out-of-Band Rejection,” *IEEE Microw. Wirel. Components Lett.*, vol. 26, no. 7, pp. 501–503, 2016, doi: 10.1109/LMWC.2016.2574997.

[50] A. K. Panda, M. Pattnaik and R. Swain, “CSRR Embedded CPW Band-Stop Filter,” *IETE J. Res.*, pp. 1–7, 2019, doi: 10.1080/03772063.2019.1684847.

[51] J. Hinojosa, M. Rossi, A. Saura-Rodenas, A. Alvarez-Melcon and F. L. Martinez-Viviente, “Compact Bandstop Half-Mode Substrate Integrated Waveguide Filter Based on a Broadside-Coupled Open Split-Ring Resonator,” *IEEE Trans. Microw. Theory Tech.*, vol. 66, no. 6, pp. 3001–3010, 2018, doi: 10.1109/TMTT.2018.2833483.

[52] S. Soeung, S. Cheab and P. W. Wong, “Lossy Asymmetrical Bandstop Filter Based on a Multiple Triplet Realization,” *IEEE Access*, vol. 6, pp. 1284–1291, 2017, doi: 10.1109/ACCESS.2017.2778267.

[53] O. Abu Safia, L. Talbi and K. Hettak, “A new type of transmission line-based metamaterial resonator and its implementation in original applications,” *IEEE Trans. Magn.*, vol. 49, no. 3, pp. 968–973, 2013, doi: 10.1109/TMAG.2012.2230248.

[54] M. Esmaeili, J. Bornemann and P. Krauss, “Substrate integrated waveguide bandstop filter using partial-height via-hole resonators in thick substrate,” *IET Microwaves, Antennas Propag.*, vol. 9, no. 12, pp. 1307–1312, 2015, doi: 10.1049/iet-map.2015.0141.

[55] D. C. H. Bong, V. Jeoti, S. Cheab and P. W. Wong, “Design and Synthesis of Chained-Response Multiband Filters,” *IEEE Access*, vol. 7, pp. 130922–130936, 2019, doi: 10.1109/ACCESS.2019.2940059.

[56] C. F. Chen, “Design of a compact microstrip quint-band filter based on the tri-mode stub-loaded stepped-impedance resonators,” *IEEE Microw. Wirel. Components Lett.*, vol. 22, no. 7, pp. 357–359, 2012, doi: 10.1109/LMWC.2012.2202894.

[57] Y. Guo, S. Kim, H. Gao and G. P. Li, “Compact High Q Configurable Quint-Band Electromagnetic Bandgap Filter,” *IEEE Access*, vol. 6, pp. 63703–63711, 2018, doi: 10.1109/ACCESS.2018.2877297.

[58] J. Ai, Y. Zhang, K. Da Xu, D. Li and Y. Fan, “Miniaturized Quint-Band Bandpass Filter Based on Multi-Mode Resonator and λ/4 Resonators with Mixed Electric and Magnetic Coupling,” *IEEE Microw. Wirel. Components Lett.*, vol. 26, no. 5, pp. 343–345, 2016, doi: 10.1109/LMWC.2016.2549643.

[59] H. Y. Gao, Z. X. Tang, X. Cao, Y. Q. Wu and B. Zhang, “Compact dual-band SIW filter with CSRRS and complementary spiral resonators,” *Microw. Opt. Technol. Lett.*, vol. 58, no. 1, pp. 1–4, Jan. 2016, doi: 10.1002/mop.29482.

[60] A. Y. Rouabhi, M. Berka, A. Benadaoudi and Z. Mahdjoub, “Investigation of dual-band bandpass filter inspired by a pair of square coupled interlinked asymmetric tapered metamaterial resonator for X-band microwave applications,” *Bull. Mater. Sci.*, vol. 45, no. 118, pp. 1–9, 2022, doi: 10.1007/s12034-022-02693-6.

[61] H. Fabian-Gongora, A. E. Martynyuk, J. Rodriguez-Cuevas, L. Martinez-Lopez, R. Martinez-Lopez and J. I. Martinez-Lopez, “Independently Tunable Closely Spaced Triband Frequency Selective Surface Unit Cell Using the Third Resonant Mode of Split Ring Slots,” *IEEE Access*, vol. 9, pp. 105564–105576, 2021, doi: 10.1109/ACCESS.2021.3100325.

[62] A. Kumar, D. K. Choudhary and R. K. Chaudhary, “Metamaterial Tri-Band Bandpass Filter using Meander-Line with Rectangular-Stub,” *Prog. Electromagn. Res. Lett.*, vol. 66, pp. 121–126, 2017.

[63] N. K. and Y. K. Singh and A, “Compact tri-band bandpass filter using three stub-loaded open-loop resonator with wide stop band and improved bandwidth response.” *ELECTRONICS LETTERS*, pp. 1950–1952, 2014, doi: 10.1049/el.2014.3425.

[64] P. Ma *et al.*, “A Design Method of Multimode Multiband Bandpass Filters,” *IEEE Trans. Microw. Theory Tech.*, vol. 66, no. 6, pp. 2791–2799, 2018, doi: 10.1109/TMTT.2018.2815682.

[65] Q. Yang, Y. C. Jiao and Z. Zhang, “Compact Multiband Bandpass Filter Using Low-Pass Filter Combined with Open Stub-Loaded Shorted Stub,” *IEEE Trans. Microw. Theory Tech.*, vol. 66, no. 4, pp. 1926–1938, 2018, doi: 10.1109/TMTT.2018.2791961.

[66] J. Tang, H. Liu, Q. Zhang, B. Ren and Y. Liu, “Miniaturized Multiband HTS Bandpass Filter Design Using a Single-Perturbed Multimode Resonator with Multitransmission Zeros,” *IEEE Trans. Appl. Supercond.*, vol. 28, no. 4, 2018, doi: 10.1109/TASC.2018.2799993.

[67] H. Wu and R. Yang, “A New Quad-Band Bandpass Filter Using Asymmetric Stepped Impedance Resonators,” *IEEE Microw. Wirel. Components Lett.*, vol. 21, no. 4, pp. 203–205, 2011, doi: 10.1109/LMWC.2011.2106153.

[68] G. Soundarya and N. Gunavathi, “Compact Dual-Band SIW Band Pass Filter Using CSRR and DGS Structure Resonators,” *Prog. Electromagn. Res. Lett.*, vol. 101, no. September, pp. 79–87, 2021, doi: 10.2528/PIERL21091301.

[69] M. Berka, H. Abdelhak, A. Amina and B. Zoubir, “Dual - Band Bandpass Filter Based on Electromagnetic Coupling of Twin Square Metamaterial Resonators (SRRs) and Complementary Resonator (CSRR) for Wireless Communications,” *J. Electron. Mater.*, vol. 50, no. 8, pp. 4887–4895, 2021, doi: 10.1007/s11664-021-09024-1.

[70] H. Hanen and G. Ali, “Design of pass band filter in hybrid architecture planar/NRD waveguide integration technology,” *7th Int. Conf. Des. Technol. Integr. Syst. Nanoscale Era, DTIS 2012*, pp. 1–3, 2012, doi: 10.1109/DTIS.2012.6232974.

[71] K. Onaka *et al.*, "28 GHz wideband filter using quartz crystal waveguide for massive MIMO antenna unit," *IEEE MTT-S Int. Microw. Symp. Dig.*, pp. 1468–1471, 2017, doi: 10.1109/MWSYM.2017.8058898.

[72] A. Abramowicz, "Unified description of coupled resonators and coupled transmission lines," *Acta Phys. Pol. A*, vol. 119, no. 4, pp. 548–552, 2011, doi: 10.12693/APhysPolA.119.548.

[73] G. Mansour, M. K. A. Rahim and H. A. Aldeeb, "Cross-Coupled Microstrip Bandpass Filters with Finite Frequency Transmission Zeros," *2021 IEEE 1st Int. Maghreb Meet. Conf. Sci. Tech. Autom. Control Comput. Eng. MI-STA 2021 - Proc.*, no. May, pp. 684–688, 2021, doi: 10.1109/MI-STA52233.2021.9464385.

[74] M. Chetioui, N. Benabdallah, N. Benahmed and L. Boumediene, "Design of Novel Cross-Coupled Trisection Bandpass Filters with Open-Loop Resonators," *Int. J. Sci. Eng. Res.*, vol. 6, no. 5, pp. 437–440, 2015, ISSN: 2229-5518.

[75] T. Rohit, R. Ramesh, S. G. Abhishek, H. Umma and R. Sandhya, "Microstrip open loop resonator using dual feed techniques for Wireless Applications," vol. 11, no. 5, pp. 13–15, 2016, doi: 10.9790/2834-1105021315.

[76] A. J. Salim, A. N. Alkhafaji, M. S. Taha and J. K. Ali, "A polygonal open-loop resonator compact bandpass filter for Bluetooth and WLAN applications," *IOP Conf. Ser. Mater. Sci. Eng.*, vol. 433, no. 1, 2018, doi: 10.1088/1757-899X/433/1/012083.

[77] M. Alaydrus, D. Widiastuti and T. Yulianto, "Designing cross-coupled bandpass filters with transmission zeros in lossy microstrip," *Proc. - 2013 Int. Conf. Inf. Technol. Electr. Eng. "Intelligent Green Technol. Sustain. Dev. ICITEE 2013*, pp. 277–280, 2013, doi: 10.1109/ICITEED.2013.6676252.

[78] N. V. Ivanov, "A new approach to microstrip coupled-resonator bandpass filter design," *Proc. 2018 IEEE Conf. Russ. Young Res. Electr. Electron. Eng. ElConRus 2018*, pp. 201–203, 2018, doi: 10.1109/EIConRus.2018.8317064.

[79] A. A. Ibrahim, A. B. Abdel-Rahman, M. A. Abdalla and H. F. A. Hamed, "Compact size microstrip coupled resonator band pass filter loaded with lumped capacitors," in *Proceedings of the 2013 2nd International Japan-Egypt Conference on Electronics, Communications and Computers, JEC-ECC 2013*, 2013, pp. 64–67, doi: 10.1109/JEC-ECC.2013.6766386.

[80] L. Ma, J. Zhuang and J. Zhou, "A cross-coupled substrate integrated waveguide filter for 28 GHz millimeter wave communications," *Proc. - IEEE Int. Symp. Circuits Syst.*, vol. 2016-July, pp. 814–817, 2016, doi: 10.1109/ISCAS.2016.7527365.

[81] Y. Zhong, Y. Yang, X. Zhu, E. Dutkiewicz, K. M. Shum and Q. Xue, "An On-Chip Bandpass Filter Using a Broadside-Coupled Meander Line Resonator with a Defected-Ground Structure," *IEEE Electron Device Lett.*, vol. 38, no. 5, pp. 626–629, 2017, doi: 10.1109/LED.2017.2690283.

[82] Z. J. Hou, Y. Yang, X. Zhu, Y. C. Li, E. Dutkiewicz and Q. Xue, "A Compact and Low-Loss Bandpass Filter Using Self-Coupled Folded-Line Resonator with Capacitive Feeding Technique," *IEEE Electron Device Lett.*, vol. 39, no. 10, pp. 1584–1587, 2018, doi: 10.1109/LED.2018.2864597.

[83] N. N. Al-Areqi, N. Seman and T. A. Rahman, "Design of microstrip parallel-coupled line band pass filters for the application in fifth-generation wireless communication," *J. Telecommun. Electron. Comput. Eng.*, vol. 9, no. 2–7, pp. 19–23, 2017. ISSN: 2289-8131.

[84] G. Wen, J. Li, F. Xie, H. Wang and Y. Huang, “Millimeter-Wave SIW Filter Based on the Stepped-Impedance Face-to-Face E-Shaped DGSs,” *IEEE MTT-S Int. Microw. Symp. Dig.*, vol. 2019-June, pp. 830–833, 2019, doi: 10.1109/mwsym.2019.8700813.

List of Publications

International Journals-Published

1. Sowjanya A, Vakula D. “Compact dual bandpass filter using dual-split ring resonator for 5G upper microwave flexible use services”, *Journal of the Korean Institute of Electromagnetic and Science*, vol. 22, no. 4, pp: 434-439, July,2022; DOI:10.26866/jees.2022.4.r.106. **(SCIE)**
2. Sowjanya A., & Vakula D. (2022). “Design of C band bandpass filter using fractal based symmetrical ring resonator”. *Advanced Electromagnetics*, *11*(3), 71–77. DOI: 10.7716/aem.v11i3.1851. **(ESCI)**
3. Ampavathina Sowjanya, Damera Vakula*, “*Metamaterial inspired compact single and multiband filters*”, in Advances in Science, Technology and Engineering Systems Journal.* 7(4), 92-97 (2022); DOI: 10.25046/aj070412. **(Scimago)**

International Journals-Under review

1. Sowjanya A, Vakula D*, “*Design of EI shaped coupled lines based bandpass filter for 5G applications”, in *International Journal of System Assurance Engineering and Management System* (IJSA). **(ESCI)**
2. Sowjanya A, Vakula D, “EI shaped metamaterial inspired structure and slotted stub loaded dual bandpass filter”, in Frequenz: Journal of RF Engineering and Telecommunications. **(SCIE)**

International Conferences Published

1. A. Sowjanya and D. Vakula, "Microstrip Band Pass Filter using Symmetrical Split Ring Resonator for X band Applications," *2019 IEEE Indian Conference on Antennas and Propogation (InCAP)*, 2019, pp. 1-4, doi: 10.1109/InCAP47789.2019.9134507.
2. A. Sowjanya and D. Vakula, "Design of Bandpass filter using Complementary Split Ring Resonators," *2021 International Applied Computational Electromagnetics Society Symposium (ACES)*, 2021, pp. 1-3, doi: 10.1109/ACES53325.2021.00150.
3. S. Ampavathina and V. Damera, "Compact Complementary Symmetric Ring Resonator Band Stop Filter for Ku band applications," *2022 IEEE Wireless Antenna and Microwave Symposium (WAMS)*, 2022, pp. 1-5, doi: 10.1109/WAMS54719.2022.9848080.
4. Sowjanya A, Vakula D, “Design of EI Shaped Coupled Lines based Bandpass Filter for 5G Applications” in *Antenna Test and Measurement Society Conference on February 18, 2021*.

Book chapter

1. Vakula, D., Sowjanaya, A. (2022). “Metamaterial Filters.” In: Narayan, S., Kesavan, A. (eds) *Handbook of Metamaterial-derived Frequency Selective Surfaces. Metamaterials Science and Technology*, Vol 3. Springer, singapore. https://doi.Org/10.1007/978-981-15-8597-5_30-1.